NAVAL POSTGRADUATE SCHOOL

MONTEREY, CALIFORNIA

THESIS

A STATISTICAL-DYNAMICAL APPROACH TO INTRASEASONAL PREDICTION OF TROPICAL CYCLOGENESIS IN THE WESTERN NORTH PACIFIC

by

Bryan D. Mundhenk

March 2009

Thesis Advisors: Tom Murphree
                                                   David W. Meyer

Approved for public release; distribution is unlimited

THIS PAGE INTENTIONALLY LEFT BLANK

REPORT DOCUMENTATION PAGE		*Form Approved OMB No. 0704-0188*
Public reporting burden for this collection of information is estimated to average 1 hour per response, including the time for reviewing instruction, searching existing data sources, gathering and maintaining the data needed, and completing and reviewing the collection of information. Send comments regarding this burden estimate or any other aspect of this collection of information, including suggestions for reducing this burden, to Washington headquarters Services, Directorate for Information Operations and Reports, 1215 Jefferson Davis Highway, Suite 1204, Arlington, VA 22202-4302, and to the Office of Management and Budget, Paperwork Reduction Project (0704-0188) Washington DC 20503.		
1. AGENCY USE ONLY *(Leave blank)*	**2. REPORT DATE** March 2009	**3. REPORT TYPE AND DATES COVERED** Master's Thesis
4. TITLE AND SUBTITLE A Statistical-Dynamical Approach to Intraseasonal Prediction of Tropical Cyclogenesis in the Western North Pacific		**5. FUNDING NUMBERS**
6. AUTHOR(S) Mundhenk, Bryan D.		
7. PERFORMING ORGANIZATION NAME(S) AND ADDRESS(ES) Naval Postgraduate School Monterey, CA 93943-5000		**8. PERFORMING ORGANIZATION REPORT NUMBER**
9. SPONSORING /MONITORING AGENCY NAME(S) AND ADDRESS(ES) N/A		**10. SPONSORING/MONITORING AGENCY REPORT NUMBER**
11. SUPPLEMENTARY NOTES The views expressed in this thesis are those of the author and do not reflect the official policy or position of the Department of Defense or the U.S. Government.		
12a. DISTRIBUTION / AVAILABILITY STATEMENT Approved for public release; distribution is unlimited		**12b. DISTRIBUTION CODE**
13. ABSTRACT We have developed a combined statistical-dynamical prediction scheme to predict the probability of tropical cyclone (TC) formation at daily, 2.5° horizontal resolution across the western North Pacific at intraseasonal lead times. Through examination of previous research and our own analysis, we chose five variables to represent the favorability of the climate system to support tropical cyclogenesis. These so-called large-scale environmental factors (LSEFs) include: low-level relative vorticity, sea surface temperature, vertical wind shear, Coriolis, and upper-level divergence. Logistic regression was employed to generate a statistical model representing the probability of TC formation at every grid point based on these LSEFs. Thorough verification of zero-lead hindcasts reveals this model displays skill and potential value for risk adverse customers. In particular, these hindcasts had a positive Brier skill score of 0.03 and a skillful relative operating characteristic skill score of 0.68. The fully coupled, one-tier NCEP Climate Forecast System was used as the dynamical model with which to forecast the LSEFs and, in turn, force the regression model. A series of individual TC case studies were conducted to demonstrate the predictive potential, at intraseasonal leads, of our statistical-dynamical method. Lastly, we investigated the applicability of intraseasonal forecasts to military planning.		
14. SUBJECT TERMS Tropical Cyclones, Western North Pacific, Tropical Cyclogenesis, Intraseasonal Forecasting, Smart Climatology, Tropical Climatology, Long-Range Forecast, Long-Range Weather Support, Tropical Genesis Parameters, NCEP Climate Forecast System		**15. NUMBER OF PAGES** 129
		16. PRICE CODE

17. SECURITY CLASSIFICATION OF REPORT Unclassified	**18. SECURITY CLASSIFICATION OF THIS PAGE** Unclassified	**19. SECURITY CLASSIFICATION OF ABSTRACT** Unclassified	**20. LIMITATION OF ABSTRACT** UU

NSN 7540-01-280-5500

Standard Form 298 (Rev. 8-98)
Prescribed by ANSI Std. Z39.18

THIS PAGE INTENTIONALLY LEFT BLANK

A STATISTICAL-DYNAMICAL APPROACH TO INTRASEASONAL PREDICTION OF TROPICAL CYCLOGENESIS IN THE WESTERN NORTH PACIFIC

Bryan D. Mundhenk
Captain, United States Air Force
B.S., University of Missouri - Columbia, 2003

Submitted in partial fulfillment of the
requirements for the degree of

MASTER OF SCIENCE IN METEOROLOGY

from the

**NAVAL POSTGRADUATE SCHOOL
March 2009**

Author: Bryan D. Mundhenk

Approved by: Tom Murphree
                    Co-Advisor

                    David W. Meyer
                    Co-Advisor

                    Philip A. Durkee
                    Chairman, Department of Meteorology

THIS PAGE INTENTIONALLY LEFT BLANK

ABSTRACT

We have developed a combined statistical-dynamical prediction scheme to predict the probability of tropical cyclone (TC) formation at daily, 2.5° horizontal resolution across the western North Pacific at intraseasonal lead times. Through examination of previous research and our own analysis, we chose five variables to represent the favorability of the climate system to support tropical cyclogenesis. These so-called large-scale environmental factors (LSEFs) include: low-level relative vorticity, sea surface temperature, vertical wind shear, Coriolis, and upper-level divergence. Logistic regression was employed to generate a statistical model representing the probability of TC formation at every grid point based on these LSEFs. Thorough verification of zero-lead hindcasts reveals this model displays skill and potential value for risk adverse customers. In particular, these hindcasts had a positive Brier skill score of 0.03 and a skillful relative operating characteristic skill score of 0.68. The fully coupled, one-tier NCEP Climate Forecast System was used as the dynamical model with which to forecast the LSEFs and, in turn, force the regression model. A series of individual TC case studies were conducted to demonstrate the predictive potential, at intraseasonal leads, of our statistical-dynamical method. Lastly, we investigated the applicability of intraseasonal forecasts to military planning.

THIS PAGE INTENTIONALLY LEFT BLANK

TABLE OF CONTENTS

LIST OF FIGURES

THIS PAGE INTENTIONALLY LEFT BLANK

LIST OF TABLES

THIS PAGE INTENTIONALLY LEFT BLANK

LIST OF ACRONYMS AND ABBREVIATIONS

14WS	14th Weather Squadron, formerly named AFCCC
ACE	Accumulated cyclone energy
AFCCC	Air Force Combat Climatology Center, now named 14WS
AFW	Air Force Weather
AIC	Akaike Information Criterion
AMIP–II	Atmospheric Model Intercomparison Project–II
BS	Brier score
BSS	Brier skill score
CFS	Climate Forecast System
C/L	Cost/loss
CPC	Climate Prediction Center
DoD	Department of Defense
DOE	Department of Energy
ECMWF	European Centre for Medium-range Weather Forecasts
ENLN	El Niño-La Niña
EPS	Ensemble Prediction System
EVD	Economic value diagram
FNMOD	Fleet Numerical Meteorological and Oceanographic Detachment
GCM	General Circulation model
GFDL	Geophysical Fluid Dynamics Laboratory
GFS	Global Forecast System
IRI	International Research Institute for Climate and Society
JASO	July, August, September, and October
JTWC	Joint Typhoon Warning Center
LSEF	Large-scale environmental factor
LTM	Long term mean
METOC	Meteorology and oceanography

MJO	Madden-Julian oscillation
MOM3	Modular Ocean Model version 3
MSLP	Mean sea level pressure
NCAR	National Center for Atmospheric Research
NCEP	National Centers for Environmental Prediction
NE	Northeast
NOAA	National Oceanic and Atmospheric Administration
NTCI	Non-tropical cyclone information
OI	Optimum interpolation
OLR	Outgoing longwave radiation
ONI	Oceanic Niño index
R1	NCEP/NCAR Reanalysis Projects
R2	NCEP/DOE AMIP–II Reanalysis
ROC	Relative operating characteristic
ROCSS	Relative operating characteristic skill score
SST	Sea surface temperature
SW	Southwest
TC	Tropical cyclone
TUTT	Tropical upper tropospheric trough
VS	Valiant Shield military exercise
WMO	World Meteorological Organization
WNP	Western North Pacific

ACKNOWLEDGMENTS

THIS PAGE INTENTIONALLY LEFT BLANK

I.   INTRODUCTION

A.   MOTIVATION

Three months before the kickoff of the Valiant Shield (VS) naval exercise, a group of U. S. Navy planners gathers in a small conference room at Pearl Harbor to compare notes. The meeting scrubs the logistics and rules of engagement for this large scale, joint forces event held in the tropical western North Pacific region near Guam. Hours later, an environment-savvy planner questions, "is the weather going to cooperate?" He continues, "How might tropical cyclones affect the ability of the different platforms to operate in the designated exercise area and period?"

This meeting may be hypothetical, but those questions are exactly the type that military planners *should* be asking and that Department of Defense (DoD) weather centers *should* be capable of answering with confidence. Unfortunately, no suitable products currently exist to answer such questions. Such mission planning well in advance of the operation(s) is not unusual in the DoD. Though this example depicts a complex exercise, the same environmental intelligence should be exploited for a multitude of missions, such as planning flight qualification training at long leads or establishing a CORONET trans-oceanic air bridge.

A gap clearly exists in DoD weather support for forecasts with lead times on the order of weeks to months. Consider the potential benefit—in dollars, hours, morale, etc.—if weather forecasters were able to provide those planners with a regional outlook for tropical cyclone activity and an idea of avenues of safe passage through the western North Pacific. This thesis will investigate one such approach that would benefit this scenario.

B. CLIMATE PREDICTION PROCESS

1. Syntax and Definitions

Below are definitions for and discussions of some key terms that are used in this paper.

a. Climatology

While *climatology* literally refers to the description and scientific study of climate (Glickman 2000), this term is used in this work to refer to a quantitative description of an element in terms of a long term average; for example, the frequency of cyclone formation for a given grid box in a region for a given unit of time. Climatology is also used throughout this thesis as the baseline forecast against which our methods will be compared. Appendix A includes a more in-depth discussion on the variations in the methods used to calculate climatologies.

b. Intraseasonal

Used in reference to a subset of forecast products and associated lead times, *intraseasonal* comprises a period bounded by a single season or other three month period. Often referred to as long-range forecasting, subseasonal forecasting, or short-term climate prediction, the lead times for intraseasonal products and techniques are typically longer than two weeks, but less than three months.

c. Prediction

The word *prediction* is readily used interchangeably with a form of the word *forecast*. Though such use may be grammatically correct, we use the word prediction to denote a quantitative scientific estimate of future climate conditions that has skill. A forecast, in contrast, is used to refer to both the prediction process, regardless of perceived skill, and the deliverable that results.

The difference here between forecast and prediction may be more psychological than meteorological. The customers for forecasts and predictions (e.g., military operators, the general public, etc.) expect that weather forecasts are readily available (e.g., a five-day forecast from the local news media). In contrast, a description of the future state of the climate system may be best thought of as a prediction that is issued only if the prediction has some perceived skill beyond a baseline forecasts (e.g., a forecast of climatological conditions). In that context, a customer should not always expect a prediction that varies from the long-term mean (LTM) for temperature over the forthcoming summer in the same way he expects a local forecast for tomorrow's high temperature.

d.   *Tropical Cyclone*

In the most general form, *tropical cyclone* refers to a closed, cyclonic circulation with its origins over a tropical ocean basin. Tropical cyclones (TCs) are classified according to their intensity, and these classifications vary somewhat by ocean basin. In the western North Pacific (WNP), a *tropical depression* is characterized by winds up to 17 ms^{-1}, a *tropical storm* has winds of 18 ms^{-1} to 32 ms^{-1}, a *typhoon* has winds 33 ms^{-1} to 66 ms^{-1}, and a *super typhoon* has winds that exceed 66 ms^{-1}.

2.   Elements of Operational Climate Prediction

The basis of this thesis is the exploratory development of a state-of-the-science climate prediction system for likely TC formation areas in a given geographical region. Though the idea of climate prediction—intraseasonal or otherwise—is not new, no available resources clearly outline the prediction process.
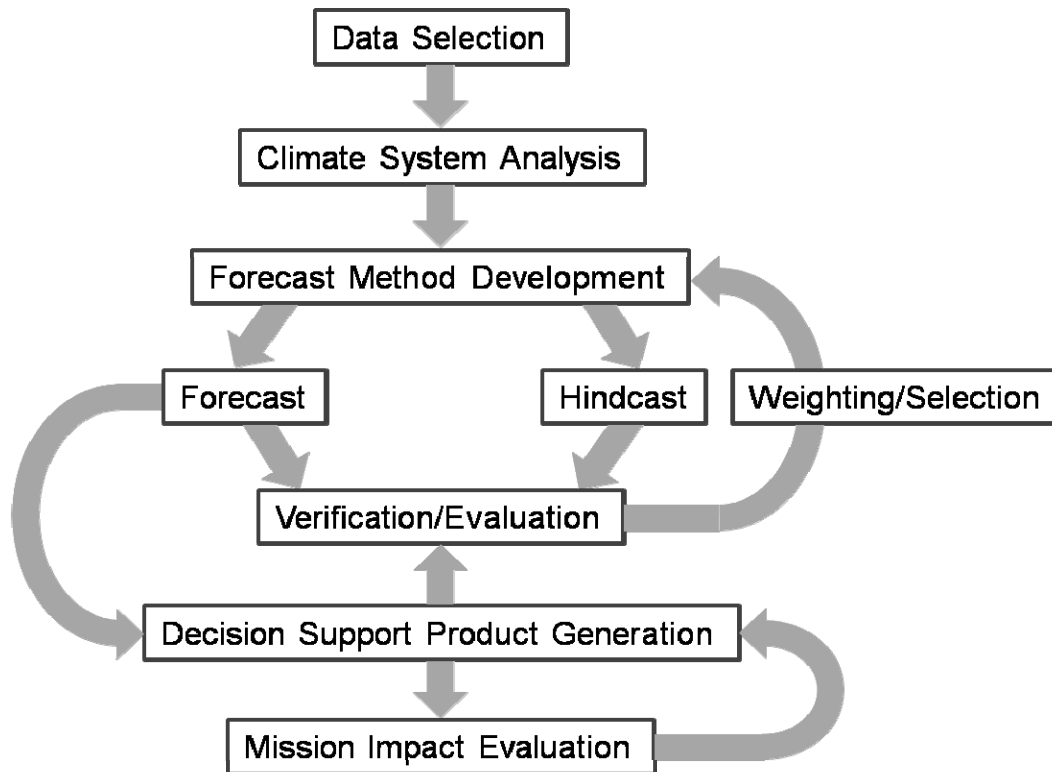
Figure 1.   Schematic of the climate prediction process.

Figure 1 provides a schematic description of a state-of-the-science approach to developing an operational climate predictions. As presented, this process is generic and may be applied to various meteorological or oceanographic elements and over various time scales. The flow of the arrows in the diagram indicates that the process is fluid, and often iterative in nature. Though the process may vary somewhat in specific cases, the depicted steps are all important to the development of an operational deliverable.

3.   Methods of Prediction

Though the *Forecast Method Development* step is only one step in the process depicted in Figure 1, the development of the forecast method is likely the most challenging component of the climate prediction process. Three primary categories of predictive methods exist in operational intraseasonal/seasonal forecasting: statistical,   dynamical,   and   a   combined   statistical-dynamical approach.

a.   Statistical

Whether the approach is projecting average conditions, constructing analogues, or applying empirical orthogonal functions, statistical methods are widely used in climate prediction. These and many other statistical, also referred to as empirical, methods use existing data sets in order to develop predictive methods based on past conditions. Such methods are mainstays for intraseasonal and seasonal climate prediction at the National Weather Service's Climate Prediction Center (CPC) and other climate prediction centers (van den Dool 2007).

b.   Dynamical

Numerical weather prediction may be the standard for day-to-day weather forecasting, but dynamical methods in intraseasonal and seasonal climate prediction are often less skillful than comparable statistical methods. Van den Dool (2007) cites that in 2005, the National Centers for Environmental Prediction (NCEP) presented an award to a group of its employees for developing the Climate Forecast System (CFS; to be discussed in Section II.B.4) that led to "the first time in history (in which) numerical seasonal predictions were on par with empirical methods."

The CFS belongs to a class of numerical models known as general circulation models (GCMs). Many GCMs were built to focus on global climate issues; therefore, they struggle when applied regionally at intraseasonal time scales. Coarse resolution, limited parameterizations, and systematic model errors all translate into limited operational use of many of the GCMs. However, one advantage of a GCM vice a purely statistical method is the ability of the numerical model to explicitly account for nonlinear processes (van den Dool 2007). The reader is directed to van den Dool (2007) for an informative discussion of the relative performance of GCMs compared to empirical methods.

c.   *Combined*

The wide use of statistical techniques in short-term climate prediction leads one to the question whether there is any benefit to using a GCM or combined statistical-dynamical approach, or whether a pure statistical forecast would perform just as well.   A combined methodology is potentially superior, since such an approach has the ability to incorporate the advantages of each approach. The method used in this thesis entails the use of a GCM to develop a prediction of the large sale environmental factors (LSEFs) that affect TC formations, and then uses these LSEFs to force a statistical model that has been trained over many years of TC and LSEF data to predict the probability of TC formation based on the GCM predictions of the LSEFs.

C.   EXISTING PRODUCTS

1.   Seasonal

Seasonal predictions of TC activity forecast the overall character for an entire TC season within an entire basin (e.g., the total number of TCs in a WNP TC season). The lead times for seasonal predictions are approximately zero to six months. Among the earliest seasonal tropical cyclone predictions were those produced at Colorado State University in the 1980s for the Atlantic basin. Prediction techniques have continued to develop and expand since these early forecasts, and now include other ocean basins (Camargo 2006).   Though seasonal prediction is not the focus of this thesis, these existing products are briefly mentioned here as they provide much of the framework from which the newer intraseasonal products are derived. Seasonal TC forecast products for the WNP are generated at various centers using statistical and dynamical methods.   The following listing of centers and products is by no means all-inclusive, but provides a glimpse into the spectrum of participants and approaches.

a. Statistical

The City University of Hong Kong has issued seasonal forecasts for the number of storms in the WNP basin since 1997. They use several environmental conditions, the most prominent of which are El Niño and the Pacific subtropical ridge, in order to forecast the number of TCs (Chan *et al.* 2001). Tropical Storm Risk, a consortium out of the United Kingdom, also issues statistical forecasts for TC activity in the WNP. In addition, they generate a forecast of the NW Pacific accumulated cyclone energy (ACE) index, based in large part on conditions in the Niño 3.75 region (Lloyd-Hughes *et al.* 2004).

b. Dynamical

The European Centre for Medium-range Weather Forecasts (ECMWF) issues seasonal forecasts of TC activity based on coupled ocean-atmosphere models (Vitart and Stockdale 2001). The International Research Institute for Climate and Society (IRI) also generates seasonal forecasts of TC frequency, but uses a "two-tier" approach. The first step, or tier, entails employing various statistical and dynamical models to forecast future sea surface temperature (SST) conditions. Then, the predicted SSTs are used to force numerical atmospheric models. Detection algorithms are then used to identify TC-like features from amidst the coarse-resolution output fields (Camargo and Zebiak 2002).

2. Intraseasonal

Intraseasonal predictions of TC activity forecast the activity for intraseasonal periods (e.g., two weeks to two months) within an ocean basin. TC prediction at intraseasonal time scales is a comparatively new area of research, which may be attributed to increasing model resolution, improving ensemble techniques, and continuing research into intraseasonal climate oscillations. Many of the centers noted in the seasonal section are active in the intraseasonal realm as well.

a. Non-DoD Products

On the intraseasonal time scale, the Madden-Julian oscillation (MJO) presents the greatest predictive potential for empirical approaches. Useful predictive skill for statistical methods are on the order of 15 to 20 days, limited by the signal-to-noise ratio of the MJO (Camargo 2006). Frank and Roundy (2006) look beyond MJO alone and generate daily probabilities of formation using a wide variety of wave modes and climate signals. More recently, Leroy and Wheeler (2008) used logistic regression in a purely statistical prediction scheme to predict the probability of TC formation in fixed zones of the Southern Hemisphere. Their predictors include one representing a smoothed climatological cycle, two representing the propagation of MJO, and two representing the leading patterns of SST variability.

Despite the promise of the budding statistical methods, Camargo (2006) contends that "while there is much room for improvement in the skill and application of empirical/statistical methods of intra-seasonal TC prediction, the greatest hope for improvement lies with dynamical/numerical models." One of the most promising players in the dynamical field is the ECMWF and their Ensemble Prediction System (EPS).

Only a few centers create subseasonal forecasts, even fewer do so operationally and make the forecasts available freely online. The CPC is among this select group, with its operational Global Tropics Benefits/Hazards Assessment product.

Figure 2.   Example CPC Global Tropics Benefits/Hazards Assessment,
issued by CPC/NCEP on 6 August 2007 and valid 14-20 August 2007
(From http://www.cpc.noaa.gov/products/precip/CWlink/ghazards/;
accessed 12 January 2009).

Figure 2 is an example of the Global Tropics Benefits/Hazards Assessment issued by CPC. This product has both the graphical depiction (as shown in Figure 2), as well as accompanying text that explains the assessment. The description for the highlighted area in the WNP labeled region "4" states (From http://www.cpc.noaa.gov/products/precip/CWlink/ghazards/; accessed 12 January 2009):

> The potential for tropical cyclone development northeast of the Philippines and in the South China Sea. Active convection is expected in this area and with areas of anticipated weak vertical wind shear and above average SSTs the prospects for tropical cyclogenesis are increased. Confidence: Moderate.

Though this product makes strides with providing outlooks for impacts on TC activity due to the forecasted state of the tropical climate system, this product is limited by its subjective combination of forecast tools. Plans for this product include making it more objective in nature (Gottschalck *et al.* 2008).

9

b. DoD Products

As of this writing, no DoD centers are actively issuing forecasts at seasonal or intraseasonal leads for the tropics. The Joint Typhoon Warning Center (JTWC) is the DoD agency responsible for issuing tropical cyclone warnings for the Indian and Pacific Oceans. Products produced by JTWC are intended for use in decision making by operational military units, though most of these products are nowcasts and/or short-term forecasts.

The Fleet Numerical Meteorological and Oceanographic Detachment – Asheville (FNMOD) is another logical place for operators/planners to turn for information regarding future tropical activity. FNMOD does maintain a *Mariners' Worldwide Climate Guide to Tropical Storms at Sea*, which appears to be a form of climatology for each basin broken down into 10-15 day periods (depending on the time of year). This guide is certainly better than having nothing at all, but contains no information about the current or forecasted state of the climate system.

Collocated with FNMOD, is the Air Force's 14th Weather Squadron (14WS; formerly known as the Air Force Combat Climatology Center (AFCCC)). While the 14WS recently began issuing long-range forecasts for select locations (i.e., Iraq, Afghanistan), no products concerning the current or forecasted state of the tropical climate system in general, or TCs in particular, are available.

D. RESEARCH MOTIVATION AND SCOPE

1. Prior Work

The idea for taking a combined statistical-dynamical approach for predicting likely cyclogenetic regions in the tropics evolved from thesis work by Meyer (2007). Though his study did not venture into the realm of forecasting, Meyer used logistic regression to calculate the probability of TC formation in weekly five-degree latitude by five-degree longitude grid blocks as a way of quantifying the impacts of changes in the large-scale environment on the likelihood of TC formation.
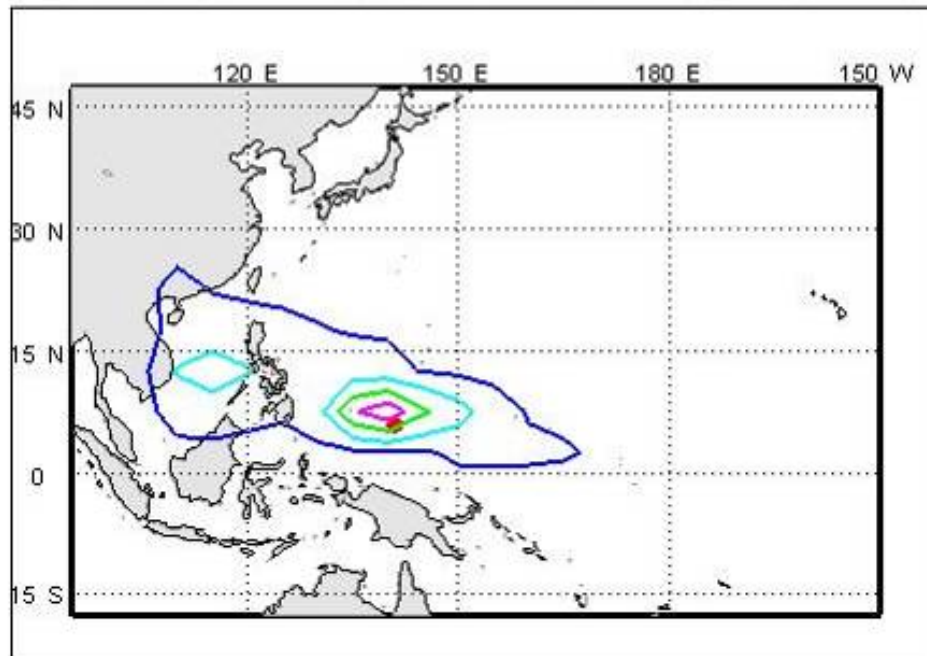
Figure 3.   Example figure generated using methods from Meyer (2007), contoured are the zero-lead hindcast probabilities of TC formation for week 26 of 2006, and the contours are at 0.01, 0.25, 0.40, and 0.55. The red dot represents a verifying TC formation location.

Figure 3 is an example plot after Meyer's work. Such plots resulted in a perceived forecast potential and a methodological basis for this thesis work.

2.   Research Questions

This thesis is an exploration into the viability of the prescribed methodology as a predictive tool at intraseasonal time scales. While many sub-questions exist, this work will primarily focus on investigating the following two questions:

1)   Can favorable regions for tropical cyclogenesis be predicted at intraseasonal lead times, by way of forcing a statistical model with available output from a GCM?

2)   Does a combined statistical-dynamical approach appear to result in skill and value beyond that which basic climatology provides?

11

As one can deduce from the preceding questions, this work will concentrate on methodology and stand as a "proof of concept." This thesis is not an attempt to advance the science of tropical dynamics; however, it may indirectly contribute to an improved understanding of, and ability to model, the large scale environmental factors that affect TC activity.

3. Thesis Organization

In order to answer the two aforementioned research questions, this work will focus on the following steps of the climate prediction process (see Figure 1): *Data Selection*, *Climate System Analysis*, *Forecast Model Development*, *Hindcast/Forecast*, and *Verification/Evaluation*.

Chapter II begins by defining the study region and time period, and then provides a brief look at the numerous data sets used in this study, as well as the methods used in developing and testing our predictive model. Also included in Chapter II is a summary of the large-scale variables thought to impact TC formation. Chapter III outlines the results of the model development and hindcasting; in addition, Chapter III demonstrates the predictive potential of the model by way of a pair of case studies. Chapter IV provides a summary of our results and conclusions, and offers suggestions for future research.

To make this thesis purposefully concise, several topics are only mentioned briefly in the text but covered more at length in the appendices. The following topics are appended to this work as references for the reader: climatology development and selection (Appendix A), calculation of variables from available output fields (Appendix B), and plots from additional case studies (Appendix C).

II.   DATA AND METHODS

A.   STUDY REGION

The western North Pacific (WNP) was chosen as the focus region for this study. Our analyses of JTWC best track TC data from 1970-2007 indicate that an average of 30 TCs—tropical depressions through super typhoons—form per year, with a standard deviation of 4.8 storms. With that, the WNP has the highest average number of TCs annually of all basins, and accounts for nearly 30% of global annual total TCs (Chan 2004). The WNP is also the only ocean basin wherein TC formation is observed throughout the year, although the majority of cyclones develop between June and November (Frank 1987). This study region was also chosen for its economic and military importance.
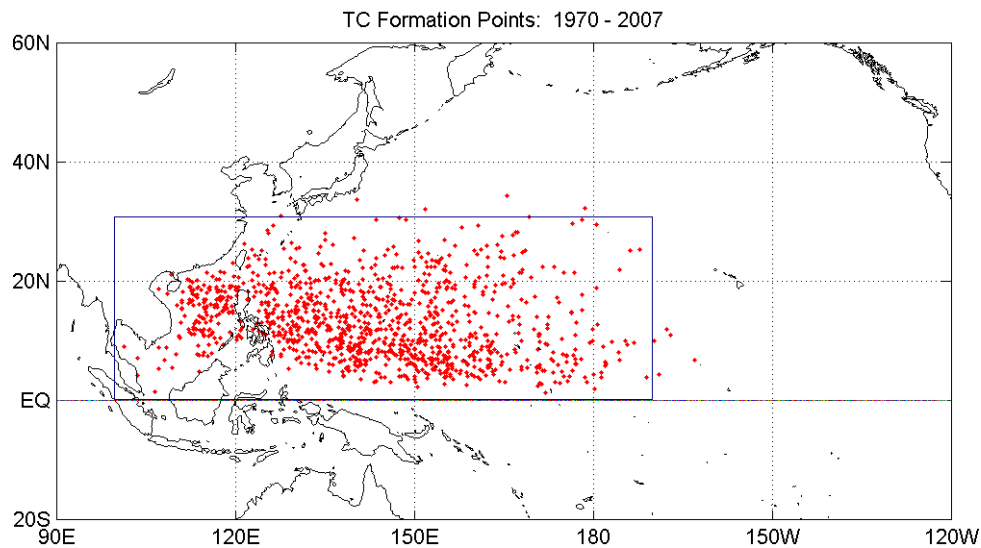
Figure 4.   Depiction of the WNP study region (outlined by the blue box) and TC formation points (red dots), constructed from JTWC WNP best track data from years 1970-2007.

The study region extends from 100°E to 190°E (170°W) and from the Equator to 30°N, as depicted in Figure 4. No literature standard exists for defining the WNP basin; however, the bounds for our study region differ no more than 10° in any one direction from the majority of other sources. One reason that

our bounds differ slightly from other studies that deal with the WNP, is that in focusing on the genesis locations there is no need to allow for the recurvature of TCs post-formation. Defining restrictive bounds also minimize the potential impacts of data dilution in our statistical verification.
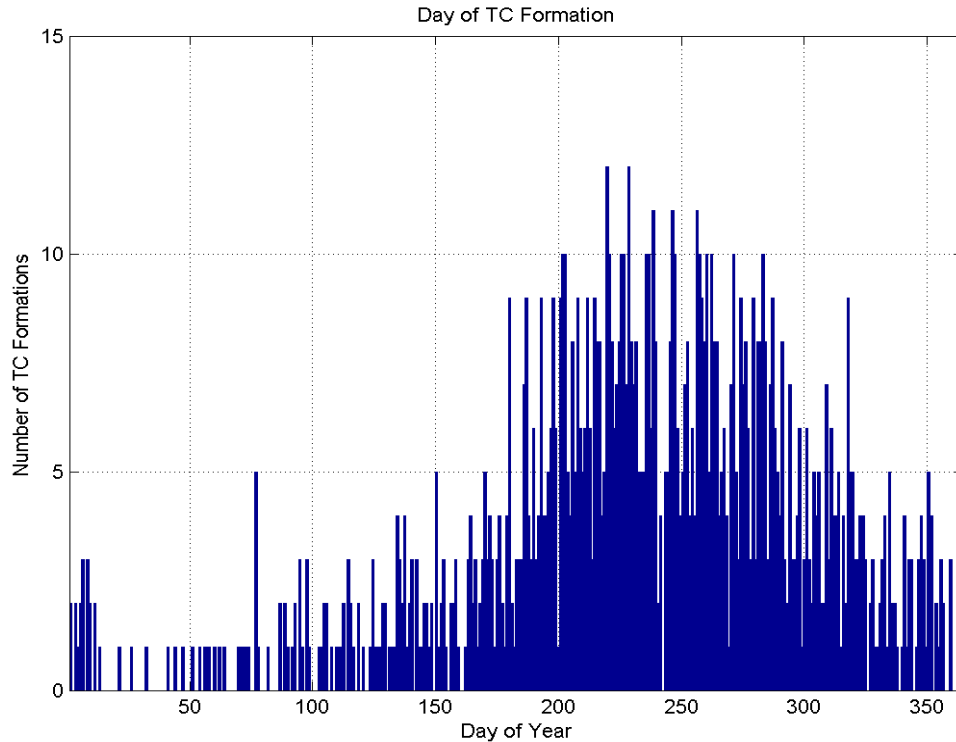
Figure 5.   Number of TC formations versus day of year, constructed with JTWC WNP best track data from years 1970-2007.

As noted earlier, TC formations are observed throughout the year in the WNP. Figure 5 displays the variation in the number of TC formations in the WNP during the period for a given Julian day. This figure also highlights the unequal distribution of formations over the course of the year. If one defines the peak formation period as June through November (as in Frank 1987), those months account for 936 of the 1122, or 83%, of the TCs; in contrast, a peak formation period of July through October (as in Sobel and Camargo 2005) accounts for 761 of the 1122, or 68%, of TC formations. Hereafter in this study the peak formation season will be defined as a period encompassing the months June through November.

Just as the temporal distribution of TC formations is not uniform throughout the year, the distribution varies spatially over the extent of the study region. Figure 6 highlights the spatial variability from grid point to grid point.
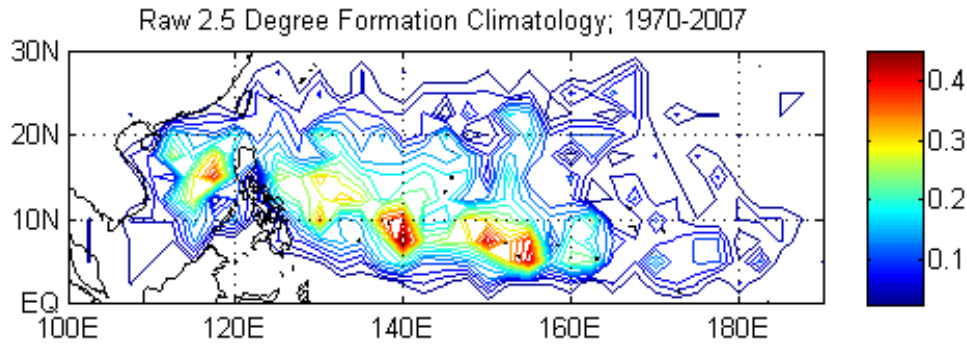
Figure 6.   Contoured probability of TC formation, constructed from binned JTWC best track data from the years 1970 - 2007. Values represent the probability that a TC will form per year in a given grid box.

Figure 6 shows what we term the "Raw 2.5 Degree Formation Climatology" that was constructed by summing the number of TC formations in the JTWC best track data for 1970-2007 within 2.5° latitude/longitude grid boxes, and then dividing the total per box by the number of years. The result is a map of the climatological, or long term mean, probability of TC formation during January-December. The probabilities are based on TC formation over the course of the entire year, so the contour values are not overly useful to most decision makers. See Appendix A for further discussion on TC formation climatology.

In this study, we attempted to develop and test a statistical-dynamical method for forecasting TC formation probabilities that is more skillful than the forecasts that could be obtained by simply using climatological TC formation probabilities (e.g., those shown in Figure 6 and discussed in Appendix A). For such a method to be more skillful than climatology, it needs to be skillful at representing climate anomalies in the large-scale environment that affect TC formations. Thus, it is useful to review the general conditions that influence TC formations in the WNP during the peak formation season. Figure 7 shows the

15

main low-level circulation features that characterize summer Conditions in the WNP. Note in this figure the band of convergent and cyclonic flow marked by the dashed line. This band is often labeled the monsoon trough (Ramage 1995), so named because of its association with summertime monsoonal flow in the region.
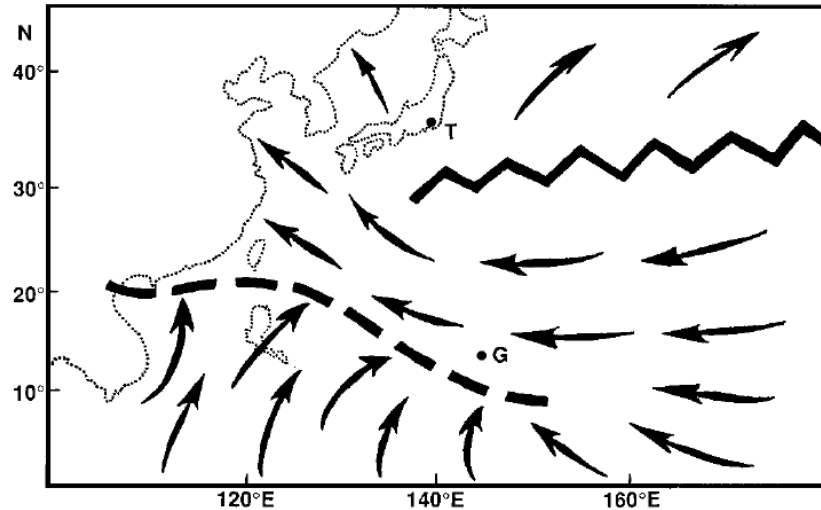
Figure 7.   Schematic depiction of summertime low-level flow over the WNP. The dashed line marks the monsoon trough and the zig-zag line indicates the mean ridge axis (From: Figure 1 (a) Lander 1996).

The monsoon trough is associated with the development of most TCs in the WNP (Xue and Neuman 1984), due to the predominantly favorable environmental factors (as described in Section II.C.). This is also indicated by the co-location of the high probabilities in Figure 6 and the climatological position of the monsoon trough in Figure 7. The position of the monsoon trough experiences normal seasonal variations through the year, as well as spatial and temporal deviations from its normal seasonal cycle. One example of a significant deviation is labeled a reverse-oriented monsoon trough, when the convergence zone extends from southwest (SW) to northeast (NE) over the WNP (Chu 2004).

B.   DATA SETS AND SOURCES

The structure, format, and availability of the primary data sets used in this thesis are described in this section. The inquisitive reader is directed to the cited

references for more information on each of these data sources. All of the data used in this thesis are freely and publically available online.

1.   JTWC Best Track

The JTWC maintains an archive of tropical cyclone data for the WNP. At a minimum, these "best track" files contain the latitude and longitude of the TC center location at six-hour intervals. These data are used for both model construction and verification in this study.

The best track archive includes all TCs identified by the JTWC, and even includes a number of storms that were determined to be of sufficient strength for classification as TCs well after the storms occurred. The aforementioned TC numbers in Section II.A. are higher than those in some prior studies that analyzed only storms that were of tropical storm intensity or greater.

The JTWC data set is not without controversy. Several researchers have noted that variations in analysis procedures, as well as changes in observational tools (satellite, aircraft, etc.) over the years, may compromise the overall consistency of the best-track [as written can be confusing] records. Furthermore, Wu *et al.* (2006) cite notable differences in the track information from JTWC vice what is available from the Regional Specialized Meteorological Centre Tokyo; among the reasons for the discrepancies are differences in the time period over which winds were averaged, and differences in each center's intensity-estimation techniques. However, efforts have been made, and are continuing, to minimize the discrepancies within the JTWC best track archive and between the JTWC archive and other sources for historical TC information (Chu *et al.* 2002). We determined that the potential problems with the JTWC best track data were not likely to significantly influence our study results.

2.   NCEP Reanalyses

Global objective analyses that assimilate numerous observational data sources with model output and span many years provide an increased ability to

investigate the physical processes that surround TC development. Prior to the introduction of these so-called reanalyses, it was difficult to consistently investigate subtle variations in the climate system. We used two reanalysis data sets: (1) the NCEP/National Center for Atmospheric Research (NCAR) Reanalysis Projects (Kalnay *et al.* 1996; Kistler *et al.* 2001); and (2) the NCEP/Department of Energy (DOE) Atmospheric Model Intercomparison Project–II (AMIP–II) Reanalysis (Kanamitsu *et al.* 2002).

The NCEP/NCAR Reanalysis Projects data set (hereafter referred to as R1), and the NCEP/DOE AMIP–II Reanalysis data set (hereafter referred to as R2) are both based on assimilating data using a fixed model at T62L28 resolution. Though both reanalyses use the same raw observational data, the R2 project attempts to correct some of the known errors in the R1 reanalysis; please review the cited publications for more details.

Though other variables were tested, the final atmospheric variables used in the construction of our regression model (see Section III.A.) are all manually derived from "A" variables. Kalnay *et al.* (1996) note that an "A indicates that the analysis variable is strongly influenced by observed data and, hence, it is in the most reliable class."

For the purposes of this study, we used daily mean fields interpolated to a 2.5° global grid. R2 was the primary dataset from which variables were derived, but R1 data was used in this research for verification and as a way to test the model's sensitivity to a specific reanalysis system.

3. NOAA OISST

Just as the atmospheric reanalyses are invaluable tools in developing empirical prediction methods, so too is a quality database of SSTs. The SST data used in developing our statistical model is the National Oceanic and Atmospheric Administration (NOAA) optimum interpolation (OI) SST analysis version 2. SST values from this dataset are available in weekly means from 1981 to present, at one degree latitude by one degree longitude horizontal

resolution on a global grid. OISST data combine in situ and satellite-derived SST measurements with biases adjustments (Reynolds *et al.* 2002).

In order to match our R1 and R2 data, the OISST fields were extrapolated from one degree resolution to 2.5° horizontal resolution and interpolated to daily values.

4.   NCEP CFS

The NCEP Climate Forecast System (CFS) is a one-tier fully coupled ocean-land-atmosphere dynamical assimilation and prediction system, which has been operational at NCEP since August 2004 (Saha *et al.* 2006). The atmospheric component of this coupled system is a reduced-resolution version of the more-familiar 2003 operational NCEP Global Forecast System (GFS), with T62L64 resolution (equivalent to ~200 km Gaussian grid); the initial conditions are obtained from the operational R2 (Saha 2008). This atmospheric component is coupled once per day, without flux correction, with the Geophysical Fluid Dynamics Laboratory (GFDL) Modular Ocean Model version 3 (MOM3). Four CFS runs are executed daily, with integrations out to nine months. Of the two runs initialized at 00Z and at 12Z, each has the same initial oceanic state, but a slightly perturbed atmospheric state. The initial conditions for these runs are one day old for both the atmospheric and oceanic variables (Saha 2008).

One appealing feature of the CFS is the availability of hindcast and bias correction fields. As noted in Section I.B.3.b., GCMs are often plagued by systematic errors. We are able to remove much of this systematic error, namely climate drift, by employing the forecast climatology that is available for all forecast lead times and the daily observed climatology. Such corrective fields are only available for a subset of variables.

From the available fields, in gridded binary format, we manually extracted daily SSTs at one-degree global coverage, daily atmospheric variables converted from their native Gaussian grid to a 2.5° latitude/longitude grid, and the appropriate bias correction fields. Once the variables were bias corrected and on

the same latitude/longitude grid, we used the SSTs and atmospheric variables to force a statistical model to provide a probability of TC formation at every grid point.

With numerous GCMs being used in climate science, one may wonder why we chose the CFS. In addition to being freely and publically available, the CFS is the first operational, dynamical model with predictive skill on par with statistical methods used at CPC (Saha *et al.* 2006). Saha *et al.* (2006) also notes that the "Niño-3.4 SST is probably the single most predictable entity [within the CFS]." Though the Niño-3.4 region is just outside of our WNP study region, we were motivated by the relative high skill of the CFS in the Pacific basin, especially since prior studies have shown that SST variability in the Niño-3.4 region is closely related to variations in the large scale environmental factors that influence TC formations in the WNP (Ford 2000; Chan 2004). In addition to the perceived skill, the CFS also offers a rudimentary ensemble construct. With two runs executed twice daily, the potential exists for a four-run ensemble with perturbed initial conditions. One could increase the number of ensemble members by incorporating runs from other days as well. The intention for the ensemble approach is to smooth out the differences between the runs in order to bring out the more predictable elements and, thereby, lead to enhanced predictive skill on average.

C. VARIABLES OF INTEREST

The existence of a set of large-scale environmental factors (LSEFs) that are influential in TC formation has been well documented over the last half century. Gray (1968, 1975, 1979) outlined a physical climatology of tropical cyclogenesis relative to six, so-called genesis parameters. Other authors vary the list of these parameters, or factors, slightly and at times condense the list (e.g., low-level relative vorticity and the Coriolis parameter may be combined into a single absolute vorticity term). Regardless of the specific list of LSEFs one chooses, the physical properties are arguably quite similar.

The LSEFs may each be necessary for tropical cyclogenesis, but a combination of these parameters alone may not be sufficient to diagnose or predict the transition from a convective disturbance into an organized TC (Frank 1987). This idea of "necessary but not sufficient" suggests that the large-scale environment may not be solely responsible for determining whether a TC forms or not. Frank (2006) contends that "individual storms form infrequently and sporadically within large areas of favorable environmental conditions due to the effects of local flow perturbations." Such a mesoscale trigger and/or perturbation in the local flow may be required to instigate tropical cyclogenesis, but abundant research supports the profound role of large-scale external forcing as a determining factor in tropical cyclogenesis (Briegel and Frank 1997).

An underlying goal of this study is to predict favorable regions for tropical cyclogenesis at intraseasonal lead times, by way of forcing a statistical model with available output from a GCM. In our case, we use the NCEP CFS as our dynamical GCM, from which not all the LSEFs are available. To remedy this, we had to accomplish two tasks. First, we had to consider other parameters that are similar to the LSEFs described in the literature and may represent the same processes, and for which intraseasonal forecasts are readily available from the CFS. Second, we had to calculate additional variables based on available model output fields. For variables requiring spatial derivatives, we employed second order centered finite differencing; see Appendix B for more information regarding the calculation of additional variables from available fields.

The genesis parameters, as proposed by Gray (1975), can be subdivided into thermodynamic and dynamic parameters. What follows is a brief look at these parameters, as well as some of the additional variables we considered. For the sake of brevity, not all of the variables that we investigated in our research are presented here. For more information on LSEFs and how they relate to TC development, the reader is directed to any of the plethora of articles and books on the subject (e.g., Gray 1975; Frank 1987).

1. Thermodynamic Parameters

Research suggests that sufficiently high SSTs and moisture in the mid-troposphere are important for only for TC formation, but also for tropical deep convection. These thermodynamic variables are often favorable for TC development over much of the tropical Pacific during much of the year (see Chapter III).

a. *Sea Surface Temperatures*

Frank (1987) contends that the high frequency of TC formation in the WNP, as compared to other ocean basins, is due, in part, to an expansive area of warm water (e.g., water warmer than 26°C).
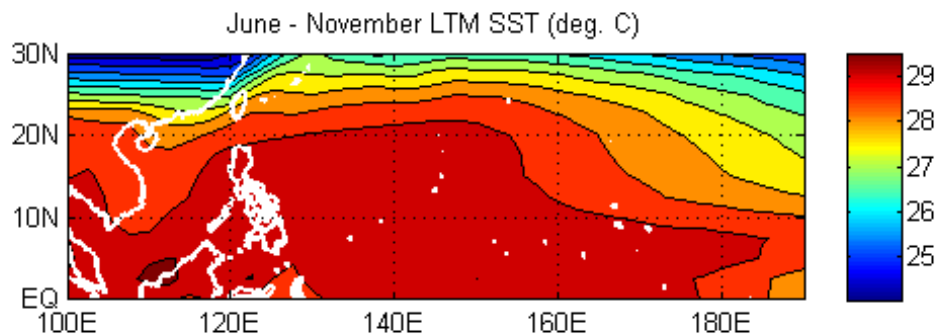
Figure 8.   Average June – November SST (in °C) conditions over the WNP for the period 1982–2000, plotted from NOAA OISST data interpolated to 2.5° horizontal resolution.

Figure 8 depicts the average SST conditions over the WNP during the peak formation season. Such a large expanse of warm water has led some researchers to conclude that SSTs may not be a primary factor affecting formation in the tropical Pacific (Chan 2004), as the temperatures are often sufficiently warm (e.g., greater than 26°C).
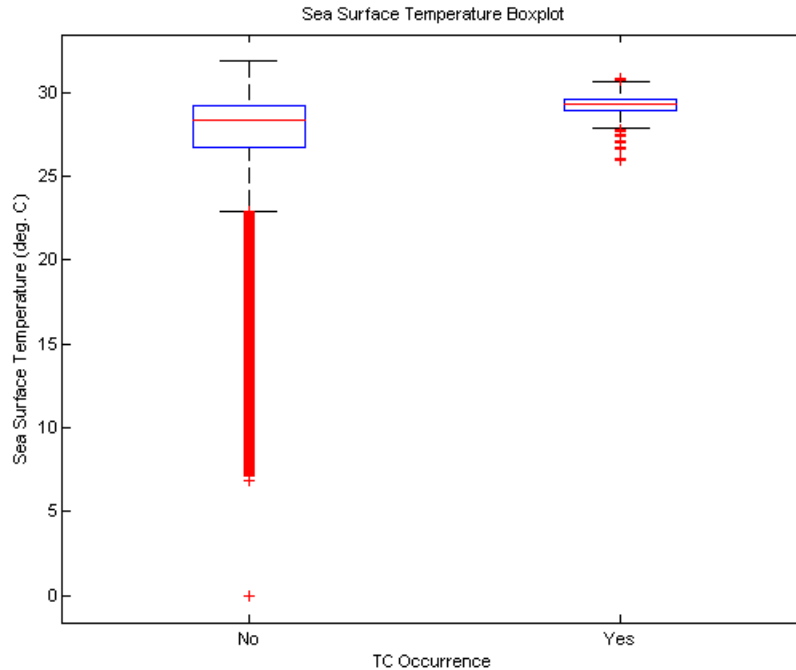
Figure 9.   Box plots of grid values of SST (in °C) grouped according to whether a TC formed in that day-grid box (indicated by Yes on the horizontal axis) or did not form in that box (indicated by No). The box height encompasses 50% of the SST data points, the whiskers (dashed lines) extend to include ~99% of the SST data points, and SST data that fell outside the whiskers (outliers) are indicated by the red "+" symbols. Constructed from NOAA OISST data with TC occurrences from the JTWC best track archive for the January–December period of 1982–2006.

The Box plots in Figure 9 separate the SSTs at 2.5° latitude x 2.5° longitude by day grid blocks according to whether a TC formed in the grid block ("Yes") or not ("No"). The comparatively constrained appearance of the "Yes" boxplot indicates that TCs seem to form in conjunction with a small range of SSTs in the upper 20s and low 30s degrees Celsius. Numerous sources, such as Frank (2006) and Meyer (2007), note that SSTs must meet or exceed 26.5°C to favorably support TC formation. These Box plots support that, and suggest that a threshold for the WNP may be even more restrictive (i.e., ≥ 28°C). Physical reasoning and the sort of relationships shown in Figure 9 indicate that

SST and TC formation probability at a given location should be directly and positively related to each other, if all other factors that influence TC formation are favorable and held constant.

b. Humidity

Early research on the climatologies of WNP TCs indicates that TCs only form in regions where seasonally averaged values of mid-tropospheric moisture are high. The physical explanation is that moist air in the middle troposphere is more conducive to deep convection and vertical coupling of the atmosphere (Gray 1975).
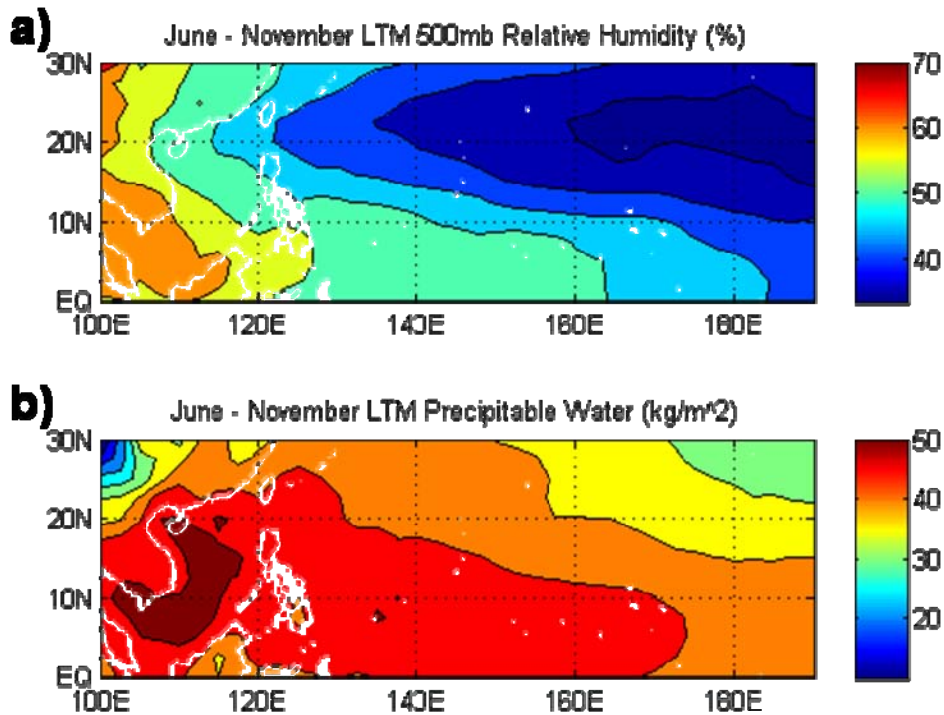
Figure 10. Average June – November a) 500mb relative humidity (in %) and b) precipitable water (in kg m^{-2}) conditions over the WNP for the period 1971–2000, plotted from R1 data.

Mid-tropospheric humidity variables are not available from the CFS. So we looked to precipitable water as a viable alternative to represent the

available environmental moisture. Figure 10 shows average conditions during the peak formation period of mid-level relative humidity and total-column precipitable water. Though the units are not directly comparable, one should note the spatial agreement of the location of high humidities to the location of greatest precipitable water. As with SST, physical reasoning indicates that, all other factors being favorable and constant, an increase in atmospheric moisture content should lead to an increase in the probability of TC formation. We confirmed this with moisture-TC formation Box plots (not shown) similar to those in Figure 9.

2.   Dynamic Parameters

As noted earlier, favorable thermodynamic conditions are often present over expansive swaths of the WNP much of the year; therefore, dynamic parameters are thought to be responsible for determining whether a TC will form in a region that is thermodynamically favorable for TC formation. Gray (1975) noted the comparatively small spatial and temporal scales over which a disturbance will interact with its surrounding dynamic environment. These subtle interactions at smaller scales provide the motivation to use data at 2.5° resolution and daily time steps for this study, versus the previous work by Meyer (2007) that used 5° data at weekly time steps.

a.   Shear

Numerous studies have found that large values of vertical wind shear in the large-scale environment tend to suppress TC formations. Though various definitions exist in literature, the most common measure of vertical wind shear is the mean vector wind at 850 mb subtracted from the mean vector wind at 200 mb. Such a calculation results in a magnitude and direction, though the magnitude alone is used in this work. Near the monsoon trough axis, vertical wind shear is minimal, allowing deep convection to be sustained and increasing the likelihood of TC formation in the region (Chan 2004).
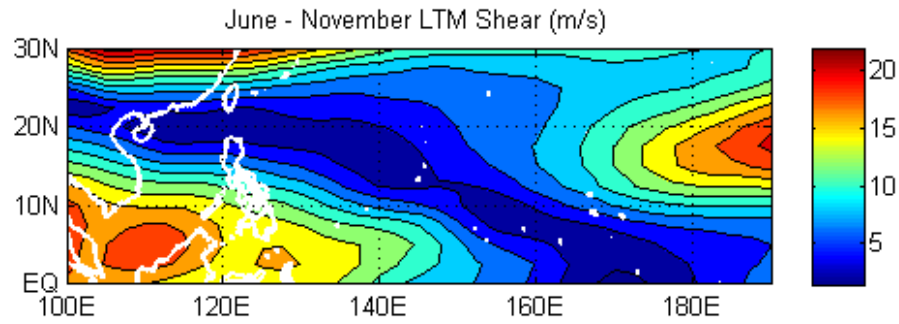
Figure 11.   Average June – November magnitude of vertical wind shear (in m s^{-1}) over the WNP for the period 1971–2000, derived from R1 data.

Figure 11 displays the mean magnitude of vertical wind shear over the WNP during the peak formation season. The reader should note the co-location of the low mean shear pattern (Figure 11), the climatological monsoon trough (Figure 7), and the highest climatological probabilities of formation (Figure 6). The Box plots in Figure 12 solidify the relationship between the magnitude of vertical wind shear and probability of TC formation—TCs form in regions of low environmental wind shear.
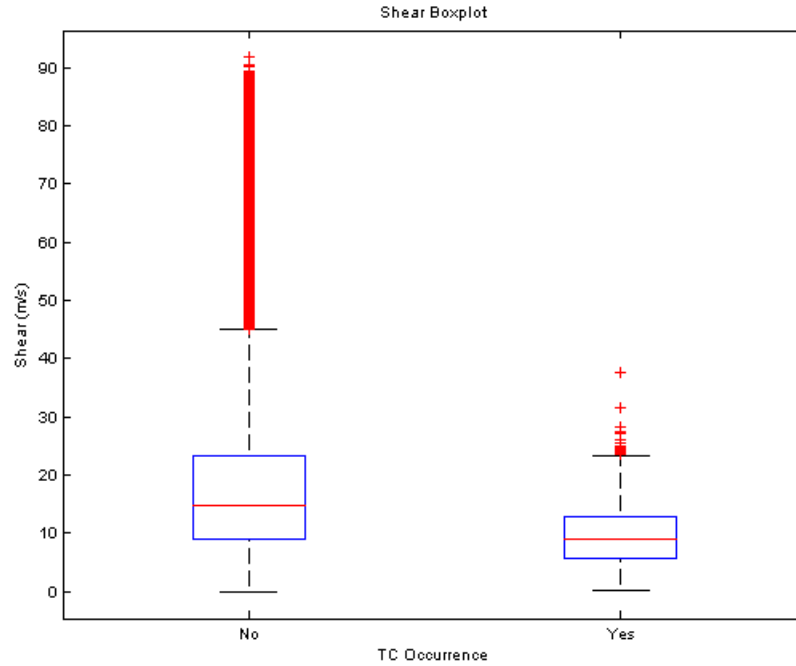
Figure 12.   Box plots of grid values of the magnitude of the mean vertical wind shear (in m s^{-1}) grouped according to whether a TC formed in that day-grid box. The box height encompasses 50% of the data points, the whiskers (dashed lines) extend to include ~99% of the data points, and points that fall outside the whiskers (outliers) are indicated by the red "+" symbols. Constructed from R2 data with TC occurrences from the JTWC best track archive for the January–December period of 1982–2006.

b.   *Upward Vertical Motion/Velocity*

During the peak formation season in the WNP, warm waters lie just to the west of the tropical upper tropospheric trough (TUTT) and near the entrance region of the climatological tropical easterly jet.   Both features contribute to regions of upper-level divergence and/or persistent upward vertical motion, both shown to be favorable for cyclogenesis (Frank 1987).

27
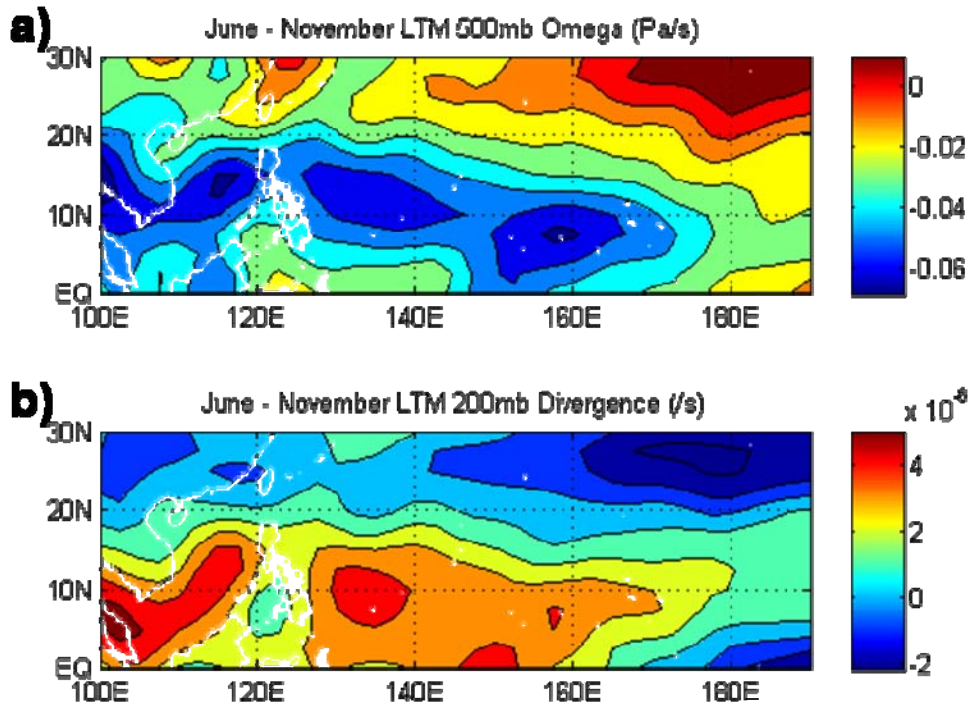
Figure 13.   Average June – November a) 500mb omega (in Pa s^{-1}) and b) 200mb divergence (in s^{-1}) conditions over the WNP for the period 1971–2000, derived from R1 data.

Just as with the moisture variables, the availability of variables from the CFS influenced our choice of the variables to use to represent vertical motion in our statistical model. A variable directly representing vertical motion is not readily available from the CFS at daily time steps, thus we opted to test 200 mb divergence (calculated from the 200 mb zonal and meridional wind fields; see Appendix B for more information regarding these calculations). Figure 13 depicts the peak season averages of 500 mb omega and 200 mb divergence.
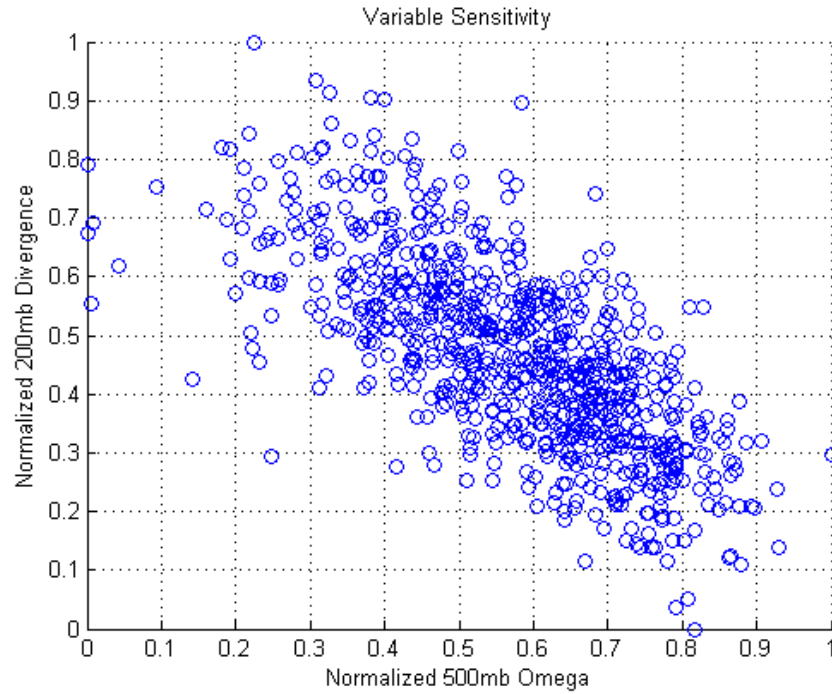
Figure 14.   Normalized January–December 500 mb omega vs. 200 mb divergence scatter plot, displaying sensitivity between the variables, constructed from R2 data for the period 1982–2006.

Though the spatial patterns in Figure 13 suggest that upper-level divergence may be a suitable alternative to the more-traditional omega, we sought to test the sensitivity of these two variables. Figure 14 is a scatter plot of normalized divergence versus omega. Knowing the opposing sign conventions, the negative slope to the elongated cluster suggests that the variables are reasonably correlated, and that divergence may be a suitable replacement for omega. The box plots in Figure 15 indicate that TCs form in the WNP when 200 mb divergence is weak, but skewed towards divergent outflow aloft.
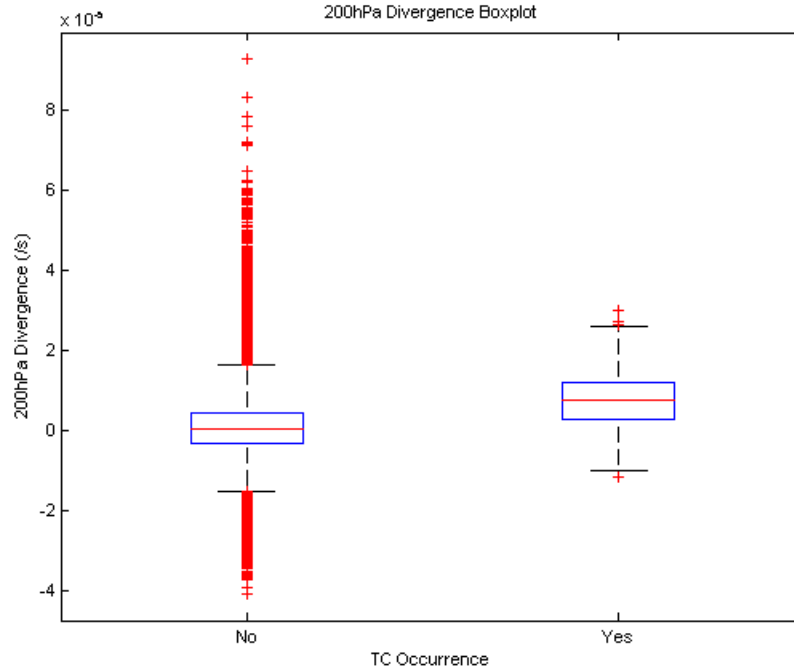
Figure 15.   Box plots of grid values of upper-level divergence (in s[-1]) grouped according to whether a TC formed in that day-grid box. The box height encompasses 50% of the data points, the whiskers (dashed lines) extend to include ~99% of the data points, and points that fall outside the whiskers (outliers) are indicated by the red "+" symbols. Constructed from R2 data with TC occurrences from the JTWC best track archive for the January–December period of 1982–2006.

c.   *Vorticity*

The final genesis parameter is vorticity in the lower troposphere. As their behavior is different, we chose to investigate relative vorticity and planetary vorticity—as represented by the Coriolis parameter *f*—separately, as well as combined into a single low-level absolute vorticity term. Frank (1987) notes that relative vorticity may result from several sources, including from the intensification of monsoon trough circulations, waves in the easterlies, or along frontal zones that extend into the tropics.

30
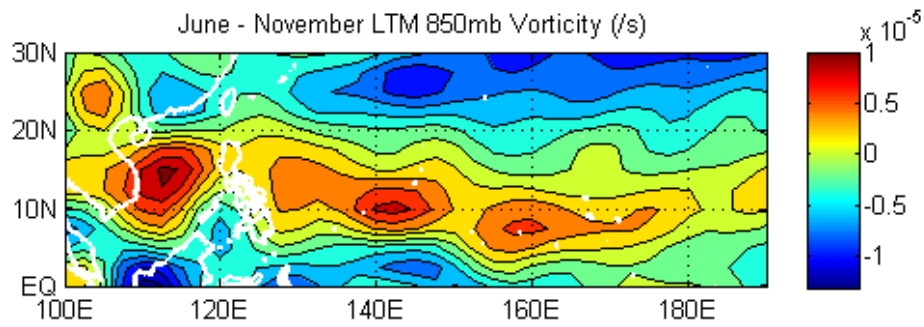
Figure 16. Average June – November 850 mb relative vorticity (in s^{-1}) conditions over the WNP for the period 1971–2000, derived from R1 data.

The spatial pattern of Figure 16 should be familiar to the reader by this point, with the greatest average values of 850 mb relative vorticity in spatial agreement with the monsoon trough figure described earlier in this chapter. Of the three mechanisms noted by Frank that intensify relative vorticity, only the monsoon trough is persistent enough to be clearly represented in this six-month composite.
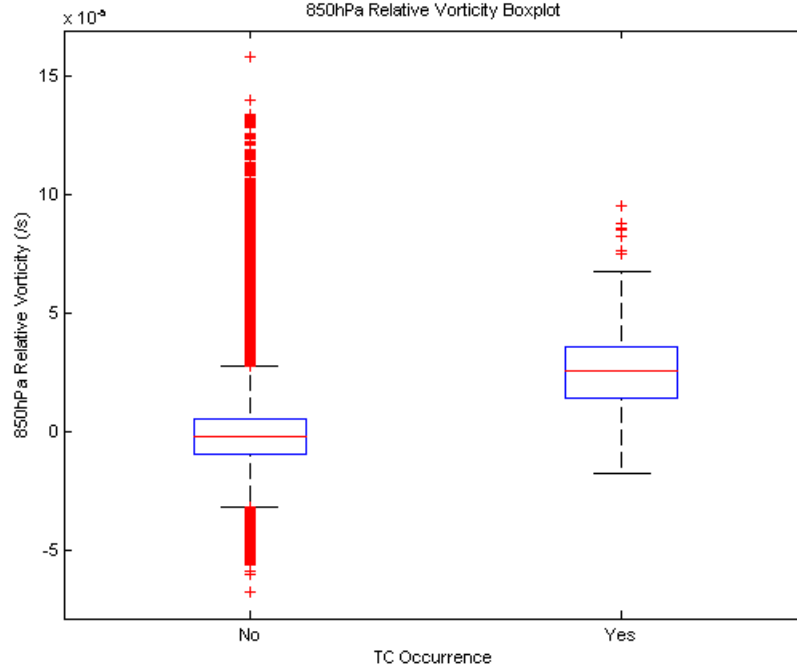
Figure 17. Box plots of grid values of low-level relative vorticity (in s[-1]) grouped according to whether a TC formed in that day-grid box. The box height encompasses 50% of the data points, the whiskers (dashed lines) extend to include ~99% of the data points, and points that fall outside the whiskers (outliers) are indicated by the red "+" symbols. Constructed from R2 data with TC occurrences from the JTWC best track archive for the January–December period of 1982–2006.

The box plots in Figure 17 support what many previous authors have found, that weak to positive low-level relative vorticity relates to an increase in TC formation probability. Not shown are similar sets of plots for planetary vorticity and absolute vorticity. In agreement with previous studies, we find that Coriolis parameter has a positive relationship with TC formation, and that the vast majority of TCs form several degrees or more from the equator.

3. Model Variable Selection

Several of the variables that are either directly available from the CFS or are easily derived from CFS output represent similar large-scale environmental conditions and processes. Thus, to represent, for example, vertical motion, we

had to choose between 200 mb divergence and 200 mb relative vorticity, since both of these variables represent vertical motion (the former does so explicitly and the latter does so implicitly). In making this sort of choice, we favored variables that:

1) have physically plausible relationships to TC formation,

2) are readily available directly from the CFS,

3) or are easily derivable from available CFS variables, and

4) are relatively skillfully predicted by the CFS.

4.   Climate Oscillations and Model Variable Relationships

Numerous prior studies describe the intraseasonal and interannual variability of TC formation, especially as they relate to climate oscillations (e.g., Ford 2000; Chan 2004). Of the climate oscillations that impact TC activity, the most often investigated are El Niño and La Niña (ENLN). ENLN are anomalous oscillations of the tropical atmosphere and ocean that can alter the large-scale environment in ways that influence TC formations, intensities, and tracks (e.g., Ford 2000). Wang and Chan (2002) offer a good illustration of how ENLN can influence TC activity. They note that during the latter months of an El Niño year, low-level anomalous westerlies encompass much of the WNP. These anomalous winds lead to positive relative vorticity anomalies in the region, which provide a favorable environment for TC formation that is both later in the year than normal, and displaced farther to the east.

In addition to ENLN, much focus has been directed at the influence of intraseasonal tropical oscillations; for example, investigations into the effects of the MJO on TC formation in the WNP. Frank and Roundy (2006) show that when MJO activity is high, TCs are more likely to form in the convectively active portions of the MJOs. As with ENLN, it is likely that the impacts of intraseasonal variations on TCs occur mainly via alterations of the LSEFs.

Though climate oscillations and their impacts on TC activity are beyond the scope of this thesis, these brief notes are included because of their relationship to the subject of this thesis: intraseasonal prediction of tropical cyclogenesis. With changes in the large-scale circulation in the tropics, the thermodynamic and/or dynamic genesis parameters may be modified; these modifications, in turn, alter the TC activity. The idea is that if oscillations (ENLN, MJO, etc.) that have been shown to impact TC formation are skillfully predicted by the CFS, including the variations in the LSEFs associated with these climate oscillations, then a statistical-dynamical method based on the relationships between the LSEFs and TC formations can be skillful regardless of the oscillatory state of the climate system.

D. PROBABILISTIC EQUATION DEVELOPMENT

1. Logistic Regression

Logistic regression, also referred to as logit regression, is an appropriate statistical tool for this application. Given a combination of independent variables, logistic regression provides the probability of occurrence of the dependant, binary variable. Let p_F be the probability of TC formation at a given grid point for a given time period (one day, in this study); since p_F is a probability it is bounded by zero and one.

The natural logarithm of the odds ratio of the probability is called *logit*, where:

$$Logit = \ln\left(\frac{p_F}{1 - p_F}\right)$$

We used the statistical analysis software *S-Plus* to find the optimal values of the intercept b_0 and the coefficients b_k for each contributing variable x_k, such that:

$$\ln\left(\frac{p_F}{1 - p_F}\right) = b_0 + b_1 x_1 + \ldots + b_k x_k$$

Then the probability of TC formation may be calculated based on a linear combination of the optimal value coefficients and explanatory variables:

$$p_F = \frac{e^{(b_0 + b_1 x_1 + \ldots + b_k x_k)}}{1 + e^{(b_0 + b_1 x_1 + \ldots + b_k x_k)}}$$

For more information regarding logistic regression, the reader is directed towards Wilks (2006), Devore (200), or most any college-level statistics text.

a.   *Dependant Variable*

Within the framework of logistic regression, TC formation at a given grid point is modeled as a binary response variable and is expressed as either zero (no formation) or one (formation observed).   As such, this approach provides the model with no information as to the strength or duration of the storm. We feel that this approach remains viable despite this limitation. McBride (1981) comments, with respect to compositing data, that "the averaging process smears out the diversity between different systems and enhances features in common" As such, we hope our method is applicable over more scenarios, as a result of including a wide variety of storms in the training of the regression model.

b.   *Independent Variables*

Technically, the approach we are using is multivariate logistic regression, as we are allowing multiple independent, or explanatory, variables to contribute to the probability. Ideally, all the independent variables in a multiple logistic regression analysis, would be just that, *independent*. As noted earlier, the LSEFs are inter-related in a linked ocean-atmosphere system, thus the variables will all have some degree of correlation with each other. This lack of true independence will allow combinations of variables to negate the need for others. For example, high relative humidity often occurs in regions of warm SST, positive low-level vorticity, and upward vertical motion. Therefore, if the latter three variables favorably exist, the addition of a humidity variable may not be required to ascertain the favorability of the large-scale environment.

2. Model Training

Statistical methods, such as logistic regression, predict the response to variables based on a historical record; therefore, one must reach a balance between the length and the quality of the climate record. For this reason, we utilize data only from the satellite era. In developing such statistical tools, one must also assume a degree of stationarity of the climate system, which we know is not entirely the case.

We used R2 and OISST data to train our statistical model; the availability of both of those datasets limited us to the years 1982 – 2006, inclusive. Various forms of the model were tested, some of which were trained over the entire year, others were trained over just the peak formation season.

When a model is trained over all months for the 25-year period, the size of the dataset becomes somewhat cumbersome [13 (latitude grid boxes in WNP) x 37 (longitude grid boxes) x 365 (days, excluding leap days) x 25 (years) = 4,389,125 day grid points per variable!]. One approach for the reducing the needed dataset is to include all the points wherein a TC was observed, but only include a portion of the remaining "non-occurrence" points. We refer to the data from all the day grid points at which a TC was not observed as non-TC information (NTCI). Various forms of the model were tested using various amounts (as percentages) of NTCI.

3. Model Selection

We made use of a series of tests to ensure our model was statistically sound and to assess the overall goodness of fit. Our goal was to develop a model that is physically defensible, stable, and reliable. The following tools are among those we relied upon to select our model from the numerous forms of the model that we tested.

a.   Akaike Information Criterion

The Akaike Information Criterion (AIC) is a goodness-of-fit measure that seeks to find a balance between model fit and complexity. The model complexity is handled by imposing a penalty for the number of terms included in the equation. A lower AIC suggests a better-fitting model. Refer to Wilks (2006) or Burnham and Anderson (2002) for more information concerning AIC.

b.   Deviance

We also used the residual deviance numbers to compare models. In a simplistic manner, the amount of deviance explained by a model suggests how much of the variability is accounted for by the combination of the included terms of the model. The logic for this test being that the greater the goodness of fit of a model, the lower the residual deviance associated with that model.

c.   Stability

To assess whether our model contains too many explanatory variables, often referred to in statistics as being *overfit*, we examined how much the variable coefficients vary when the model is constructed over different training periods. A model is said to be more stable, and having a lower probability of being overfit, the less the coefficients vary when derived from different training periods.

d.   Physical Plausibility

A viable model must indicate relationships that fit the conceptual models identified in prior studies and noted in the section on LSEFs. For example, we expect SSTs to have a positive relationship with the likelihood of TC formation. A model that suggests a negative relationship between SST and the likelihood of TC formation would be suspect. In our research, we encountered models that suggested humidity and the probability of TC formation are inversely related; such a negative coefficient is not physically defensible and likely results from multicollinearity between the LSEFs included in the model.   This

multicollinearity may result from a lack of independence among predictor variables, in this case between humidity and the other variables included in the regression equation (e.g., SST, divergence; see also Devore 2000).

4.   Model Verification

We made use of several key metrics for assessing the skill and value of our model when the model was used to conduct multi-year zero-lead hindcasting and non-zero lead hindcasting case studies. Such metrics include the number of hits and misses, the Brier score (BS) and Brier skill score (BSS), the reliability diagram, the relative operating characteristic (ROC) curve, and the economic value diagram (EVD).

5.   Motivations for a Probabilistic Forecast

Among the reasons for selecting multivariate logistic regression as the statistical tool by which to develop a statistical-dynamical prediction method are the potential benefits of producing probabilistic forecasts. In order to reap these benefits, the probabilities must represent true probabilities. The probabilities may not be true probabilities if the model is ill constructed. Among the potential benefits of probabilistic forecasts, is that customers may use the true probabilities to compare to the risk profile of a given mission and, thereby adjust their decision making. Also, such probabilistic output allows for a relatively straightforward conversion to anomaly-type forecasts that may be useful deliverable for many decision makers.

E.   SUMMARY OF PREDICTION METHOD

Figure 18 is a schematic of the process involved in creating and operationalizing the prediction process used in this thesis. This process is a combined statistical-dynamical one, wherein one uses a numerical model to force a statistical model to generate ensemble based, probabilistic, intraseasonal predictions of TC formations.
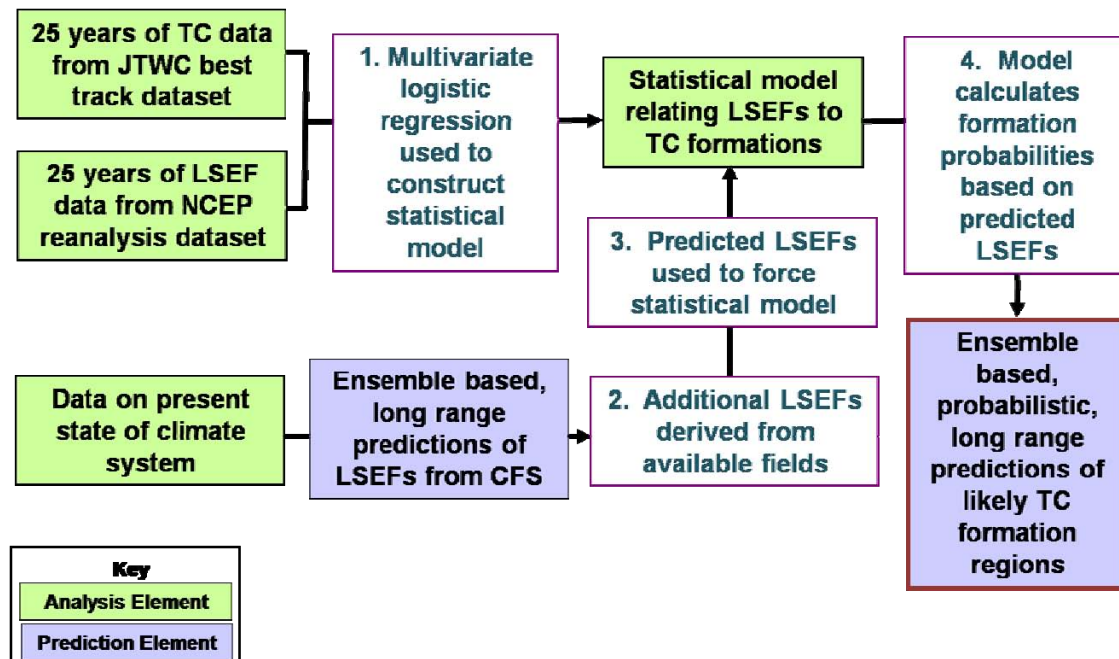
Figure 18.   Depiction of the process for generating intraseasonal predictions of tropical cyclogenesis.

THIS PAGE INTENTIONALLY LEFT BLANK

III.   RESULTS

A.   REGRESSION MODEL

The underlying goal in generating a regression model, is to construct an equation for the probability of TC formation for individual day grid points based on the values of corresponding atmospheric and oceanic variables. Multivariate logistic regression was used to find optimal values of the intercept b_0 and the coefficients b_k for each contributing variable x_k, such that the probability of TC formation p_F at any given day grid point is:

$$p_F = \frac{e^{(b_0+b_1x_1+...+b_6x_6)}}{1+e^{(b_0+b_1x_1+...+b_6x_6)}}$$

Table 1 below lists the variables and coefficients that are included in the model we chose. The paragraphs that follow highlight some of key details as to how this model was constructed and why it was chosen from amongst the many model permutations tested.

Table 1.   Variable coefficients and related statistics, generated over a June-November training period for the years 1982-2006.

	Variable		Regression Coefficient	Significance Rank	Standard Error	t Value
-	(Intercept)	b_0	-27.41179	-	1.81639	-15.09
x_1	850mb Rel. Vorticity	b_1	167645.1	1	7074.82	23.69
x_2	850mb Rel. Vorticity^2	b_2	-1679802094.0	2	112033900	-14.99
x_3	SST	b_3	0.6567593	3	0.06061	10.83
x_4	Vertical Wind Shear	b_4	-0.05990173	4	0.00687	-8.71
x_5	Coriolis Parameter	b_5	15861.34	5	2646.58	5.99
x_6	200 mb Divergence	b_6	24729.49	6	6152.83	4.01

As one can see, the variables selected for inclusion in the model include: 850 mb relative vorticity, 850 mb relative vorticity squared, SST, vertical wind shear, Coriolis, and 200 mb divergence. The magnitude of the regression coefficients are not indicative of the relative importance of that term, but are

reflections of the units of the variable. In addition, the units of the coefficients are the inverse of the units of the associated variable, thus the linear combination of the variables and their coefficients is unitless. One may also note what is not included in this equation that appears in the original listing of genesis parameters by Gray (1975), that being a term representing mid-level humidity. The results from statistical testing indicated a significant degree of multicollinearity between such a moisture variable and the other terms of the equation. The exclusion of a moisture variable is not to say it is not important for the formation of TCs, but rather that the combination of the other variables (cyclonic low-level circulation over warm ocean water, etc.) act as a suitable proxy for a moisture variable.

Of the included variables, SST is the only one directly available from the CFS. The Coriolis parameter is a function of latitude, and thus requires no model input. The remaining variables are all calculated from the 200 mb and 850 mb zonal and meridional winds, which are available from the CFS. Despite the need for these calculations, we feel that these variables are likely more predictable within the CFS than other variables that are more dependent upon parameterizations. For example, a variable for precipitation rate within the CFS would be highly dependent upon the convective parameterization scheme; whereas, the upper-level component winds are based more on observational data assimilated directly into the model and integrated via the primitive equations.

As aforementioned, a key factor in selecting a regression model is to ensure physically plausibility. All the included variables have been shown to be influential, or are known to be closely related to variables that have been shown influential, in tropical cyclogenesis. In addition, the sign on each coefficient fits the conceptual model of that variable's relationship to TC formation. More specifically, low-level relative vorticity, Coriolis parameter, SST, and upper-level divergence each have positive coefficients, and an increase in one or all of those variables translates into a more favorable environment for TC formation. The negative coefficient on the vertical wind shear term indicates that the lower the

42

vertical wind shear, the more favorable TC formation. The negative coefficient on the squared vorticity term is plausible as well, as described later in this section.

The significance ranks listed in Table 1 are based on the probability that the given term is not significant to the performance of our model per the Chi-squared test. These rankings may be interpreted as indicating that 850 mb relative vorticity has the lowest probability of not being significant to our model, and thus may be viewed as the most statistically influential component of the model. All of the terms included in this model are statistically significant to the regression model; therefore, even though the 200 mb divergence term has the lowest significance rank, it is still a significant contributor to the model.

An issue that plagued the development of this model was the persistence of storms after the formation day. In developing the model, we assigned a hit, or occurrence value of one, to the day grid point at which the JTWC best track data placed the formation point for each given storm. As the LSEFs appeared to vary little from the day of formation to the days immediately surrounding the formation day, the regression model was forced to discern the difference in the LSEFs between those days, in essence asking why was one day a hit and the following day—with nearly identical LSEFs—a non-occurrence point? To make matters worse, the R2 data used in the training of the models often depicts the storm tracks well. Therefore, the LSEFs following the JTWC formation date were often more favorable than on the formation date. This is especially true for the dynamic variables. As a result, we needed a way to focus the model in on the day of formation and introduce a variable or mechanism to the model to identify when a well-developed storm is being depicted by the assimilated reanalysis fields.

We adopted three modifications in the construction of this model to focus on the formation day and to reduce the model predicted probabilities associated with storms that have already formed. First, we adopted a mean sea level pressure (MSLP) filter. Before including a non-occurrence day grid block into the

regression, we filtered out blocks for which the MSLP was less than 990 mb. Second, we reduced the NTCI to 40%; this allowed us to randomly eliminate some blocks associated with storms that have already formed, while still retaining 784,660 non-occurrence points in the development of the regression model. Third, we added the squared 850 mb relative vorticity term.

The squared 850 mb relative vorticity term forces a non-linear response to the 850 mb relative vorticity in the generalized linear model. Of all the LSEFs, the low-level vorticity appears to change the most through the life of a TC. In order to focus our model in the formation day—rather than when a storm is a well-developed circulation center—we included this vorticity squared term into the regression model. With its negative coefficient, this term acts to decrease the probability of TC formation as the relative vorticity increases. In essence, we are attempting to decrease the likelihood of formation in regions where a TC already exists.

Other variables considered for inclusion, but not appearing in the final form of the model include, but are not limited to, 200 mb relative vorticity, thickness, MSLP, precipitable water, and 850 mb divergence. We also entertained the inclusion of combinations of several variables, such as absolute vorticity rather than relative vorticity and the Coriolis parameter separately, and a combined upper-level minus low-level divergence term.

The final form of the model outlined in Table 1 was trained only on the peak formation period, June through November, for the years 1982 through 2006. To evaluate the stability of the model (see Section II.D.3.c), we developed the regression equation several times, each time excluding one year from the training period. Table 2 lists the coefficients from some of these runs. The variations in the coefficients are minor; therefore, we concluded that our model is stable and not overfit. Excluding years also provided us with years of independent data (years over which the model was not trained) with which to conduct additional verification.

44

Table 2.   Comparison of regression coefficients for models with altered training periods. The training period for the full model is all years during 1982-2006.

Variable	Full Model	Excluding 1982	Excluding 1997	Excluding 2001	Excluding 2006
(Intercept)	-27.41179	-27.51922	-27.44453	-27.40436	-27.17824
Rel. Vorticity	167645.1	164535.9	165662.7	166313	171080.2
Rel. Vorticity^2	-1679802094	-1641682993	-1638789695	-1668518817	-1770825439
SST	0.6567593	0.661396	0.6575657	0.6569342	0.6482437
Shear	-0.05990173	-0.06006378	-0.05951317	-0.05778334	-0.05813202
Coriolis	15861.34	16133.2	16637.09	15938.68	16204.37
Divergence	24729.49	26888.63	24222.44	23897.41	23509.69

This model was trained on data with daily temporal resolution, which poses two potential challenges. As TCs are rare events—626 formations from among 785,286 day grid blocks in the training period—the daily probability of TC formation is incredibly low. This is true even for the most favorable locations (i.e., the climatological position of the monsoon trough) and times of year. For example, daily probabilities during the height of the peak formation period in favorable regions seldom exceed 0.05, or 5%. Such low probabilities—even if the probabilities are reliable—may be a challenge for forecasters and operators to interpret. In addition, at daily scales, the predictability at intraseasonal leads of the variables included within this model tends to be low.
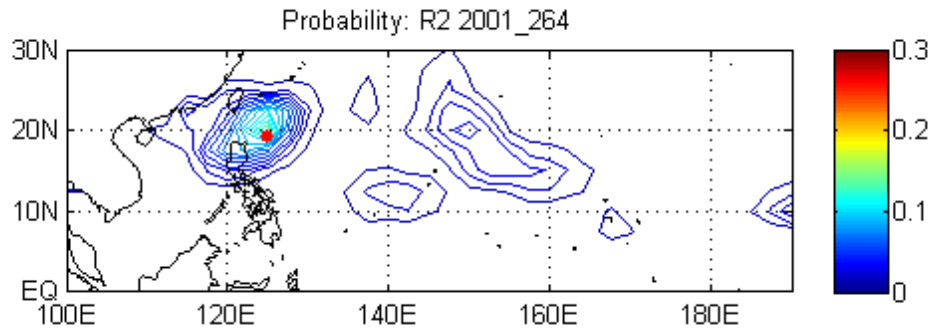
Figure 19.   Example of contoured, seven-day summed probabilities, centered about the 264th day (21 September) of 2001, constructed from R2 and OISST fields using the model described above. The red dot indicates the verification point for a TC that formed on 21 September 2001.

In order to address these problems concerning daily probabilities, we investigated non-native versions of the probabilistic output. The version upon which we settled was a summed seven-day probability. When using TC formations to verify this model output, we compared the TC formation date and location to the sum of the output probabilities for the seven days centered on the formation day: the three days prior to formation, the day of formation, and the three days following formation. Figure 19 is an example of seven-day summed probabilities from a hindcast valid 21 September 2001; the days summed to create this plot are 18 September through 24 September. The subsequent plot (not shown) would be valid on 22 September 2001, and be the summation of 19 September to 25 September daily probabilities. The reasons for favoring this seven-day summation were threefold. First, the probabilities of formation at daily time steps are small due to the rarity of TC formation, so the summation increases the probabilities in active grid blocks to values that may be used in decision-making by users. Second, the daily output of summed seven-day probabilities should enhance the predictability within the model, as it reduces the potential impacts of timing error within the forecast fields, and provides a better fit with the time averaging approach that tends to enhance the skill of long lead forecasts. Third, this approach enhances the usefulness as a planning product;

46

for example, if operators are planning an intraseasonal lead times multi-day transits of the WNP, a multi-day probability forecast may be a better match to the planning process. The probabilities shown in the remainder of this thesis are seven-day summed probabilities, unless otherwise specified.

B. VERIFICATION OF THE REGRESSION MODEL

As depicted in Figure 1 of this thesis, *Verification/Evaluation* is a vital step in the climate prediction process. Such verification and evaluation is required for two primary reasons: to identify potential shortfalls or weaknesses that may be corrected be re-doing the model development stage, and to ascertain the potential skill and value the method offers potential users.

In our verification of this regression model, we faced two complicating factors. First, we are actually predicting the favorability of the large-scale environment to support TC formations not formations themselves. This shortcoming returns to the idea that the LSEFs used in the model are necessary, but may not be sufficient, as noted in Section II.C. This complication arises when one uses actual TC occurrences to verify what are essentially forecasts for the propensity for TC formation based on environmental factors. The second complicating factor is that few techniques exist to verify spatial-distributed predictions of events that are as rare as TC formations.

Other organizations that are delving into the realm of intraseasonal climate prediction appear to be struggling with verification as well. With no standard approach as to how to verify such predictions, we feel the best approach to verification is to use several methods in concert.

1. Quantitative Verification

The first class of verification we explored was quantitative verification. For the sake of brevity, we note only the key points for each quantitative verification technique. The reader is directed to references, such as Wilks (2006) or Eckel (2008), for additional details on the construction and interpretation of these

verification techniques. Paramount in quantitative verification is having sufficient forecasts to verify. In order to encompass a sufficient number of storms, the verification in this section is for multi-year zero-lead hindcasts over dependant data. The period of verification, unless otherwise specified, is the June through November peak formation period, as this matches the period over which the model was trained and reduces the potential for data dilution from the months when few storms develop. Over this period for the years 1982 to 2006, 626 storms were identified by the JTWC in the region we define as the WNP, versus 752 storms if the verification period is expanded to encompass every day of the year for the same years. So relatively few TCs were left out of the verification process when we limited ourselves to verifying using just June-November TCs.

Many of the quantitative verification techniques that follow are based on dichotomous observation values; a value of one if the event is observed, or zero if the event is not observed. For our verifications, we opted to credit an observed value to any grid point that fell at or within a 2.5° radius of the JTWC formation point. We feel a 2.5° radius about the formation point accounts for the spatial influence of a forming TC, as well as accounts for some of the uncertainty in the formation location in the JTWC best track data.

To provide us with a standardized measure of performance based on our predictions of the probability of formation, we used the Brier skill score (BSS). Over the peak formation season, our model results in a BSS of 0.029055 (0.028211…0.02994). The ranges included in the parentheses represent a 95% confidence interval, generated through jackknifing each of the years in the training period. Recall that positive values of the BSS represent improvement over the sample climatology baseline; thus, our model shows notable skill. When verifying the model over the full year, the BSS increases to 0.032555 (0.031927…0.033182). Eckel (2008) notes that BSS is vulnerable to dataset dilution, which likely accounts for this increase in the skill score when verifying over the entire year.
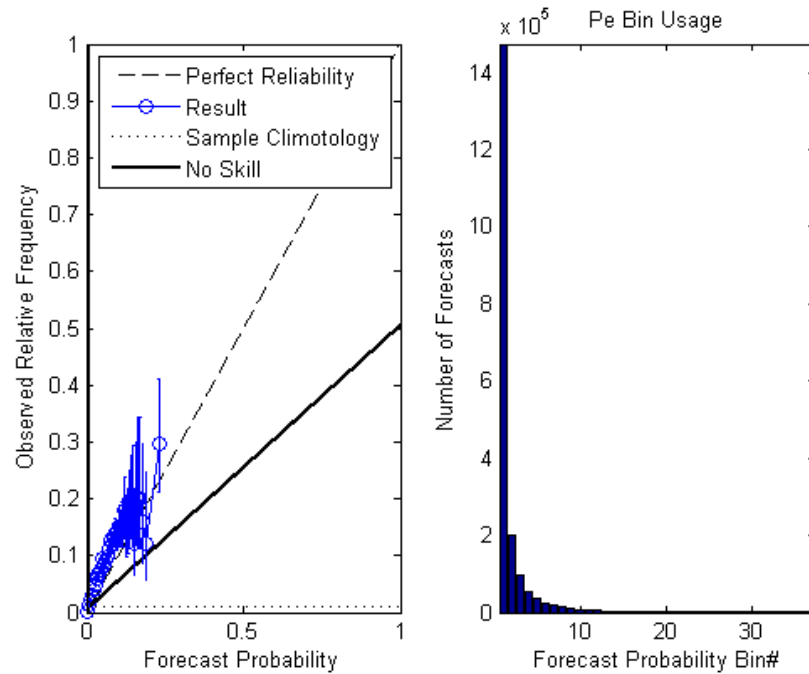
Figure 20.   Reliability diagram (left) and bin histogram (right) generated with minimum bin intervals of 0.005 for the zero-lead hindcasts, from the model outlined in Table 1 over the June – November period for 1982 to 2006; error bars represent a 95% confidence interval.
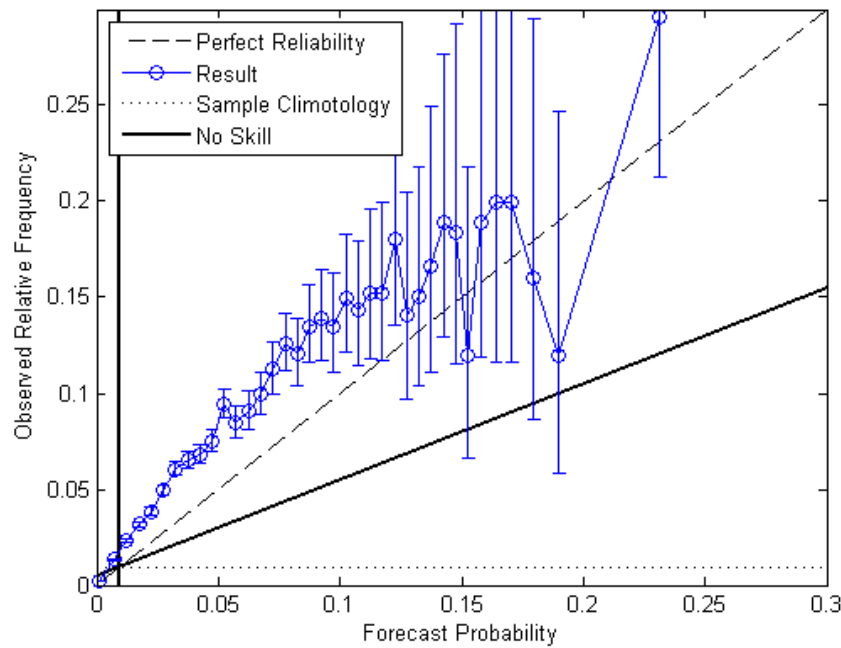
Figure 21.   The same reliability diagram as in Figure 20, but focused in on the lower probabilities; error bars represent a 95% confidence interval.

Figures 20 and 21 depict the reliability diagrams for zero-lead hindcasts with the model outlined in Table 1, for the peak formation seasons of the years 1982 through 2006. The reliability diagram for a perfectly reliable model would lie along the diagonal indicated by the dashed line. Points within the region defined by the solid lines indicate positive skill. The figures show graphically what we learned from the BSS, that this model exhibits skill over the sample climatology baseline. The line connecting the results points is above the diagonal, indicating that the model slightly underforecasted TC formations. The sporadic behavior—as captured by the error bars—in the "higher" probabilities is likely due to the drop in number of points in those bins. From these reliability diagrams, we obtain an approximate BSS of 0.02852, reliability of 0.000065693, resolution of 0.00032856, and uncertainty of 0.0092171.
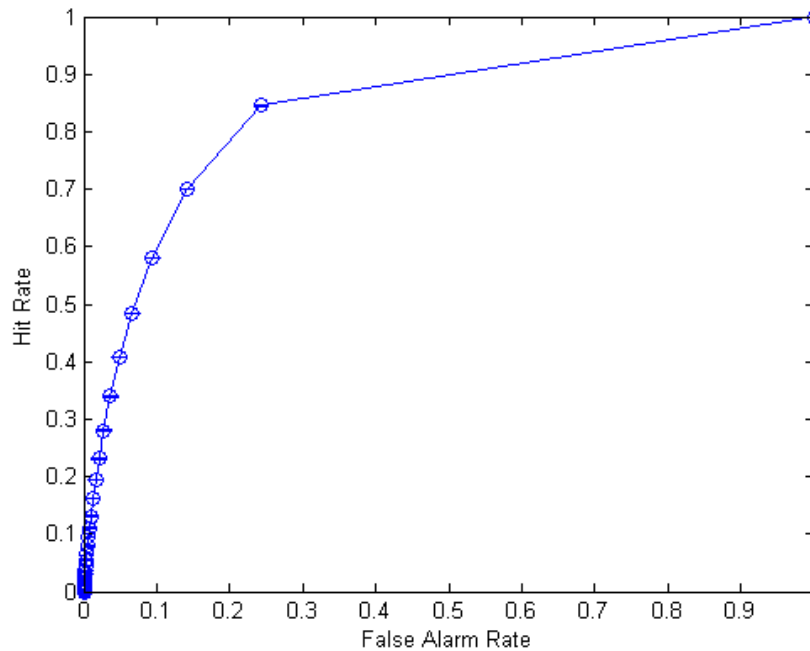
Figure 22.   ROC diagram for the zero-lead hindcasts over the peak formation season for the years 1982 to 2006.

In addition to having skill, a worthwhile predictive method must also offer utility and value to the user. The relative operating characteristic (ROC) diagram and economic value diagram (EVD) are two graphical tools that one may use to

ascertain whether a method may offer such value and utility. Figure 22 shows the ROC diagram for the zero-lead hindcasts over the aforementioned verification period. A diagonal line (not shown) connecting (0,0) with (1,1) would represent zero resolution or no discrimination. Forecasts with better discrimination have ROC curves approaching the upper-left corner of the diagram (Wilks 2006). As a result, one can see that the model exhibits fair discrimination and offers potential utility to the user. Along with the ROC diagram, one may calculate a ROC skill score (ROCSS), which has a value of one for a perfect forecast and is less than zero if the forecast is worse than the sample climatology forecast. The ROCSS for these hindcasts is 0.68325.
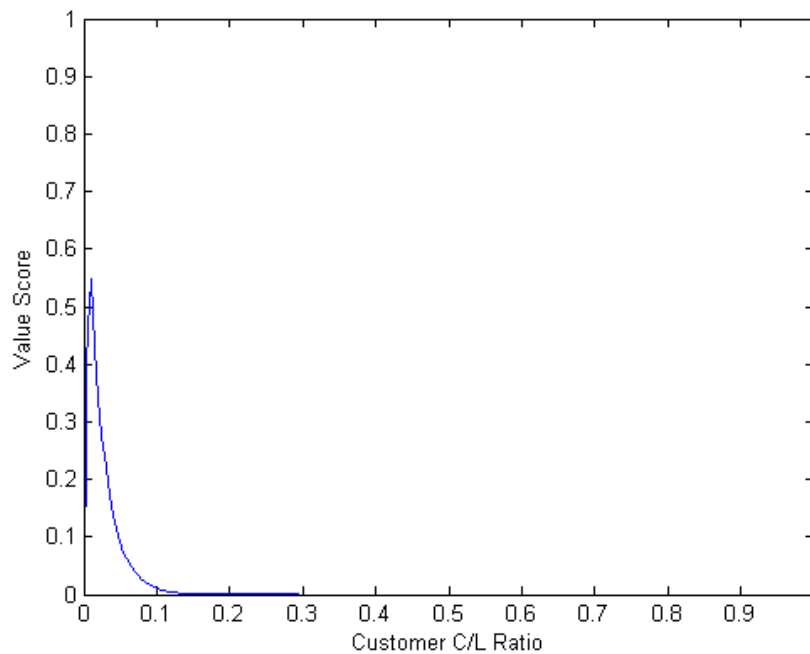
Figure 23.   EVD for the zero-lead hindcasts over the peak formation season for the years 1982 to 2006.

An EVD, as shown in Figure 23, plots value score versus cost/loss (C/L) ratio, and is a representation of the potential value added by following the forecast guidance for each customer (as defined by their C/L ratio). While initially one may not be impressed by the EVD in Figure 23 due to its skew, this EVD actually depicts significant potential value for risk adverse customers. Whether a

customer defines their C/L ratio in terms of dollars, sortie hours, or crew morale, most customers would be risk adverse (low C/L ratio) to a hit by a TC. A hypothetical example may be in order. Let us imagine a cruiser is steaming towards Subic Bay and the forecast calls for a TC; the captain can either divert around the storm at an additional cost of $100,000 above and beyond typical operating costs. Alternately, the captain may maintain course and if the cruiser is hit may suffer damages worth $1M in equipment and lost time. With these numbers this customer would have a C/L ratio of $100,000/$1,000,000 or 0.1, and thus should be highly risk adverse. For such a customer, the EVD indicates that the model has the potential to be very valuable in mission planning. While this example is grossly oversimplified, it reveals in the basic idea associated with the EVD and, thus, the potential benefits of this model.

2. Qualitative Verification

While qualitative verification is often not as definitive as quantitative verification, it does offer the advantage of allowing us to verify using purely independent data. Options for independent data include using runs generated with a year left of out of model development, then verifying over that excluded year, or using another variable source (such as R1 data for atmospheric variables).
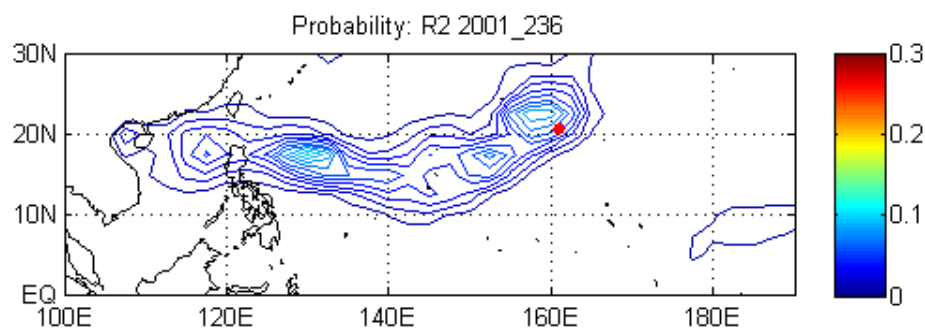
Figure 24. Example of contoured, seven-day summed probabilities, centered about the 236th day (24 August) of 2001, constructed from R2 and OISST fields. The red dot indicates the verification point for a TC that formed on 24 August 2001.

52

Figure 24 is a contour plot of probabilities for the period of 21-27 August 2001. The model used in generating this plot was trained over a period that excluded the year 2001; therefore, this plot was generated with independent data. Plots such as that in Figure 24 indicate that the methodology proposed in this thesis may prove beneficial, as this zero-lead hindcast shows "high" probabilities that resemble those expected from reverse monsoon trough conditions that are very different from those that would be expected from typical monsoon trough climatological conditions in August.
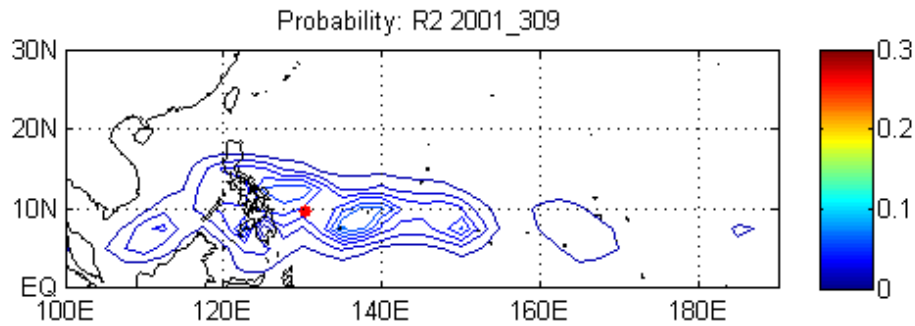
Figure 25. Example of contoured, seven-day summed probabilities, centered about the 309th day (5 November) of 2001, constructed from R2 and OISST fields. The red dot indicates the verification point for a TC that formed on 5 November 2001.

Figure 25 shows a zero-lead hindcast in which the pattern of model probabilities resembles the pattern that might be expected from climatological monsoon trough conditions. This figure represents situations in which the model proability patterns are similar to climatological patterns. But even when the model patterns resemble climatology, the model may add value by providing a more accurate prediction of the magnitude of the probabilities, as discussed in the next section.

3.   Comparison to Climatology

The preceding plots provide hope as to the potential usefulness of our proposed method for predicting TC formations. One may wonder how this method compares to climatology, but with climatology comes the question of what form of climatology is the best against which to compare our method. See Appendix A for a brief discussion on the various forms of climatology one may select.

The idea of hits and misses is commonplace in verification, and one we shall use here. A simple subtraction of the climatological formation probability from the hindcast probability at every day grid block yields a difference matrix. Using the JTWC best track formation points, a hit (miss) is defined as occurring when the difference at the day grid block of formation is positive (negative). Scoring over the years 1982 through 2006, our model had 681 hits and 81 misses, for a hit rate of 89%.
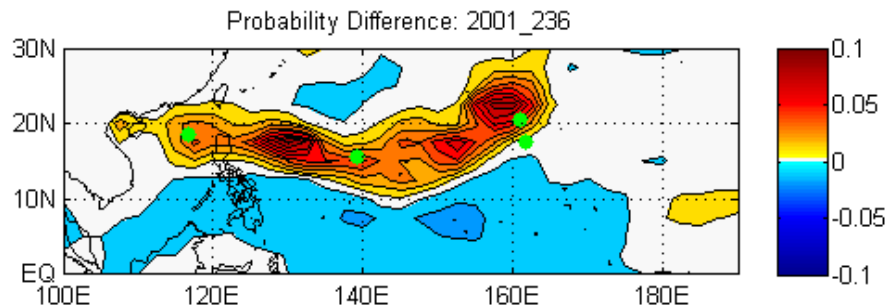
Figure 26.   Plot of the difference matrix resulting from subtracting climatological probabilities from hindcast probabilities centered on 24 August 2001, the same day used in Figure 24. Green dots denote the formation points for the four storms that formed with in the seven-day period of 21 – 27 August 2001.

One may also plot this difference matrix; Figure 26 is an example of such a plot. Warm (cool) colors represent regions where the probabilities from the model are higher (lower) than the climatological probabilities. This approach is akin to an anomaly forecast, where the positive regions may be interpreted as

having a greater than normal likelihood of TC formation. The period of 21-27 August 2001, which is depicted in Figures 24 and 26, was unusually active along 20°N. This difference product highlights this activity, but it also indicates that the probability of formation along the climatological position of the monsoon trough is lower than climatology suggests. In some cases, knowing that formation is less likely in a region when compared to climatology may be just as beneficial as knowing that formation is more likely in some other region.

4.   Climate Oscillations

Section II.C.4 briefly introduced the impacts of ENLN on TC formation. If our model accurately depicts the favorability of the large-scale environment, then it should depict a shift in the probabilities associated with the changes in the large scale environment that are associated with ENLN.
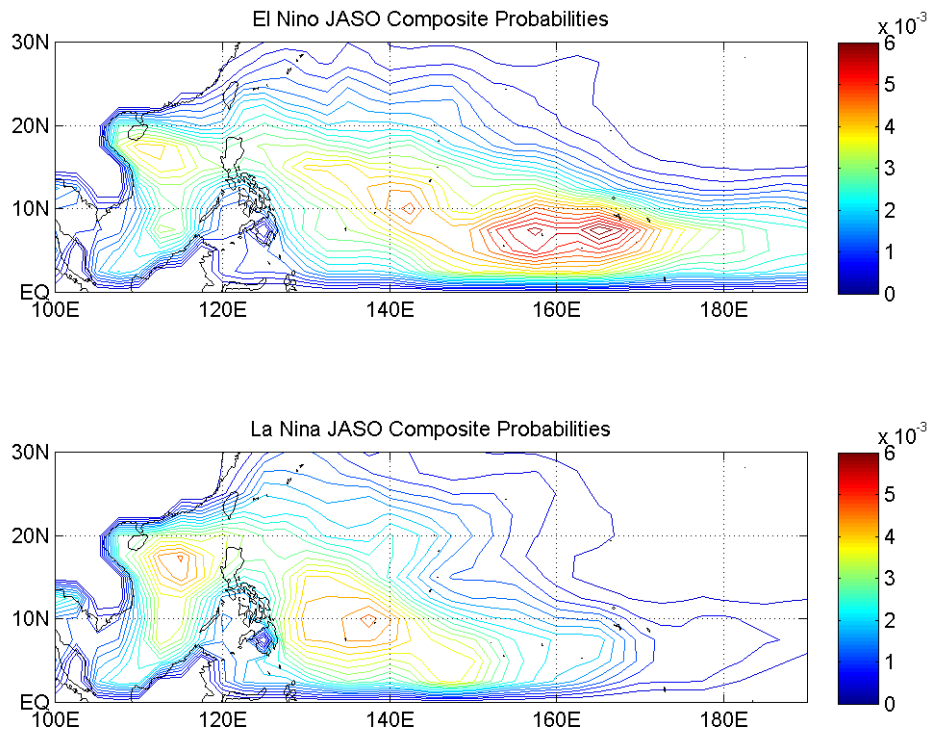
Figure 27.   Average daily probabilities for the JASO period from composited El Niño years (top) and La Niña years (bottom).

Defining ENLN years based on the Oceanic Niño index (ONI), we can take 1982, 1987, 1991, and 1997 as classic (non-Modoki) El Niño years and 1985, 1988, 1999, and 2000 as La Niña years. Averaging the daily probabilities from the zero-lead hindcasts over the July, August, September, and October (JASO) period, yields the probability patterns shown in Figure 27. Note the shift in the highest probability regions between the two plots, these shifts are similar to those described in prior studies of the impacts of ENLN on TC formations (e.g., Ford 2000). For example, the high probabilities that extend farther to the east during the El Niño years are representative of the eastward shift of the regions of warm water, low-level cyclonic flow/convergence, and low vertical wind shear from their climatological positions. In contrast, slightly higher probabilities near the Maritime Continent in the bottom panel of Figure 27 are due to the westward shift of favorable LSEFs during La Niña years.

5.   Conditional Climatologies

Another potential use for our model that emerged during this research was the possibility of creating conditional climatologies in the manner of constructed analogues. The underlying idea is that rather than generating a climatology plot based on the raw formation data, we could generate a plot based on model-generated probabilities. This approach could be as basic as generating an annual climatology based on LTM conditions, or as complex as conditioning based on time of year, ENLN, et cetera.
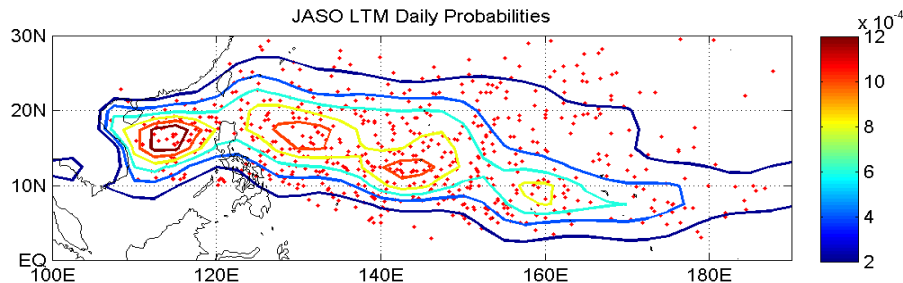
Figure 28.   Probabilities from LTM JASO R1 and OISST variables. The red dots indicate the formation points for all JASO TCs from 1971 – 2000.

Figure 28 depicts contours of daily probabilities for the JASO period, based on LTM R1 and LTM OISST LSEF values composited over the years 1971 –2000 and 1982 – 2000, respectively. The period of 1971 – 2000 is used for this and other long-term mean conditions, as it represents the current World Meteorological Organization (WMO) standard, 30-year climatology period. This plot is not a perfect representation of the raw climatology; for example, the formation points clustered around 25°N and 165°E are not captured well by the contours despite the density of storms in that location.
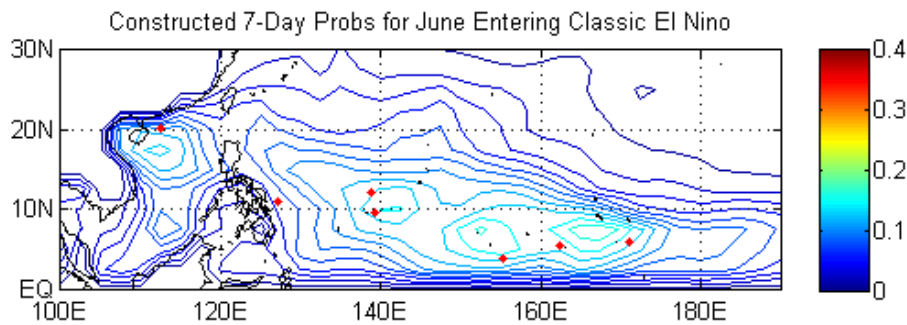
Figure 29.   Contoured, seven-day probabilities, constructed from R2 and OISST fields. The red dots indicate the verification point for TCs that formed during such conditions.

The concept of a constructed analogue is combining past anomaly patterns such that the resulting combination reflects the desired state of the climate (van den Dool 2007). As an example, we constructed a probability plot for the month of June when the climate system is entering into an El Niño pattern. Using the ONI, such conditions were met during the years 1991, 1997, and 2002. Averaging the probabilities from our model for these three months (one month each for three years) and dividing to give us seven-day probabilities, results in what is depicted in Figure 29. In essence, the result is an improved representation of expected probabilities for a week in the month of June when an El Niño event is developing.

Though this method is not without limitation, it has a remarkable advantage in that this approach does not require dynamical input. As a result, this constructed analogue approach may be useful for providing tropical activity outlooks at extended lead times.

6. Verification Against Deep Convection

As noted in the beginning of the section on verification, many of the verification methods we have discussed thus far are problematic because they verify against observed TC formations, even though the model predicts the propensity for formation, not actual formations. Thus, we chose to also verify against outgoing longwave radiation (OLR), since low OLR values indicate deep convection and thus a large-scale environment that is likely to be favorable for TC formation.
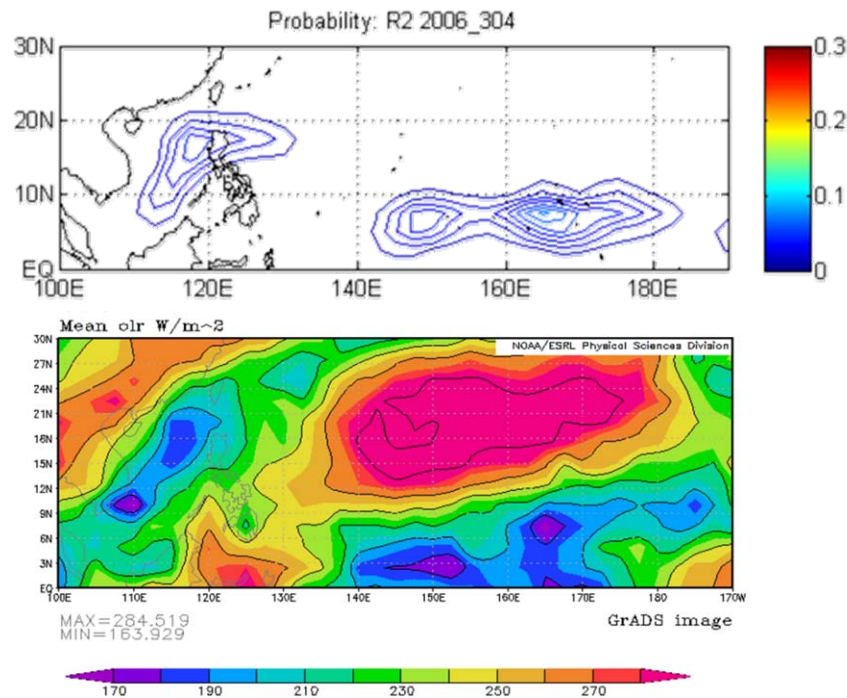
Figure 30. Comparison of zero-lead hindcast probabilities (top) and OLR (bottom). OLR image provided by Physical Sciences Division, Earth System Research Laboratory, NOAA, Boulder, Colorado, from their Web site at http://www.esrl.noaa.gov/psd/.

Figure 30 is presented as an example of model-derived probabilities for 28 October through 3 November 2006 and the corresponding NOAA Interpolated OLR. Note in the tropics the general correspondence between the higher probabilities and the low OLR values (cool colors) that correspond to cold high cloud tops and deep convection. This sort of correspondence indicates that the model is capable of identifying deep convective regions that are favorable for TC formation, and has the potential to be useful in intraseasonal predictions of tropical convective activity. To operationalize such an approach for predicting convective activity, the Coriolis term should be removed from the regression model.

7. Verification in Other Basins

This final form of verification is one that tests whether the model truly represents a physically sound combination of LSEFs. Earlier authors presented their genesis-parameters as relevant to TC formations in all tropical ocean basins. As a result, one is left to wonder how the model, as described in Table 1, would perform on fully independent data in basins other than the WNP. Figure 31 is an example of a probability plot that results when the Pacific-trained model is used to generate probabilities for the North Atlantic basin.
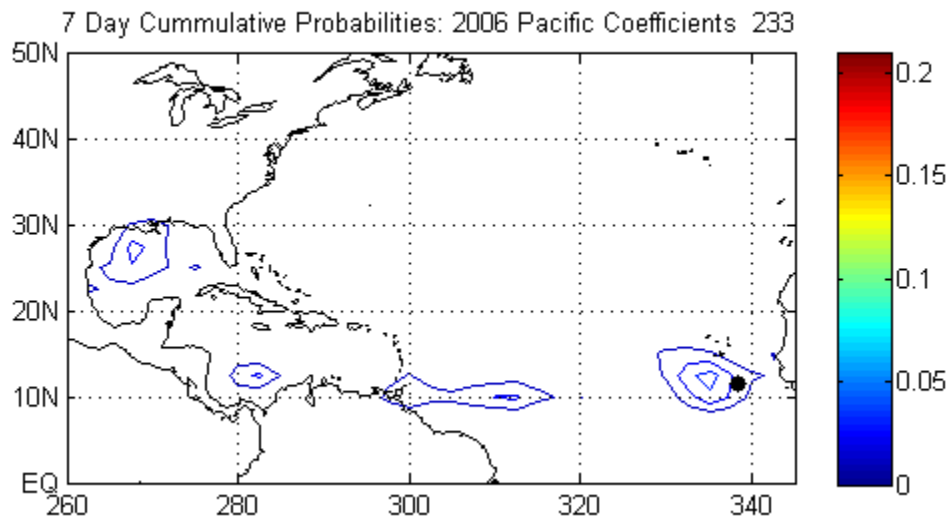
Figure 31. Example of contoured, seven-day summed probabilities over the Atlantic basin, centered about the 233rd day (21 August) of 2006, constructed from R2 and OISST fields using the model trained on the WNP. The black dot indicates the verification point for a TC that formed on 21 August 2006.

Quantitative verification of the storms that developed into tropical storms or hurricanes in the Atlantic during the months of June through November and years 1982-2006 yields promising results. Over that period, hits number 273 and misses 16, with a BSS of 0.019476 (0.018584...0.020306) and a ROCSS of 0.58959. These positive results suggest that the LSEFs that influence TC formation are the same regardless of the ocean basin. This cross-basin verification confirms what was proposed by authors such as Gray and Frank, that the same set of LSEFs influence TC formation regardless of the ocean basin. Though the model is likely better tuned if trained over the basin over which it will be used as a predictive tool, this comparison suggests that one basic model may be skillfully applied to multiple basins.

8. Model Shortcomings

Two potential shortcomings were identified in the verification of the zero-lead hindcasts. Both of these shortcomings deal with the post-formation environment. First, the conditions that follow the formation day are likely to be represented by the model as remaining favorable for formation, despite a TC having already formed. The impacts of this shortcoming may be minimized by noting that the probabilities represent the favorability of the large-scale environment for TC formation, and if a TC forms the high probabilities may represent the likely track of the storm. Second, TCs may act to enhance or suppress the formation of other tropical cyclones (Frank 1982). Due to the coarse resolution of the CFS, it may poorly represent the TC-environment feedback. Further study would be required to assess the impacts of this second shortcoming, though such research ventures beyond the scope of this thesis.

C. VARIATIONS OF THE REGRESSION MODEL

The previous verification sections have tested a model containing terms for 850 mb relative vorticity, 850 mb relative vorticity squared, SST, vertical wind shear, Coriolis parameter, and 200 mb divergence, and trained over the peak formation period for the years 1982-2006. Through the course of this thesis research, numerous forms of the model were tested, in addition to this final model. For example, we varied the training period of the model, such as training the model over the entire year and over JASO, rather than just over the peak formation period. We also investigated the inclusion and/or combination of other variables as noted earlier in Section III.A. Using the suite of metrics and verification techniques listed in Chapter II, we selected the final model from among the many tested. For the sake of brevity, only verification for the final model has been presented in this thesis.

D. FINDINGS FROM CFS CASE STUDIES

The previous sections have explored the validity of the statistical model in identifying likely formation regions. The associated verification metrics represent

the potential skill, value, and applications as defined by the zero-lead hindcasts. In this section we demonstrate the ability to use the CFS as the source of LSEF values with which to force the regression model and generate forecast probabilities (see Figure 18). The availability and format of CFS output fields negates the use of many of the quantitative verification metrics that were possible with the reanalysis-based, zero-lead hindcasts. As a result, in order to investigate the predictive potential of the proposed technique, we will present a pair of case studies. The first case study is of a pair of storms from 2008 using operational CFS data; the data used for Case 1 is exactly what is readily available on a daily basis, and that could be used to operationalize the method proposed in this thesis. The second case study is one from 2003 using archived CFS hindcast fields. Plots from some additional case studies are included in Appendix C.

1.   Non-Zero Lead Hindcasts: Case 1

TC activity in the 2008 TC season in the WNP was relatively low, for reasons that are not yet clear. From this low activity season, we examined two rather low intensity TCs. Our model should be robust enough to predict TCs in low activity seasons and TCs that do not reach high intensities. The only thing that may be notable about these two TCs, Mekkhala (20W) and Higos (21W), is that the JTWC has traced their origins back to the same day in 2008.

Disturbances that would develop into Mekkhala and Higos were identified for as early as 27 September (see Figure 32 for formation points). Mekkhala, developing in the South China Sea, would grow to tropical depression strength by the following day, and be a named tropical storm another day later, on 29 September. Similarly, Higos, forming in the WNP, would reach tropical depression strength, and then tropical storm strength on 29 September.
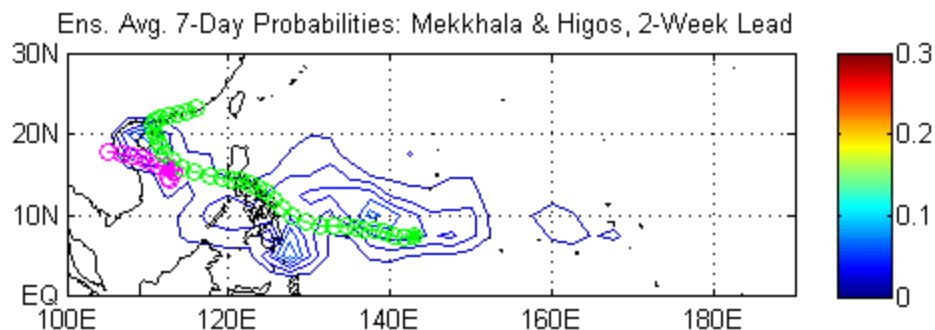
Figure 32.   CFS ensemble mean probabilities from runs initiated on 13 September 2008, valid 24-30 September 2008. Formation points (solid circles) and tracks (open circles) are included for Mekkhala (magenta) and Higos (green).

Figure 32 is a plot of the mean seven-day probabilities from the four-member ensemble. From this plot alone, it appears the CFS predicted the potential for above-average TC activity in the greater monsoon trough region at a two-week lead (tau: 336 hours). The difference plot in Figure 33 confirms that the CFS-based probabilities were higher at both formation points than what climatology would have provided.
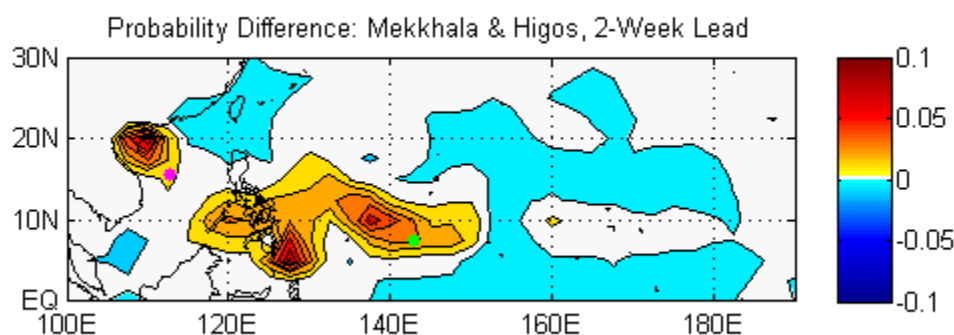
Figure 33.   A probability difference plot of the CFS ensemble mean probabilities (as in Figure 32) minus the climatological formation probabilities for the same period. Formation points are included for Mekkhala (magenta) and Higos (green).
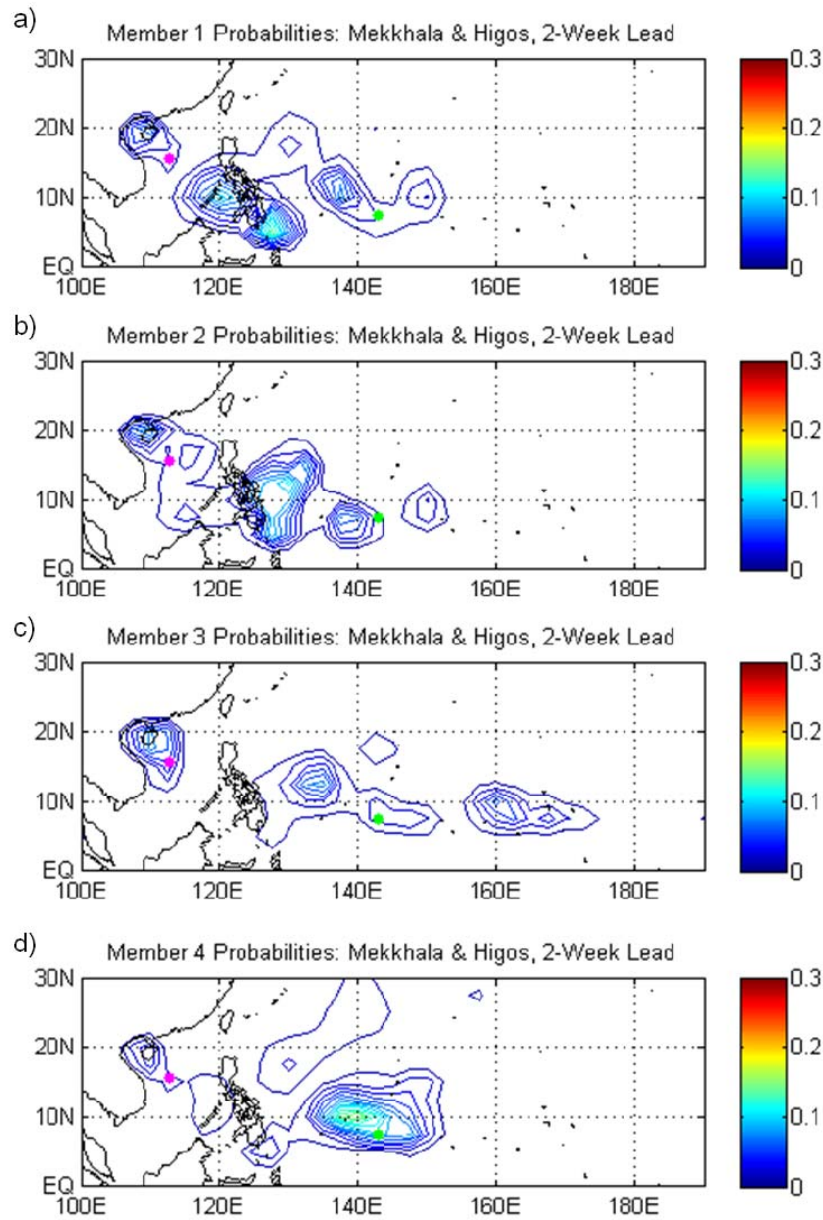
Figure 34. Seven-day probabilities from each of the four ensemble members, initiated on 13 September 2008, valid 24-30 September 2008. Formation points are included for Mekkhala (magenta) and Higos (green).

Figure 34 separates the ensemble mean plot in Figure 32 into individual ensemble members. Recall that the members are identical models, but have different initial conditions and/or initiation times (00Z or 12Z). These minor variations between the members do result, as shown in Figure 34, in pronounced

differences after a two-week integration. A quick comparison of these seven-day probabilities reveals that no one member performed better than the others for both of these storms, although member four appeared to strongly predict the development of Higos.

The contoured probability plots like those in Figure 34 represent summed daily probabilities. In addition to the spatial variability of the individual members, we could also analyze the temporal variations between the members. This additional degree of variability is not shown in this report, although the variations are what one would expect when comparing runs of any dynamical model—timing differences exist from run-to-run. The spatial and temporal variability between members highlights what was first mentioned in Section II.B.4, that the ensemble approach smoothes out differences between the runs, and highlights the more predictable elements of the climate system. Thus, this ensemble approach should lead to enhanced predictive skill overall, although there will, of course, be exceptions.

As highlighted earlier, ensemble member four appeared to capture the formation of Higos. We explored the individual LSEFs that contributed to the probabilities plotted in panel d of Figure 34. Figure 35 displays those LSEFs for the day of formation, 27 September 2008.
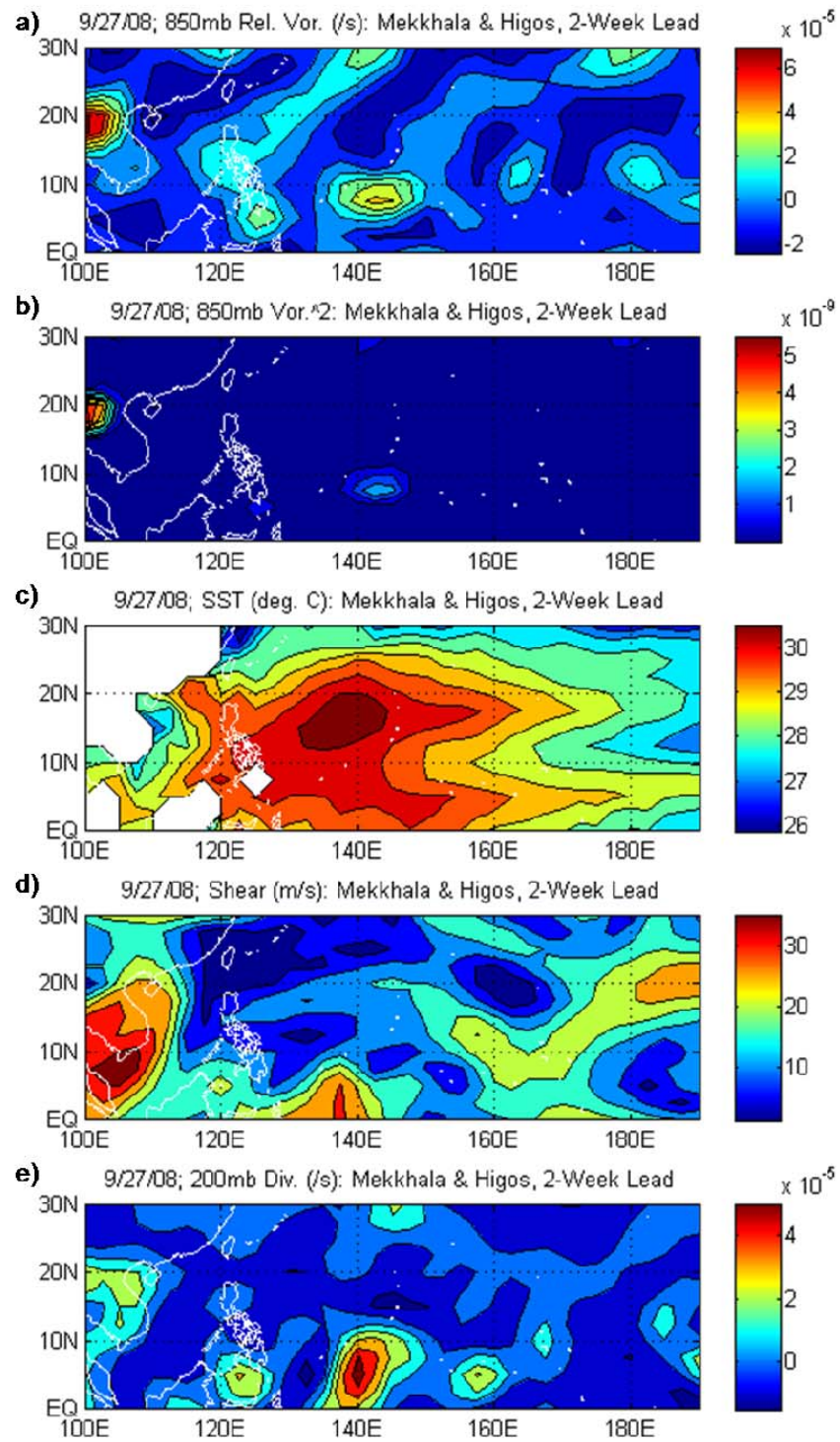
Figure 35.   Individual LSEFs from ensemble member four for the formation
day, 27 September 2008.

The panels in Figure 35 depict the LSEFs for the formation day in the order of their statistical significance in the regression model: a) 850 mb relative vorticity, b) 850 mb relative vorticity squared, c) SST, d) vertical wind shear, and e) 200 mb divergence. The Coriolis term is not shown, as it is a simple function of latitude, and thus does not vary by member or run. The regression model, when applied to variables from member four, predicted the highest probabilities of formation for the week centered on the formation day to be near 10°N and 140°E, very close to the actual formation location. Though the panels in Figure 35 are for the formation day alone, they reveal why the high probabilities are predicted where they are. The region surrounding 10°N and 140°E is forecasted to experience high low-level relative vorticity, very warm SSTs, near a low shear zone, and positive upper-level divergence.
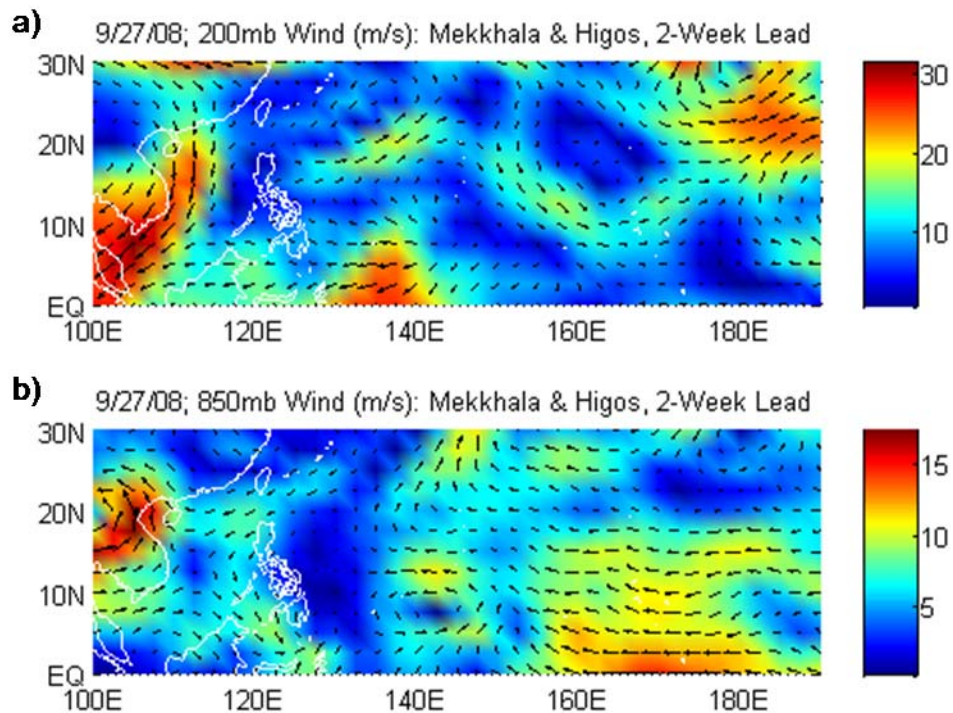
Figure 36.   Winds at a) 200 mb and b) 850 mb from a two-week lead of ensemble member four valid for the formation day, 27 September 2008.

The vorticity, vorticity squared, shear, and divergence terms included in the regression model are all calculated from the zonal and meridonal winds

67

available from the CFS. Figure 36 depicts the 200 mb and 850 mb winds from member four on formation day; the component winds used to create these full-wind plots are the same used to calculate the variables in Figure 35, except SST. Note the cyclonic circulation at 850 mb and anticyclonic outflow at 200 mb forecasted by member four for the formation day at a two-week lead.

In this particular case study, a well-trained forecaster might have been able to use just the CFS output fields (as in Figure 36) to foresee the development of Higos around 10°N and 140°E. Some readers may then question, why would one not just use the available CFS dynamical output to forecast tropical cyclogenesis? Many of the potential benefits of the combined statistical-dynamical approach have been noted implicitly elsewhere in this thesis. We feel that from the dynamical perspective, employing an ensemble minimizes the impacts of spatial and temporal errors within the model. If we analyzed member three, rather than member four, in the preceding figures, one would see that both the timing and strength of the circulation would have been inaccurate; therefore, a forecaster would have likely miss-forecasted the formation of Higos. A reason why operational numerical weather prediction is seldom used beyond ten days to two weeks is that longer leads are often beyond the limit of predictability of individual weather elements. Exploiting the expanded predictability of the large-scale circulations and ocean memory may extend the predictability of this combined method, vice the predictability of individual elements. Furthermore, the regression model represents a physically- and statistically-sound combination of LSEFs, which allows one to produce a reliable, repeatable prediction of TC formation. Rather than having to intuitively compare multiple output fields and subjectively generate a forecast, the contoured plots from the proposed method are easily generated and interpreted by forecasters or users. For these reasons, we feel that this combined statistical-dynamical method is a viable approach to intraseasonal prediction of tropical cyclogenesis.
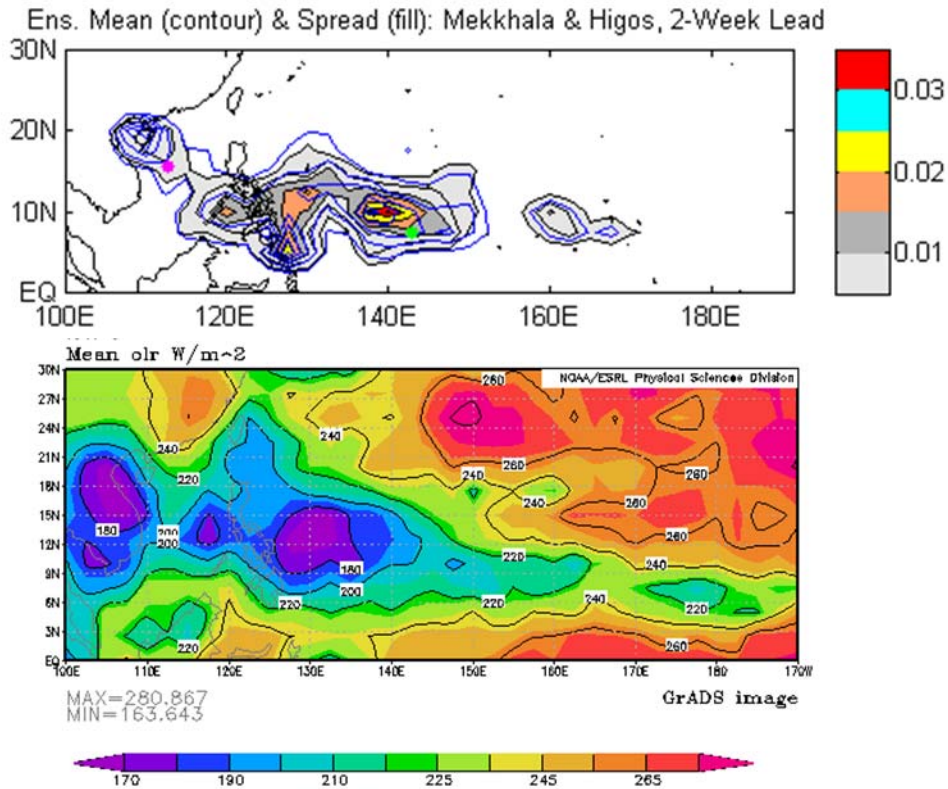
Figure 37.   Comparison of CFS-based TC formation probabilities in the form of an ensemble mean/spread plot (top) and OLR (bottom) for the same period. OLR image provided by Physical Sciences Division, Earth System Research Laboratory, NOAA, Boulder, Colorado, from their Web site at http://www.esrl.noaa.gov/psd/.

As noted earlier, in addition to intraseasonal prediction of tropical cyclogenesis, this method appears to highlight regions of likely tropical deep convection. Figure 37 is a comparison of CFS-based forecast probabilities, in the form of an ensemble mean/spread plot, and OLR for the period of 24-30 September 08. Whether verified against the formation of Mekkhala and Higos, difference from climatology, or against deep convection, the CFS-based probabilities from this case study show promise for this combined approach at a lead time of two weeks.

2.   Non-Zero Lead Hindcasts: Case 2

As a second case study into the predictive potential based on CFS, we focused on Ketsana and Parma (20W and 21W, respectively), two storms that formed on 18 October 2003. Rather than constructing a four-member ensemble from the operational CFS, we used the archived ensemble mean from the CFS hindcast project. This ensemble mean is an average of all 15 members initialized in one month from the CFS hindcast project. As a result, the initial conditions of the ensemble mean are staggered over the period of a month. Like other CFS runs, the integrations extended out to nine months. These ensemble mean runs are available once per month in the CFS archive, with the valid times beginning on the ninth day of every month. Thus we were able to work with a nine-day lead (tau: 144 hours) and a 39-day lead (tau: 864 hours) in this case study.
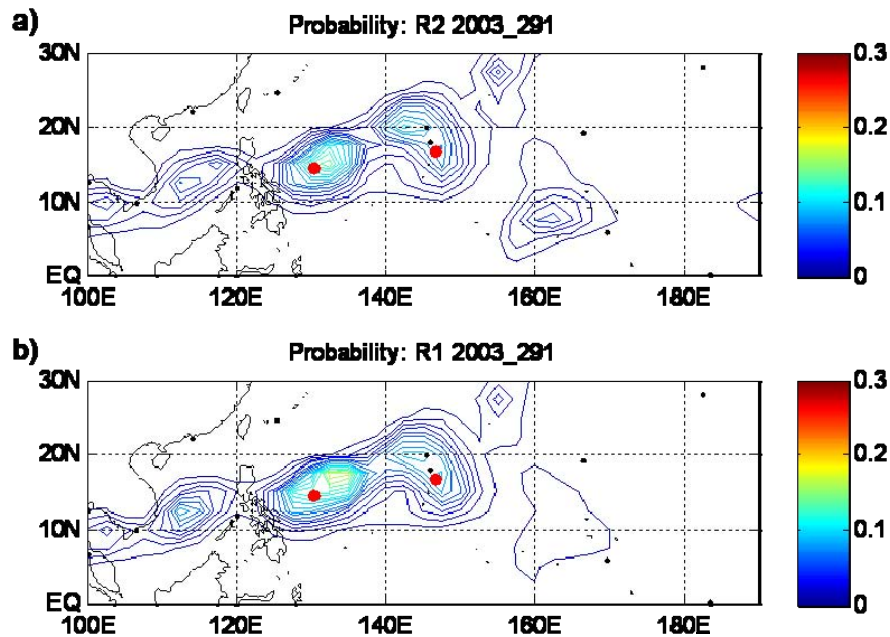
Figure 38.   Contoured, seven-day summed probabilities, centered about 18 August 2003, constructed from a) R2 and OISST and b) R1 and OISST fields. The red dots indicate the formation points for Ketsana (right) and Parma (left).

This second case study was chosen not for its perceived performance based on the CFS, but rather for its unusual reverse-oriented monsoon trough and high probabilities visible in the zero-lead hindcast (Figure 38). Figure 38 displays the high probabilities that extend SW to NE over the WNP when using both the R1 and R2 reanalyses. The strong similarity between the R2-based (top) and R1-based (bottom) plots suggest that our model is not overly sensitive to the specific analysis and assimilation system. The logical question that follows is whether the 15-member CFS ensemble mean would predict this unusual activity.
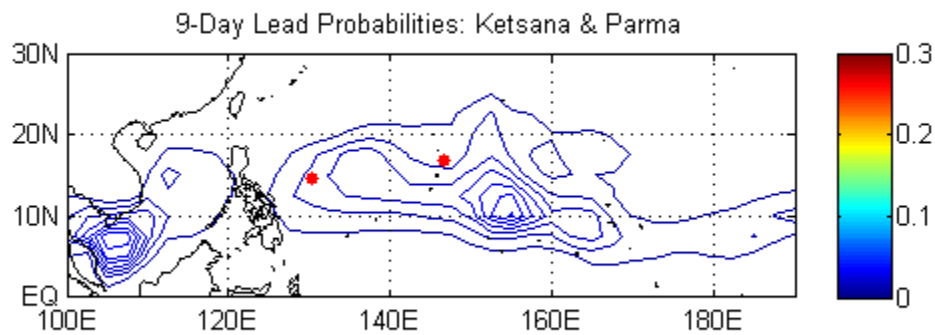
Figure 39.   Contoured, seven-day probabilities, centered on 18 October 2003, constructed from the archived CFS ensemble mean at a nine-day lead. The red dots indicate the formation points for Ketsana and Parma.

To assess the predictive potential, we first investigated the nine-day lead forecast. Figure 39 depicts the probabilities of TC formation for the period 15-21 October 2003, based on archive CFS ensemble mean fields with a nine-day lead from the day of formation. The formation points for both Ketsana and Parma are included within the 0.5% minimum contour.

Figure 40 is the same as Figure 39, but from fields with a 39-day lead from the day of formation. While the contours do suggest activity around 15°N, the

71

CFS-based probabilities at such a lead are notably different from the reanalysis-based, zero-lead probabilities (Figure 38) and do not indicate reverse monsoon trough conditions.
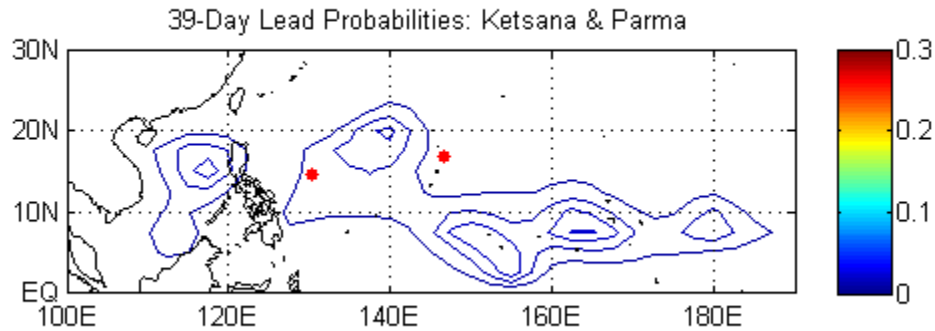
Figure 40.   Contoured, seven-day probabilities, centered on 18 October 2003, constructed from the archived CFS ensemble mean at a 39-day lead. The red dots indicate the formation points for Ketsana and Parma.

Visual comparisons between Figure 38 and Figures 39 and 40 indicate differences between the CFS-based probabilities and the reanalysis-based probabilities in both magnitude and spatial distribution. As aforementioned, this case was chosen, in part, because of the high probabilities found in the zero-lead hindcast; both formation points were predicted with probabilities on the order of 0.1 or a 10% probability.   In contrast, the CFS-based probabilities at the formation points range from approximately 0.004 to 0.013. Also, the reanalysis-based probabilities depict favorable formation in a reverse-oriented monsoon trough pattern, while the CFS-based plots show a poleward extension of the contoured probabilities from the climatologically-favored monsoon trough region.

One is left to wonder what accounts for the difference between the CFS-based and reanalysis-based probabilities. Is it a weakness of the regression model and/or of the CFS? Is something unique about this case that is causing these differences?
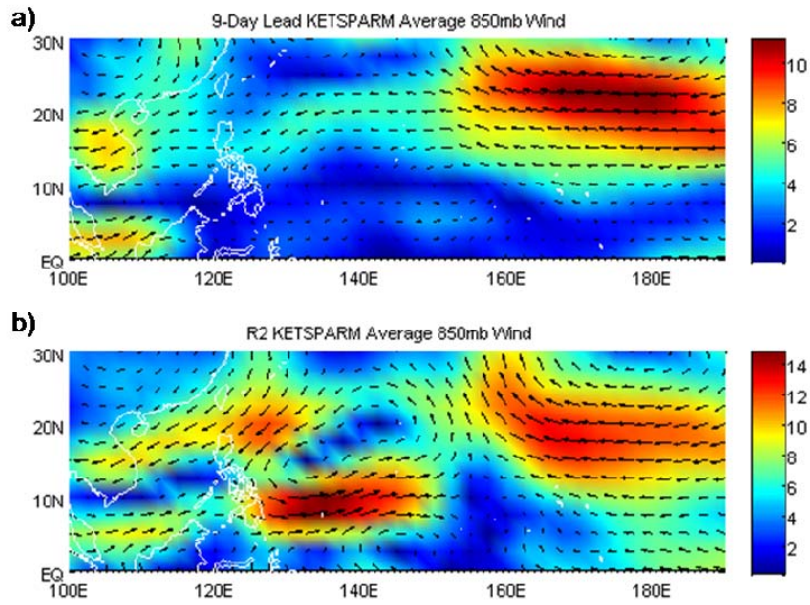
Figure 41.   Comparison of 850 mb winds for the period 15-21 October 2003, from a) nine-day lead from the CFS ensemble mean and b) zero-lead R2 data. Note the different scales.
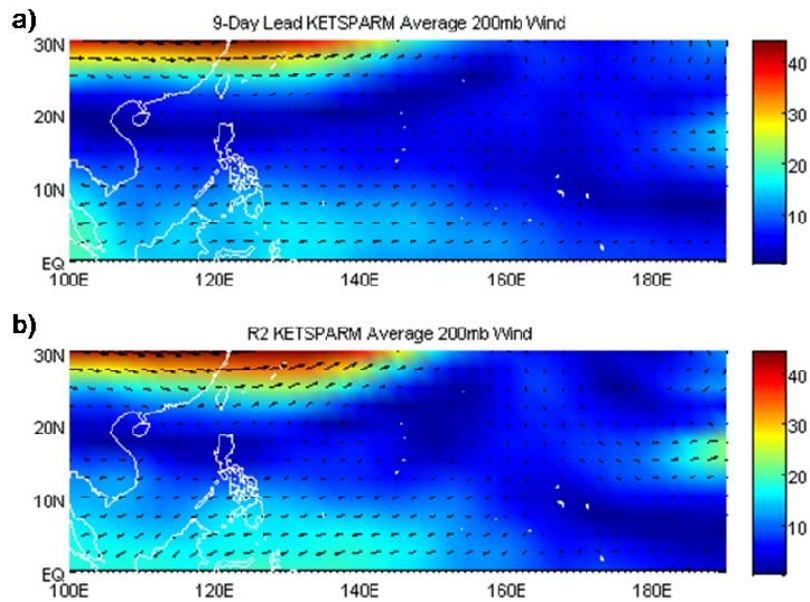
Figure 42.   Comparison of 200 mb winds for the period 15-21 October 2003, from a) nine-day lead from the CFS ensemble mean and b) zero-lead R2 data.

Figures 41 and 42 are comparisons of the 850 mb winds and 200 mb winds, respectively, from averaged CFS ensemble mean output (at a nine-day lead) and averaged R2 data (at zero-lead) for the same period, 15-21 October 2003. As discussed in the case study 1, the magnitude and distribution of the model probabilities are sensitive to these wind fields. From Figures 41-42, one can start to hypothesize why the probabilities are different when the regression model is forced with CFS and with R2 LSEF values. For example, the 850 mb winds (Figure 41) are similar in direction in most locations *except* the region extending from 125°E to 150°E and straddling 10°N. These robust westerlies indicated by the R2 data, at zero lead, have a profound impact on the reanalysis-based probabilities, in that they increase the vertical wind shear in that region and amplify low-level relative vorticity to the north. As a result, the region 125°E to 150°E and straddling 10°N is no longer favorable for TC formation, and enhances the probability of TC formation to the immediate north of the westerlies. These westerlies were not predicted by the CFS fields at a nine-day lead; therefore, the climatologically favored location for TC genesis is not displaced. The differences in the 200 mb winds are not as profound. Overall, it appears that temporally summing the bias-corrected ensemble mean fields tends to smooth the CFS fields such that they represent climatology. In the absence of any other predictable elements, seeing the CFS tend towards climatology is reassuring. This tendency is likely due in part to the bias correction we applied to the CFS output.
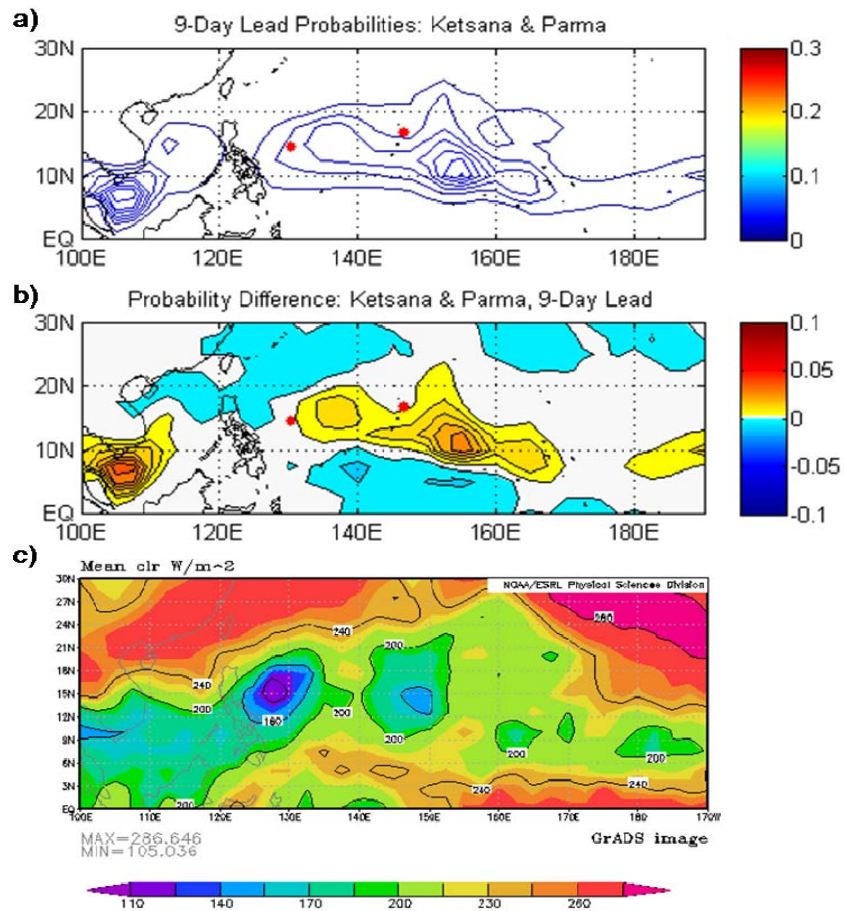
Figure 43.   Comparison of a) CFS-based probabilities (repeat of Fig. 39), b) probability difference, and c) OLR, for the period 15-21 October 2003. The red dots indicate the formation points for Ketsana and Parma.

From this case study, we observe that the 15-member CFS hindcast ensemble mean may be too much like climatology to yield formation probabilities that deviate greatly from climatology. Despite the differences between the R2 and CFS-forecasted 850 mb winds, the probability difference plot in panel b) of Figure 43 highlights that the model still predicts probabilities higher than climatology in the region. In addition, a visual comparison between the CFS-based probabilities and the OLR plot for the same period, Figure 43 panels a) and c), suggests that this period may have been a convectively active period across much of the WNP, and that the CFS-based probabilities did a fair job in predicting this activity.

3.   General Observations

The earlier sections on the verification of the zero-lead hindcasts established a skillful benchmark for evaluating non-zero lead hindcasts and actual forecasts. The two non-zero lead hindcast case studies presented in the preceding section indicate that our combined statistical-dynamical method for intraseasonal prediction of regions favorable for tropical cyclogenesis has the potential to produce useful forecasts from the existing version of the CFS.

Some of the differences between the CFS-based probabilities and the reanalysis-based probabilities are likely due to the differing mechanics of the two systems. Though the output we used was at 2.5° horizontal resolution for both systems, the effective portrayal of the assimilated observational data is different. The R2 assimilates data from a multitude of observational sources directly onto its Gaussian grid; therefore, it is conceivable that if a TC were forming or present over the WNP, the reanalysis data would represent the TC. While similar data is included into the CFS as initial conditions, as the model is integrated forward in time, the coarse-resolution numerics and physics mean that the smaller scale features in the LSEFs associated with TCs that are forming or present will in general be less well represented than in the R1 or R2 fields that force the zero-lead hindcasts. Thus, in general, the CFS is likely to predict LSEF magnitudes and gradients that are weaker than those in R1 and R2.

One should recall that dynamical models, especially GCMs, though based on physical laws, are unable to resolve at all spatial and temporal scales and are sensitive to their often-problematic parameterizations. Nevertheless, it is important to remember that the CFS is not a simplified physics, coarse resolution atmospheric model. Indeed, it is a fully coupled, one-tier dynamical prediction system. With our proposed application, the coupling in the CFS is rather important. At short lead times, a forecast is mostly affected by atmospheric initial conditions. But at longer lead times, the ocean plays a greater role and can allow relatively high predictability in a time averaged forecasts.

We saw with the first case study that applying an ensemble approach to the operational CFS may increase the predictability by smoothing out differences between the members and enhancing the more predictable elements of the climate system. The second case suggested that it might be possible to over smooth, by using the archived ensemble mean summed over seven days. It was promising, however, that the CFS appears to trend towards a plausible, climatological state, rather than toward a model bias state.

The first case study indicates that it may be possible to use raw output fields from the CFS to predict individual TC formations. For the aforementioned reasons, we believe that until the single-element predictability is increased in dynamical models, using the raw output at daily resolutions will often lead one astray at intraseasonal leads. By statistically combining several variables and summing temporally, the predictability is likely increased and more reflective of the large-scale environment that is known to impact TC development.

THIS PAGE INTENTIONALLY LEFT BLANK

IV. SUMMARY, CONCLUSIONS, AND RECOMMENDATIONS

A. KEY RESULTS AND CONCLUSIONS

This thesis is an exploration into the viability of employing a combined statistical-dynamical predictive method for forecasting TC formation probabilities at intraseasonal time scales. The primary focus of this work was to assess the feasibility of using such a method to predict favorable regions for tropical cyclogenesis. We also investigated whether this combined statistical-dynamical approach appears to result in skill and value beyond that which basic climatology provides.

Our proposed predictive method involves forcing a statistical model with available output from a GCM. We began by investigating various atmospheric and oceanic variables in order to decide upon which LSEFs, or genesis parameters, to include as explanatory variables in our model. The chosen statistical model, summarized in Table 1, contains terms for 850 mb relative vorticity, 850 mb relative vorticity squared, SST, vertical wind shear, Coriolis parameter, and 200 mb divergence. Each of these variables was found to be necessary, both statistically and conceptually, but together may not be sufficient to forecast actual formation. Multivariate logistic regression was used to develop a statistical model for the probability of TC formation based on the favorability of the large-scale environment as defined by a linear combination of these LSEFs. As an aside, this work with the LSEFs also suggests that the variable thresholds, as defined by studies during the past several decades, should be made more restrictive. For example, the oft-cited criterion that SST in the WNP must be ≥ 26.5°C for TC formation may be increased to ≥ 28°C (as suggested by Figure 9).

The predictive potential of our method was first assessed by thorough quantitative and qualitative verification of reanalysis-based, zero-lead hindcasts. The model shows great potential, with a BSS of 0.0291 (0.0282…0.0299), a ROCSS of 0.683, reliable summed seven-day probabilities, and potential added

value for risk adverse customers. In addition, the zero-lead hindcasts performed well in dealing with climate oscillations, in developing conditional climatologies, in verification against deep convection, and even in quantitative verification in the Atlantic basin.

The second assessment of the predictive potential of this technique came by way of by two CFS case studies, where we generated non-zero lead hindcasts for past TCs. The availability and format of CFS data confined much of the verification of these studies to be qualitative in nature. We explored an ensemble approach as a way to smooth out the spatial and temporal variability between members, and highlight the more predictable elements. Both the ensemble approach and the combination of LSEFs together lead to expanded predictability of the large-scale circulations, vice the limited predictability of individual elements. Results from these intraseasonal-lead case studies are promising, but also suggest much work remains when it comes to dynamical weather prediction on the intraseasonal scale. Purely dynamical intraseasonal forecasts are not overly skillful (van den Dool 2007), so our statistical-dynamical method appears to be a useful complement to existing alternatives for intraseasonal forecasting of TC formations.

Overall, our method provides a stable, reliable, and repeatable approach to intraseasonal TC formation prediction that is applicable throughout the year and, apparently, in more than just the WNP basin. Our method allows forecasters to objectively and quantitatively merge information about all the LSEFs to produce an ensemble based, probabilistic forecast of the potential for TC formation and the favorability of the climate system compared to long term mean climatological probabilities. A single contoured plot, spanning a seven-day period is easy to interpret and may even be presented directly to users. A typical rule of thumb in forecasting is to use a numerical model only when you have confidence in its output. While we agree with that mantra, we are intrigued by the suggestion that the bias-corrected CFS fields tend toward climatology when the predictability in the climate system is low. If such is the case, this method

could be employed regularly and would, at the very least, depict a probabilistic representation of TC formation climatology.

The concept of climatology appears throughout this thesis, both as the reference forecast against which the proposed technique was judged and as a potential tool in itself. Not all climatologies are created equal, however. See Appendix A for a brief discussion on the variations of climatology used in this work. In this thesis, the choice of climatology impacts the verification results.

Plots of the difference in the probabilities generated by our method and those from climatology provide an intriguing presentation of the skill and value of our method. Such plots can be viewed as probability anomalies and clearly reveal where our method predicts higher and lower likelihood of formation than climatology. Operationally, a forecast for no (or less-likely) activity may be just as beneficial as a forecast for highly-probable formation. For example, an extended area of probabilities lower than climatology may suggest safer passage for a carrier strike group wishing to transit the region.

Using the data and methods outlined in Chapter II, we believe that the model, as described and verified in Chapter III, presents a viable approach to intraseasonal prediction of tropical cyclogenesis. The numerous preceding pages were presented not as a testament to amount of code written or number of variations tested in this research, but rather as an explanation and validation of this combined statistical-dynamical approach in intraseasonal TC prediction.

B.   APPLICABILITY TO DOD OPERATIONS

O'Lenic *et al.* (2007), in discussing recent developments in operational long-range climate prediction at CPC, state "improvements in the science and production methods of LRFs [long-range forecasts] are increasingly being driven by users, who are finding an increasing number of applications, and demanding improved access to forecast information." While this is encouraging and may be true in the civilian sector, we are of the opinion that the preponderance of DoD customers do not know of what Air Force Weather (AFW) and Navy METOC

communities are truly capable. As the products and procedures of these two communities are driven by requirements, if customers do not require a product, it will likely go uninvestigated.

The majority of day-to-day military scheduling and planning is focused on operations and exercises that will occur weeks or months later. Translating the *weeks to months* of lead times of the planning realm into meteorological terms, we draw a parallel between the time scale of military planning and *intraseasonal* forecasts. In contrast, the preponderance of weather support provided by the AFW and Navy METOC communities is focused on short-range forecasting (lead times of 72 hours or less) or nowcasting (lead times less than three hours). This indicates that weather support is out of synch with the majority of the planning done by its military customers.

Arguably, the planning phase is when weather support may have the greatest positive impact on military operations, by alerting planners to the potential conditions that may impact their operations, while the planners still have time to mitigate the impacts of some environmental conditions and exploit the opportunities provided by other environmental conditions. For planners of many military operations, short-range forecasts come too late in the process to have much influence on the planning. In many of these cases, skillful long-range forecasts (e.g., lead times of two week or longer) could be very useful in determining where and when to conduct an operation, what assets and tactics to employ, etc. (personal communication CDR Van Gurley 2005; CDR Tony Miller 2009).

Due to a lack of freely available forecast products at the intraseasonal scale, even an accessible, understandable depiction of climatology or of a conditional climatology has potential value for military planners. The DoD lacks many such a products. Previous theses (e.g., Tournay 2008; Moss 2007) and sections from this report highlight the power of state-of-the-science climatology, or "smart" climatology. Creating state-of-the-science climatologies—using the

latest data sets, knowledge of climate oscillations, etc.—offers a significant improvement in environmental intelligence for DoD planners.

Active intraseasonal prediction has the potential to add value beyond climatology. By exploiting the predictability within the climate system, via statistical, dynamical, or combined methods, skillful weather information may be provided to military planners and operators. It is important for military centers to undertake such prediction in addition to civilian centers, as the military is often focused on regions and variables not covered by civilian products. For example, civilian forecasting centers generally focus on TC landfall locations or the number of TCs in a season. While TC landfall and seasonal counts are important, for the military, information at much greater temporal and spatial resolution, and over the open ocean, would likely prove beneficial. For example, Navy and Air Force planners would benefit from insight into periods and regions safe for ship and aviation operations. The technique proposed in this thesis has other benefits as well. Among these benefits is that an operational version of this process could be a fully-automated process that could be delivered to forecasters and customers in multiple formats, to include those via geographic information systems.

As evidenced by the demands placed on civilian forecast centers from customers, one is led to conclude that if DoD planners and operators saw the potential value-added from heeding long-range weather intelligence, they too would demand more of it. Products stemming from intraseasonal predictions need not be starkly different from short-term forecasts to which customers are accustomed. For example, the ship avoidance chart from JTWC (as in Figure 44) is routinely presented to operators for decision-making. Potential deliverables from the method proposed in this thesis could be very similar to such ship avoidance charts. In fact, the similarity of products would aid in fostering seamless weather support for planning to mission execution from the users' perspectives.
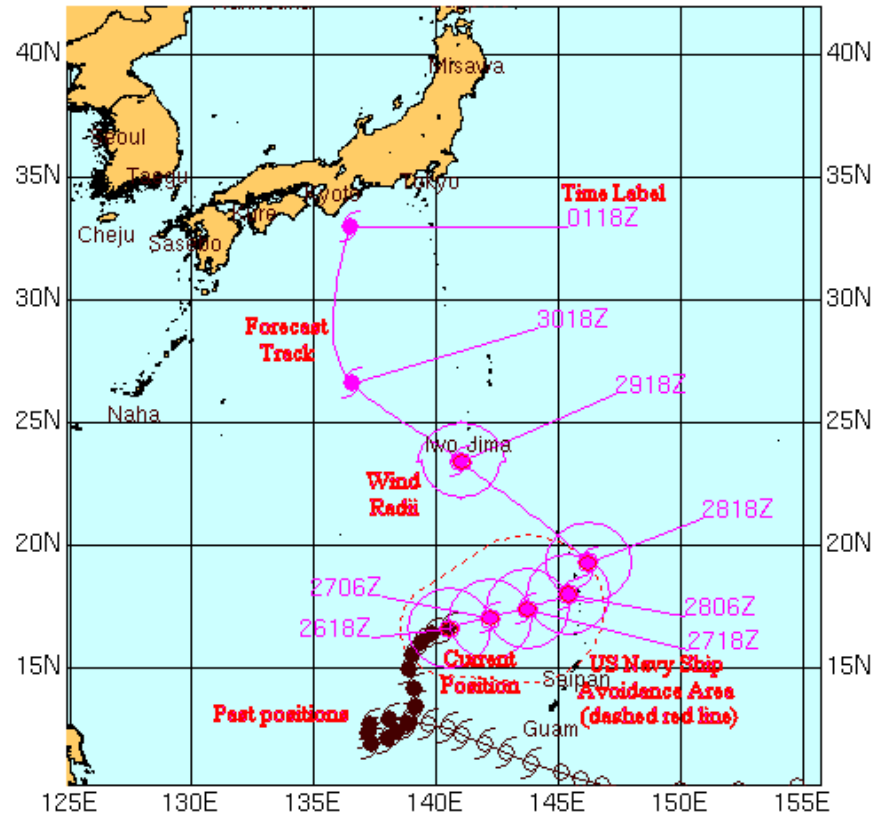
Figure 44. Example JTWC ship avoidance chart (From
http://metocph.nmci.navy.mil/jtwc/legend/ship_key.html; accessed 27
February 2009).

Whether the mission is a trans-oceanic air bridge, carrier strike group flight qualification training, or a major multi-national naval exercise, no current DoD products exist, beyond antiquated climatology products, to aid mission planners is assessing the likely state of climate system weeks to months in advance. The method proposed in this thesis, and others like it, could add value for numerous customers, and certainly has the potential for saving units' time and tax dollars. This thesis represents a test of this concept. We propose that this and similar products be presented to customers to see what applications and demands emerge throughout the DoD.

C.   AREAS FOR FURTHER RESEARCH

The previous sections have shown that this approach demonstrates intriguing potential, and that ample room remains for further research and exploration.

1.   Technique Exploration

As this was a proof of concept for the technique, further exploration into the mechanics of the approach seems prudent. The order of the following ideas for future research does not represent priority.

1)   Vary the regression model based on end strength and/or growth rate of the included storms. Preliminary work confirms the common thought that not all TCs form and behave in the same manner. The method used in this thesis was founded on the idea that compositing numerous storms smooths out the differences and enhances the features in common. However, could one construct a more skillful model if end strength and/or growth rate were taken into consideration?

2)   As mentioned in Section III.B.8, some of the apparent shortcomings of this model deal with the post-formation environment. We were able to mitigate these shortcomings by adjusting the NTCI, filtering out data according to MSLP from the model construction process, and including the relative vorticity squared term. In order to better highlight the conditions at *formation*, one should uniformly define the formation day in the best track archive and consider constructing a regression model excluding data surrounding the track post-formation.

3)   Future research should investigate further the best method for including NTCI in the development of the regression model. This research should attempt to answer questions such as: To what extent should NTCI from regions or periods in which TCs have never formed be used to train the model? Should all NTCI come just from locations and months in which TCs have been observed to occur?

4)   From the available reanalyses and CFS fields, we calculated several of our LSEFs using second order centered finite differencing (see Appendix B). One may consider using a more advanced method to calculate variables, such as Legendre polynomials for meridional differentiation and Fourier analysis for zonal spatial differentiation.

5)   As we observed with the CFS case study, a delicate balance appears to exist between predictability and resolution (as in the model's difference from climatology). The construct of the current operational CFS allows one to readily create a four-member ensemble. While keeping the balance issue in mind, one may explore the idea of creating an expanded ensemble by using runs initialized on multiple days. Such an approach would more closely resemble the approach CPC takes in using the CFS in seasonal forecasting.

6)   A struggle throughout this thesis process concerned the issue of how best to verify the propensity for TC formation. Other centers with similar spatial forecasts of rare events seem to struggle as well, and no industry standard exists for the verification of such products. The approach we took uses an assemblage of tools, most of which inevitably verify the propensity for formation against actual formations.   The issue of verification needs to be explored further.   Could we numerically score against OLR or some other variable that represents favorable LSEFs?

7)   While numerous combinations of possible LSEFs were tested for inclusion into the regression equation in this research, additional work could be accomplished in this area.   Ideal candidates are oceanic variables, such as mixed layer depth.   In addition, one may consider additional non-linear relationships between variables and TC formation or between separate variables. For example, we experienced an improvement in our model's performance by the addition of the vorticity-squared term.

8)   Prior work by Meyer (2007) and others indicate that the same LSEFs that influence formation may also influence the intensity of a TC.

Subsequent research may investigate the potential for generating near-term estimates for the intensity of a storm that has formed, or may soon form, based on the predicted conditions of the large-scale environment.

2.   Data Exploitation

As mentioned in Section II.B. regarding the importance of the reanalysis data sets, the logistic regression approach we employed would not have been possible if the atmospheric and SST reanalysis datasets were not available. Similarly, this approach would not have been viable without the existence of the CFS data set, including an extensive hindcast archive. Current and forthcoming data sources offer potential avenues through which to improve the combined statistical-dynamical method proposed in this thesis.

1)   As noted throughout this thesis, the model was trained on reanalysis data and applied in proof-of-concept testing using CFS data. Though it would require a substantial storage and coding investment initially, one should consider using the CFS to both train and test such a model. In addition to accounting for the subtle biases and nuances within the model, this approach would allow for the testing of more variables—especially oceanic variables— thought to impact TC formation. It was not so much the storage or coding that pushed us away from this approach for this thesis, but rather the limited days for which hindcast data is available. Would enough storms be captured by a purely-CFS approach to successfully train and test a regression model? In addition, we felt it was important to first use reanalysis values of the LSEFs in building the regression model, so that a relatively skillful benchmark based on zero-lead hindcasting could be established. But future studies could consider building a regression model based solely on forecasted LSEFs.

2)   Short of using the CFS data, one may consider employing an ocean reanalysis, or the forthcoming coupled reanalysis from NCEP, to investigate the use of oceanic LSEFs other than SST. We hypothesize that a term representing mixed layer depth may be a more skillful predictor than SST.

In addition, such oceanic variables are known to better represent long term climate system memory. Thus, the use of better or additional oceanic LSEFs than SST could provide a better match between the model's terms and the climate system variables that best represent intraseasonal predictability.

3)   Low skill in CFS intraseasonal predictions of atmospheric variables is likely a weak point for our technique. While there is no reason to believe that the current CFS is inferior at such leads compared to other GCMs, one may find it worthwhile to explore other GCMs, such as those from the Goddard Space Flight Center or Australian Bureau of Meteorology.   Though more computationally demanding, the most intriguing approach may be to employ a multi-model ensemble approach to generate the necessary LSEF fields.

4)   Future plans for the CFS include an operational T126 version. Though we feel that LSEFs must occur over an adequate spatial and temporal scale to affect TC formation, a higher resolution model may generate higher magnitudes and gradients, and more skillful predictions of the LSEFs. Experimental runs by CPC of a high-resolution T254 and T382 CFS have shown that it has the potential to predict individual TCs and may have skill in characterizing overall TC activity (Schemm *et al.* 2008).   Undeniably, a comparison between a high-resolution CFS, or comparable system (e.g., from ECMWF), and a lower-resolution combined approach as proposed in this thesis would be worthwhile.

APPENDIX A.   VARIATIONS OF CLIMATOLOGY

Climatology is used throughout this thesis as a baseline against which we compare our statistical-dynamical prediction method. Not all climatologies are created equal, however. The following paragraphs highlight the forms of climatology applied in or mentioned in this work, all of which are legitimate, but distinct, forms of climatology.

The most basic form of climatology is sample climatology. As used in this thesis, the sample climatology is the average rate of occurrence based on the verification dataset. For example if a TC hit is observed 10 times out of 1,000 possible day grid points, the sample climatology would be 10/1,000 or 0.01. This form of climatology is used in quantitative verification such as the BSS.

We also use various forms of raw climatology based on the JTWC best track data. Figure 6 in Chapter II is an example plot of raw climatology. This plotted data was created by treating each of the 2.5° x 2.5° grid blocks in the WNP as individual bins. Looping through a set period of time (e.g., 1970 to 2007), we counted the number of formations that occur in each bin, then divided the number in each bin by the length of time for the given time interval. Based on the time interval one chooses, the output values vary numerically—as daily, weekly, monthly, etc. probabilities—but the spatial distribution does not. A shortcoming of this raw spatial climatology is its lack of day-to-day variation, in that the magnitude and distribution of daily probabilities for 27 March are the same as 26 August, which we know is not typically the case in the real climate system.

A more robust version of climatology, still based on the JTWC data, is one that varies in magnitude throughout the year. This form of climatology was created by taking a 28-day, Loess-smoothed form of the daily observed TC formations for the WNP, dividing by the number of days in the period to give us a daily probability that a TC will form somewhere in the WNP on a given day.

These daily probabilities were multiplied by a normalized spatial distribution of the likelihood of TC formation in the WNP. The result is a climatology that displays an annual cycle and spatial variation in the output probabilities. This is the form of climatology used in creating the difference plots depicted in Chapter III of this work.

Figure 45 is an example of the components involved in generating such a form of climatology: a) a smoothed version of daily formation counts, b) a normalized distribution of spatial climatology, and c) an example of the resulting daily probabilities for 1 August. This form of climatology vaguely resembles the approach taken by Leroy and Wheeler (2008), who generated a climatological seasonal cycle based on raw probabilities smoothed through harmonic analysis.
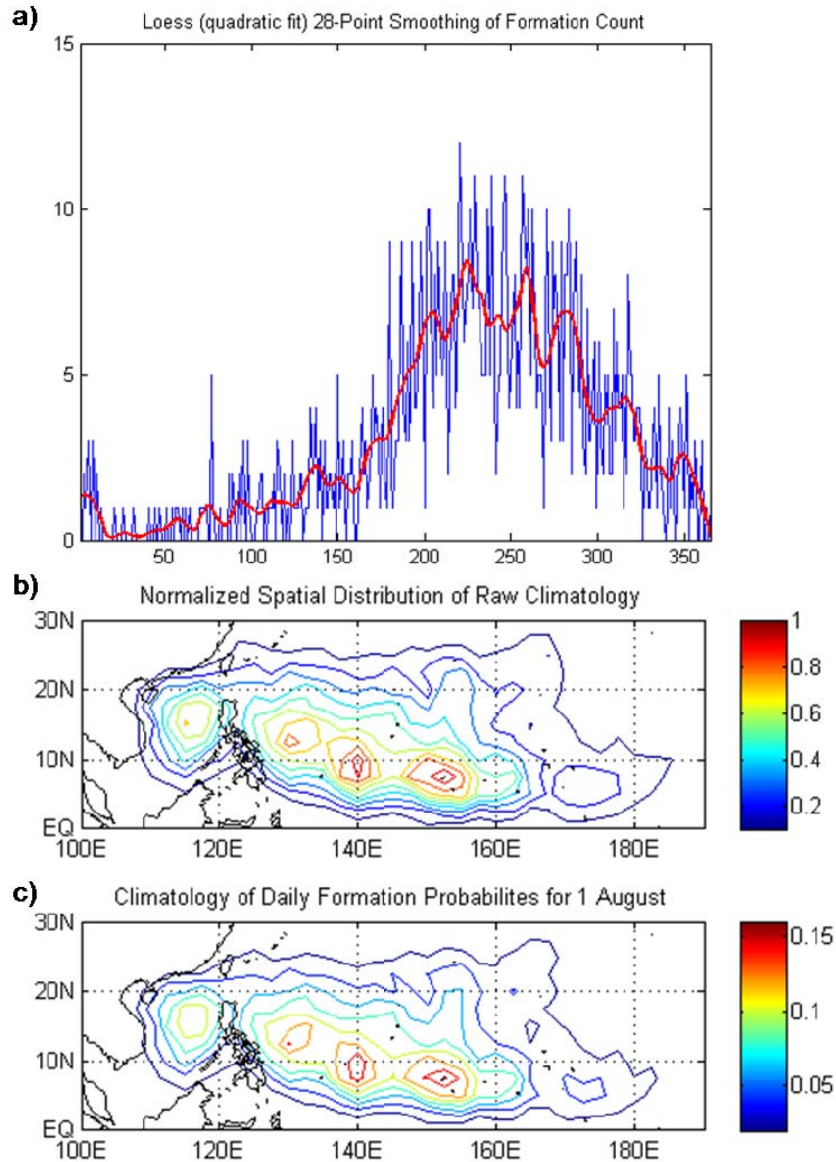
Figure 45. Components used to create a more robust climatology against which to compare our method; a) a smoothed form of daily formation counts, b) a normalized distribution of spatial climatology, and c) an example of the resulting daily climatology for 1 August.

These preceding forms of climatology are all based on the observational JTWC best track data. An approach to generating a pseudo-climatology is mentioned in Section III.B.5. Rather than generating probabilities based on the number of TCs observed for a given spatial and temporal scale, this approach uses the regression model outlined in Table 1 to generate a probability of TC at

every grid point based on LTM LSEFs. A notable benefit of this approach is that it is not sensitive to the number of TC formations. For example, if one wants to create climatology for the probability of TC formation for a forthcoming exercise in the month of May, a method relaying on raw JTWC data would depict patchy probabilities due to the limited number of storms (e.g., 53 in the month of May for the years 1970 to 2006). The spottiness of the output would not accurately reflect the large-scale environment, but rather roughly contour the individual storm formation points. In contrast, the LTM LSEFs (from one of the NCEP reanalyses) when processed by our regression model would result in a depiction of climatology much more indicative of the favorability of the typical climate system in the month of May.

As noted, each of the preceding forms of climatology is a different, but legitimate, approach to representing climatology. Climatology is both a useful tool and a baseline reference forecast. In a situation where no pronounced predictable elements appear in the climate system, a state-of-the-science climatology may be the best intraseasonal/seasonal outlook one has to offer.

APPENDIX B.   CALCULATION OF VARIABLES

As only a limited number of variables are available at daily timesteps from the CFS, we had to calculate additional variables based on available model output fields. In this work, we employed second order centered finite differencing for variables requiring spatial derivatives.

For example, a variable directly representing vertical motion is not readily available from the CFS. We surmise that some degree of uplift would exist (especially in and around the monsoon trough) if low-level convergence and/or upper-level divergence exist. As such, we opted to—among other variables— derive 200 mb divergence based on available 200 mb zonal and meridional wind fields.

Take equation 2.21 from Carlson (1998), where horizontal divergence on a fixed pressure level is given by:

$$\nabla_p \bullet V = \left(\frac{\partial u}{\partial x} + \frac{\partial v}{\partial y} \right)_p$$

Holding the area constant, to represent the fixed model grid spacing, the horizontal divergence in second order centered finite difference form of divergence at 200 mb (D_{200}) becomes:

$$D_{200} = \left(\frac{U_{j+1} - U_{j-1}}{2\Delta x} + \frac{V_{i+1} - V_{i-1}}{2\Delta y} \right)_{200}$$

Where D_{200} is the horizontal divergence at 200 mb, U is the zonal wind, V is the meridional wind, Δx is the zonal (east-west) grid spacing, and Δy is the meridional (north-south) grid spacing. Also, j and i are the longitudinal and latitudinal indexes, respectively.

Then converting the above equation into MATLAB syntax, the equation for 200 mb divergence for an array of size (41,144,365) becomes:

93

```
for i = 2:40
   for j = 2:143
      for k = 1:365
         dy = 111319.49*2.5;    % Spacing in meters, based on WGS-84
         dx(i) = cosd(i)*111319.49*2.5;
         dudx(i,j,k) = (U_200(i,j+1,k) - U_200(i,j-1,k))/(2*dx(i));
         dvdy(i,j,k) = (V_200(i-1,j,k) - V_200(i+1,j,k))/(2*dy);
      end
   end
end

DIV_200 = dudx+dvdy;         % Divergence at 200mb; s$^{-1}$
```

Note that MATLAB indexes top to bottom, thus requiring an opposite convention on the latitudinal index. Also, U_200 and V_200 are predefined variables representing three-dimensional arrays of the 200mb zonal and meridional winds, respectively.

With this spatial finite differencing, we could just as easily used fourth order finite differencing methods. With the model output variables from which such additional variables are calculated being at 2.5° horizontal resolution, we felt that fourth order methods would overly smooth the gradients. Figure 46 is a comparison of second order versus fourth order finite differencing for 200 mb divergence for a sample day in 1991.
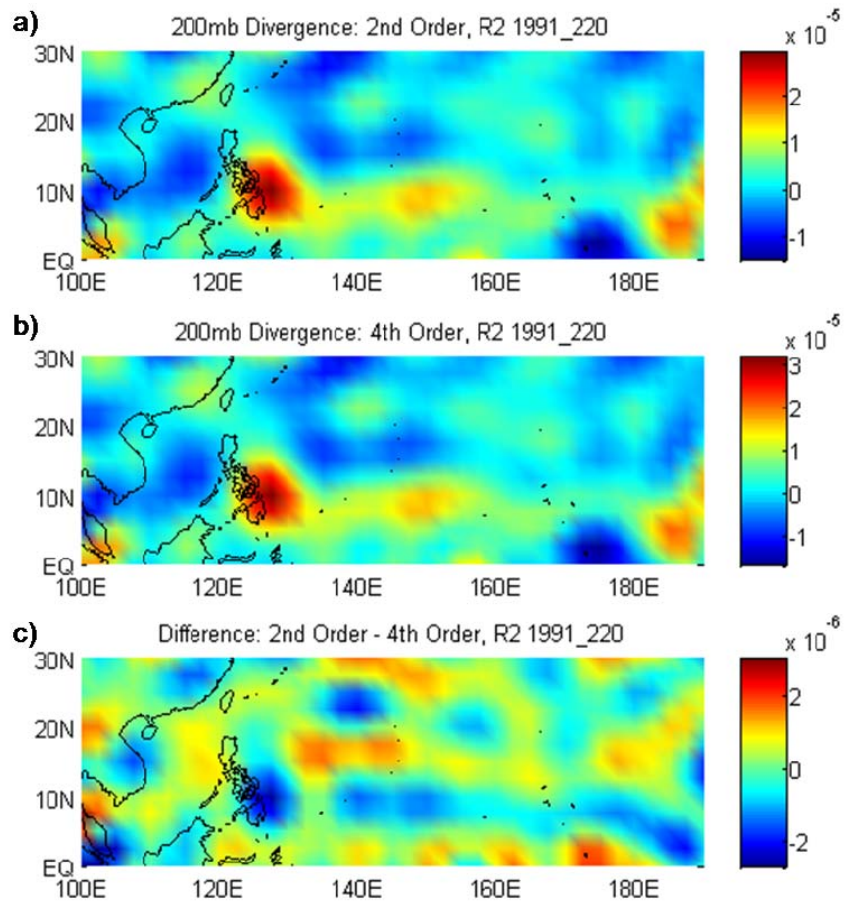
Figure 46.   Comparison of a) second order finite differencing and b) fourth order finite differencing for 200 mb divergence on 8 August 1991, constructed from R2 wind fields. Panel c) is the difference between a) and b). Note the different scales between the divergence and difference plots.

As noted in Section IV.C.1.3)., the calculation of additional variables from the available model output fields is an area open to further research. While the second order centered finite differencing allows us to readily calculate several variables that are based on spatial derivatives, the five-degree "reach" about each grid point does result in some gradient loss versus what we might get if such variables were directly predicted by the CFS.

THIS PAGE INTENTIONALLY LEFT BLANK

APPENDIX C. ADDITIONAL CASE STUDIES

Operational CFS Cases

As an additional resource for the reader, this section includes additional plots for storms that occurred in the WNP during the fall of 2008. The probability plots that follow are based on the operational CFS, and thus are generated from the four-member ensemble. The construct of these cases mirrors Case 1 in Section III.D.1.

The genesis of Jangmi (19W) may be traced back to 24 September 2008. Due to the limited availability of daily operational CFS fields, the lead time for this case is limited to a four-day lead. Figure 47 depicts the seven-day summed probabilities at a four-day lead and a comparison composite OLR plot for the day seven-day period.
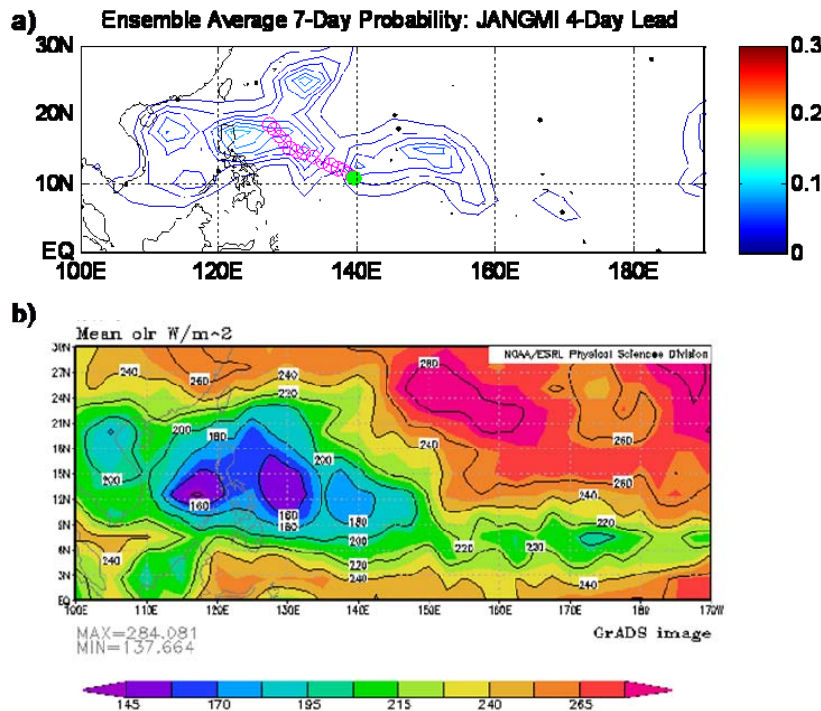

Figure 47. Comparison of a) CFS-based TC formation probabilities from the ensemble mean at a 4-day lead and b) OLR for the period of 21-27 September 2008. The formation point and storm track is marked by the green dot and magenta circles, respectively.

97

Maysak (24W) was a weak storm whose origins may be traced back to 5 November 2008. Figure 48 depicts the seven-day summed probabilities at a two-week lead, at a three-week lead, and a comparison composite OLR plot for the day seven-day period.

Figure 48.   Comparison of a) CFS-based TC formation probabilities from the ensemble mean at a 2-week lead, b) at a 3-week lead, and c) OLR for the period of 2-8 November 2008 The formation point and storm track is marked by the green dot and magenta circles, respectively.

As a late season storm with unusual formation dynamics, Dolphin (27W) makes an interesting case study. JTWC notes the beginnings of Dolphin as early as 8 December 2008. Figure 49 displays the seven-day summed probabilities at

a two-week lead, at a three-week lead, and a comparison composite OLR plot for the day seven-day period about which the probability plots are centered.
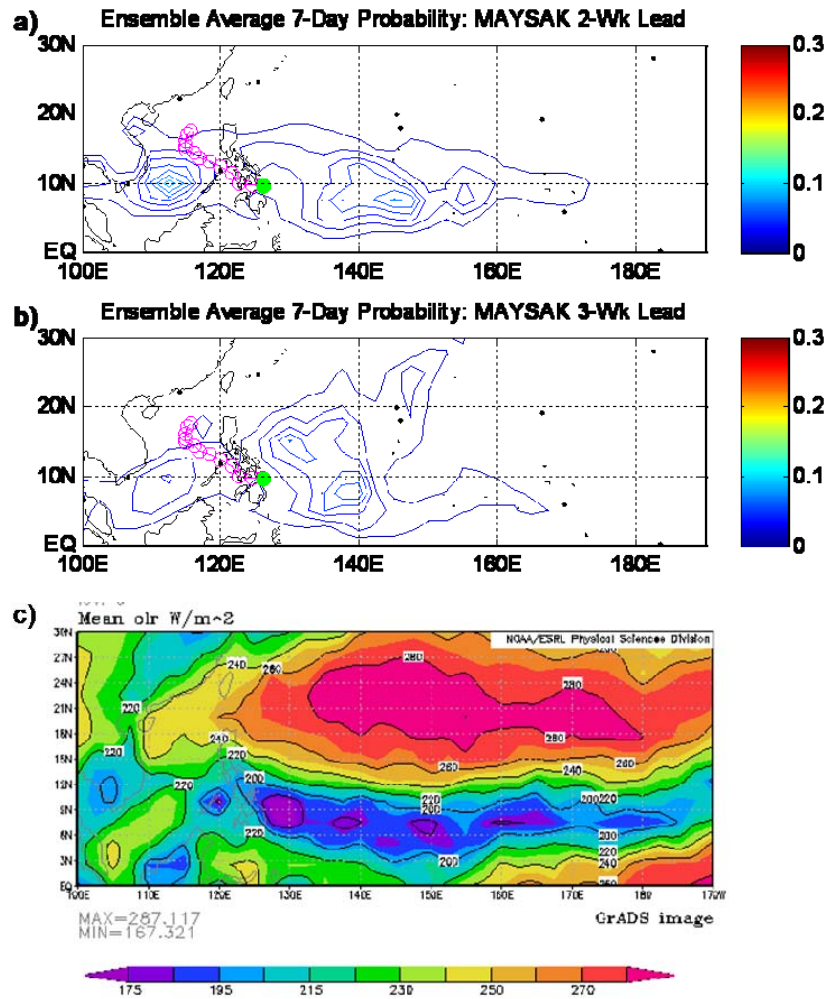

Figure 49.   Comparison of a) CFS-based TC formation probabilities from the ensemble mean at a 2-week lead, b) at a 3-week lead, and c) OLR for the period of 5-11 December 2008 The formation point and storm track is marked by the green dot and magenta circles, respectively.

Hindcast CFS Cases

In contrast to the above cases that were based on daily, operational CFS output, the cases in this section are based on archived hindcast CFS data. Though archived data is used, the lead times are still true-to-form, thus the

probability plots are contours of probabilities based on forecast variable fields. The data used for generating these case studies mirrors the 15-member ensemble mean data used for Case 2 in Section III.D.2.

Jelawat (13W) formed on 31 July 2000, in a location well removed from the climatologically favored formation regions. Figure 50 provides a visual comparison between the CFS-based probabilities and OLR over the same seven-day period.
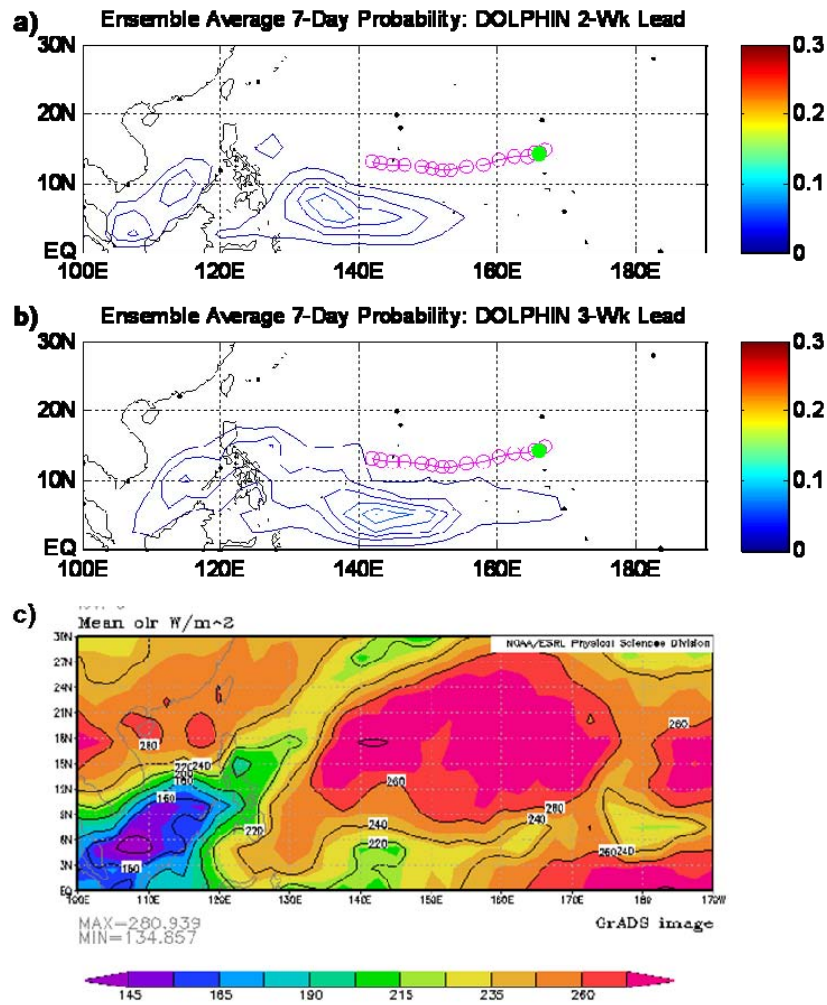

Figure 50.   Comparison of a) CFS-based TC formation probabilities from the ensemble mean at a 22-day lead and b) OLR for the period of 28 July - 3 August 2000. The formation point for Jelawat is highlighted by the magenta dot.

JTWC lists the formation day for Krosa (24W) as 3 October 2001. Figure 51 offers a visual comparison between the seven-day summed CFS-based probabilities centered on 3 October 2001, based on the 15-member ensemble mean, and OLR over the same seven-day period.
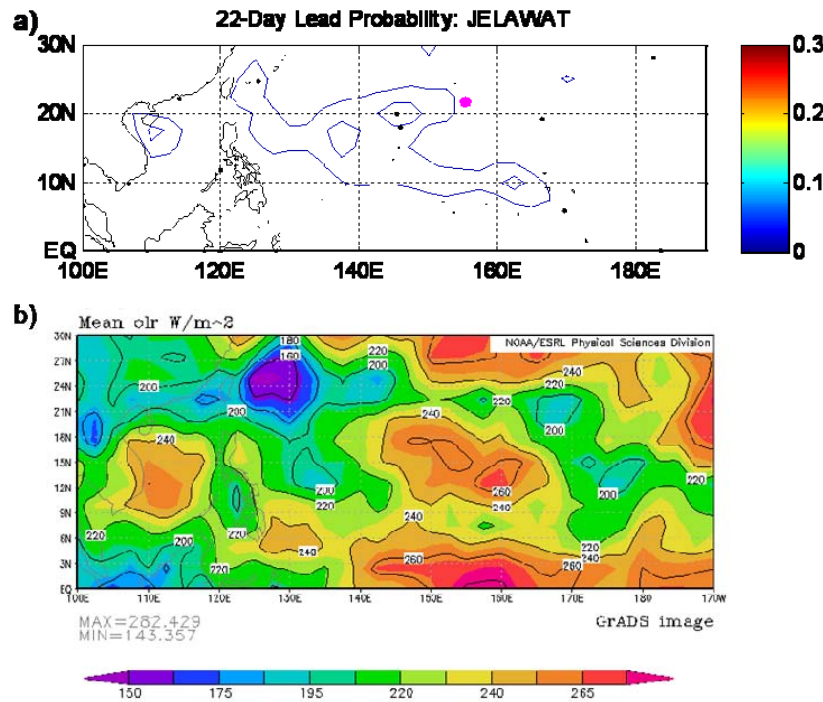
Figure 51.   Comparison of a) CFS-based TC formation probabilities from the ensemble mean at a 24-day lead and b) OLR for the period of 30 September - 6 October 2001. The formation point for Krosa is marked by the magenta dot.

As a final case study, Mindulle (10W) formed on 21 September 2004. The panels in Figure 52 represent a) the CFS-based probabilities from a 12-day lead, b) the CFS-based probabilities from a 43-day lead, and c) the NOAA interpolated OLR image from the same period. The OLR images displayed in this appendix and throughout this thesis are courtesy of the Physical Sciences Division, Earth System Research Laboratory, NOAA, Boulder, Colorado, from their Web site at http://www.esrl.noaa.gov/psd/.
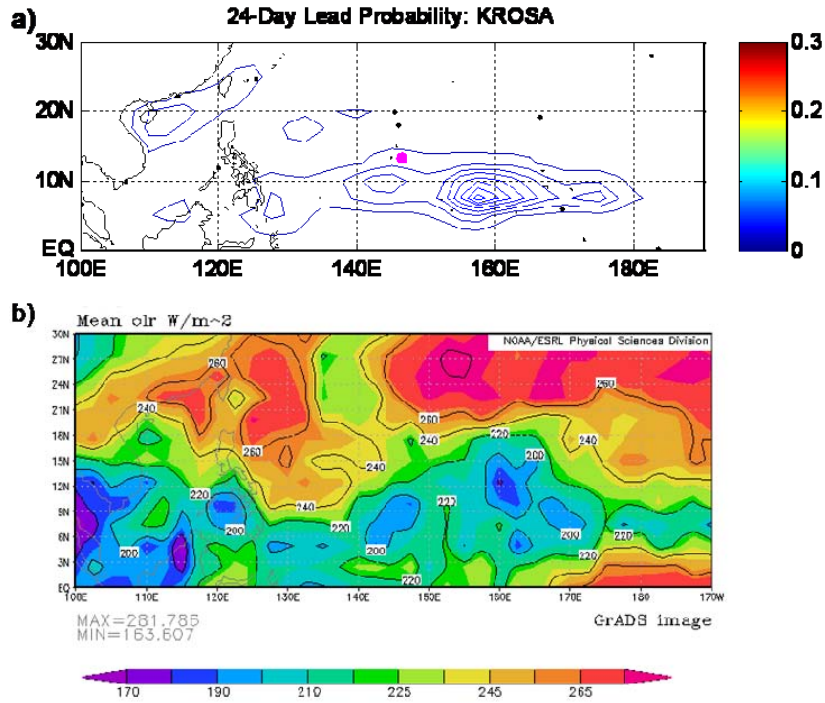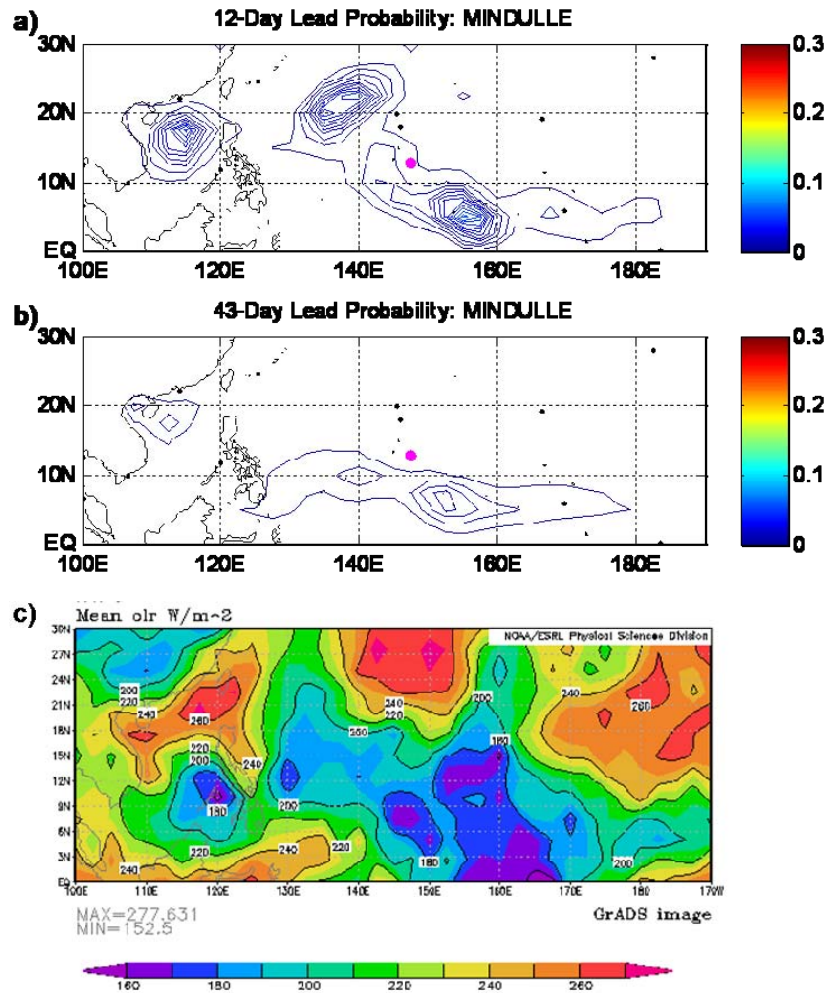
Figure 52. Comparison of a) CFS-based TC formation probabilities from the ensemble mean at a 12-day lead, b) a 43-day lead, and c) OLR for the period of 18-24 June 2004. The formation point for Mindulle is marked by the magenta dot.

LIST OF REFERENCES

Burnham, K. P., and D. R. Anderson, 2002: *Model Selection and Multimodel Inference: A Practical Information-Theoretic Approach*. 2nd ed. Springer-Verlag, New York, New York, USA. 488 pp.

Briegel, L. M., and W. M. Frank, 1997: Large-scale influences on tropical cyclogenesis in the western North Pacific. *Mon. Wea. Rev.*, **125**, 1397-1413.

Camargo, S. J., 2006: Short-term climate (seasonal and intra-seasonal) prediction of tropical cyclone activity and intensity. *Proc. The Sixth WMO International Workshop on Tropical Cyclones*, San José, Costa Rica, World Meteo. Org., 493-499.

————. and S. E. Zebiak, 2002: Improving the detection and tracking of tropical storms in atmospheric general circulation models. *Wea. Forecasting*, **17**, 1152-1162.

Carlson, T. N., 1998: *Mid-Latitude Weather Systems*. Amer. Meteor. Soc. 507 pp.

Chan, J. C. L., 2004: Variations in the activity of tropical cyclones over the western North Pacific. *Hurricanes and Typhoons: Past, Present, and Future*, R. J. Murnane and K.-B. Liu, Eds., Columbia University Press, 269-296.

————. J. E. Shi, and C. M. Lam, 2001: Improvements in the seasonal forecasting of tropical cyclone activity over the western North Pacific, *Wea. Forecasting*, **16**, 997-1004.

Chu, J.-H., C. R. Sampson, A. S. Levine, and E. Fukada, 2002: The Joint Typhoon Warning Center tropical cyclone best-tracks, 1945-2000. Tech. Rep. NRL/MR/7540-02-16, 26 pp.

Chu, P.-S., 2004: ENSO and tropical cyclone activity. *Hurricanes and Typhoons: Past, Present, and Future*, R. J. Murnane and K.-B. Liu, Eds., Columbia University Press, 297-332.

Devore, J. L., 2000: *Probability and Statistics for Engineering and the Sciences*. 5th ed. Duxbury, 775 pp.

Eckel, F. A., 2008: *Introduction to Ensemble Forecasting*. Naval Postgraduate School, lecture notes for MR4324 and MR4325.

Ford, B. W., 2000: El Nino and La Nina effects on tropical cyclones: the mechanisms. M.S. thesis, Dept. of Meteorology, Naval Postgraduate School, 190 pp.

Frank, W. M., 1982: Large-scale characteristics of tropical cyclones. *Mon. Wea. Rev.*, **110**, 572–586.

————. 1987: Tropical cyclone formation. *A Global View of Tropical Cyclones*, R. L. Elsberry, W. M. Frank, G. J. Holland, J. D. Jarrell, and R. L. Southern, Eds., Office of Naval Research, 53-90.

————. 2006: External influences on formation. *Proc. The Sixth WMO International Workshop on Tropical Cyclones*, San José, Costa Rica, World Meteo. Org., 261-265.

————. and P. E. Roundy, 2006: The role of tropical waves in tropical cyclogenesis. *Mon. Wea. Rev.*, **134**, 2397–2417.

Glickman, T., Ed. 2000: *Glossary of Meteorology*. 2nd ed. Amer. Meteor. Soc., 855 pp.

Gottschalck, J., Q. Zhang, W. Wang, M. L'Heureux, and P. Peng, 2008: MJO monitoring and assessment at the Climate Prediction Center and initial impressions of the CFS as an MJO forecast tool. Presentation, *NOAA CTB - COLA Joint Seminar Series*, 23 April 2008.

Gray, W. M., 1968: Global view of the origin of tropical disturbances and storms. *Mon. Wea. Rev.*, **96**, 669-700.

————. 1975: Tropical cyclone genesis in the western North Pacific. U.S. Navy Tech. Rep. NEPRF TP 16-75, 66 pp.

————. 1979: Tropical cyclone origin, movement and intensity characteristics based on data compositing techniques. U.S. Navy Tech. Rep. NEPRF CR 79-06, 126 pp.

Kalnay, E., M. Kanamitsu, R. Kistler, W. Collins, D. Deaven, L. Gandin, M. Iredell, S. Saha, G. White, J. Woollen, Y. Zhu, A. Leetmaa, R. Reynolds, M. Chelliah, W. Ebisuzaki, W. Higgins, J. Janowiak, K. Mo, C. Ropelewski, J. Wang, R. Jenne, and D. Joseph, 1996: The NCEP/NCAR 40-Year Reanalysis Project. *Bull. Amer. Meteor. Soc.*, **77**, 437-471.

Kanamitsu, M., W. Ebisuzaki, J. Woollen, S.-K. Yang, J. J. Hnilo, M. Fiorino, and G. L. Potter, 2002: NCEP–DOE AMIP-II Reanalysis (R-2). *Bull. Amer. Meteor. Soc.*, **83**, 1631–1643.

Kistler, R., E. Kalnay, W. Collins, S. Saha, G. White, J. Woollen, M. Chelliah, W. Ebisuzaki, M. Kanamitsu, V. Kousky, H. van den Dool, R. Jenne, and M. Fiorino, 2001: The NCEP-NCAR 50-Year Reanalysis: Monthly means CD-ROM and documentation. *Bull. Amer. Meteor. Soc.*, **82**, 247-267.

Lander, M. A., 1996: Specific tropical cyclone track types and unusual tropical cyclone motion associated with a reverse-oriented monsoon trough in the western North Pacific. *Wea. Forecasting*, **11**, 170-186.

Leroy, A., and M. C. Wheeler, 2008: Statistical prediction of weekly tropical cyclone activity in the Southern Hemisphere. *Mon. Wea. Rev.*, **136**, 3637-3654.

Lloyd-Hughes, B., M. A. Saunders, and P. Rockett, 2004: A consolidated CLIPER model for improved August-September ENSO prediction skill, *Wea. Forecasting*, **19**, 1089-1105.

McBride, J. L., 1981: Observational analysis of tropical cyclone formation. Part III: Budget analysis. *J. Atmos. Sci.*, **38**, 1152-1166.

Meyer, D. W., 2007: Relationships between global warming and tropical cyclone activity in the western North Pacific. M.S. thesis, Dept. of Operations Research, Naval Postgraduate School, 163 pp.

Moss, S. M., 2007: Long-range operational military forecasts for Afghanistan. M.S. thesis, Dept. of Meteorology, Naval Postgraduate School, 99 pp.

O'Lenic, E. A., D. A. Unger, M. S. Halpert, and K. S. Pelman, 2008: Developments in operational long-range climate prediction at CPC. *Wea. Forecasting*, **23**, 496-515.

Ramage, C. S., 1995: *Forecasters Guide to Tropical Meteorology: AWS TR 240 Updated.* AWS/TR-95/001. Air Weather Service, 392 pp.

Reynolds, R.W., N.A. Rayner, T.M. Smith, D.C. Stokes, and W. Wang, 2002: An improved in situ and satellite SST analysis for climate. *J. Climate*, **15**, 1609-1625.

Saha, S., 2008: Documentation of operational NCEP CFS data files. [Available online at http://cfs.ncep.noaa.gov/cfs_data.pdf]. Accessed March 2009.

————. S. Nadiga, C. Thiaw, J. Wang, W. Wang, Q. Zhang, H.M. van den Dool, H.L. Pan, S. Moorthi, D. Behringer, D. Stokes, M. Peña, S. Lord, G. White, W. Ebisuzaki, P. Peng, and P. Xie, 2006: The NCEP Climate Forecast System. *J. Climate*, **19**, 3483–3517.

Schemm, J.-K. E., L. Long, S. Saha, and S. Moorthi, 2008: Application of the T382 CFS forecasts for dynamic hurricane season prediction. *Proc. 33rd Climate Diagnostics and Prediction Workshop*, Lincoln, NE, NOAA/CLIVAR.

Sobel, A. H., and S. J. Camargo, 2005: Influence of western North Pacific tropical cyclones on their large-scale environment. *J. Atmos. Sci*, **62**, 3396-3407.

Tournay, R. C., Jr., 2008: Long-range statistical forecasting of Korean summer precipitation. M.S. thesis, Dept. of Meteorology, Naval Postgraduate School, 145 pp.

van den Dool, H., 2007: *Empirical Methods in Short-Term Climate Prediction*. Oxford University Press, 215pp.

Vitart, F. D., and T. N. Stockdale, 2001: Seasonal forecasting of tropical storms using coupled GCM integrations. *Mon. Wea. Rev.*, **129**, 2521-2537.

Wang, B., and J.C.L. Chan, 2002: How strong ENSO events affect tropical Storm activity over the western North Pacific. *J. Climate*, **15**, 1643–1658.

Wilks, D. S., 2006: *Statistical Methods in the Atmospheric Sciences*. 2nd ed. Academic Press, 627 pp.

Wu, M.-C., K.-H. Yeung, and W.-L. Chang, 2006: Trends in western North Pacific tropical cyclone intensity. *Eos Trans. AGU*, **87(48)**, 537-538.

Xue, Z. and C. J. Neumann, 1984: Frequency and motion of western North Pacific tropical cyclones. NWS NHC Report No. 23, 91 pp.

INITIAL DISTRIBUTION LIST

1. Defense Technical Information Center
   Ft. Belvoir, Virginia

2. Dudley Knox Library
   Naval Postgraduate School
   Monterey, California

3. Prof. Tom Murphree
   Naval Postgraduate School
   Monterey, California

4. Mr. David W. Meyer
   Naval Postgraduate School
   Monterey, California

5. Maj. Frederick Eckel, USAF
   Naval Postgraduate School
   Monterey, California

6. Air Force Weather Technical Library
   Asheville, North Carolina